THE UNIVERSITY
of EDINBURGH

Frequency-Based Radar Waveform Design for Target Classification Performance Optimisation Using Fisher Analysis

Sultan Alshirah

A thesis submitted for the degree of Doctor of Philosophy.
The University of Edinburgh.
July 2020

Abstract

This thesis presents non-adaptive radar waveform and receiver designs to improve radar target identification performance. The designs are based on the theory of Fisher discriminants analysis and Fisher separability functions. Introducing Fisher discriminants analysis in waveform design for target maximisation is the first contribution of this thesis. By using the concepts of Fisher analysis both for 2-class or multiclass scenarios, a separability rational function can be derived for practical extended targets classification. The separability functions are formulated to maximise the distance between the means of data classes while minimising their variance. Fisher separability is used as an objective function for the optimisation problem to find the optimal waveform that maximises it under constant energy constraints. The classifiers are derived and inspired by Fisher minimum distance classifiers. The second contribution of the thesis is deriving low-energy low-covariance (LELC) closed-form solutions for the optimisation problem under additive white Gaussian noise (AWGN) conditions. These solutions perform well especially when the signal-to-noise ratio is low. Further, a closed-form solution for the optimisation problem is derived for the 2-class scenario. The solution achieves classification performance comparable to solutions obtained using general optimisation solvers. The proposed waveform and receiver design methods are tested using synthetic and real target data and is shown to achieve better performance than the wideband chirp and other non-adaptive waveform design methods reported in the literature.

Lay Summary

Radars are electronic systems that operate similarly to how bats use sound echoes to see in the dark. Bats use the echo of their screeches (sound waves) to locate and detect objects around them whenever seeing is not possible. The difference is that radars sends a mix of electricity and magnetic waves instead of sound waves. Radar electromagnetic waves can travel faster than sound waves and cover more distance enabling the radar to detect and locate remote objects.

In the early days of radars, it is common to have a predefined restricted shape of radar waves. The shape of radar waves is commonly known as "the radar waveform". The radar would have a radar waveform that is used for all its operation. Modern radars have more advanced hardware that allows them to use more variety of radar waveforms with much less restrictions.

Research shows that different objects, that reflect radar waves back to the radar, can have different effects on the shape of radar echoes. This means that by recording these different effects and using them as reference, the radar can recognise the objects that reflected their waves. These effects also depends on orientation of object, its shape and its movements.

The research also shows that it is possible to design the radar waveform to make recognising objects and their effects on radar echoes better. This makes the radar more efficient and more often correct when recognising targets. This can be very important in many scenarios. For example, the radar need to be very accurate in recognising if a remote object on the ground in an enemy tank or a civilian ambulance.

In this thesis, we propose methods to design radar waveforms mathematically that should improve the odds of the radar being correct in recognising remote objects. Our design makes objects effect on echoes mathematically more separable and more different. This makes recognising the effects and the object better in radars. Our design methods are set so that the waveform can be calculated outside the radar hardware once and then used in radars. Usually calculating waveforms using our method might require a lot of calculations and need to

be done with computer. However, in this thesis we also define situations where the number of calculations can be reduced significantly. In these situations, an equation can define the waveform directly. The proposed methods also are designed to recognise the target using single echo with no need to change the waveform between echoes. We call this type of methods "non-adaptive" design methods. By using computer simulation and some real recorded objects effects, we can study and see how good our design methods in comparison to other methods proposed by other researchers. The comparison is based on the estimated odds of the radar correctly recognising an object. The results show that our methods achieve higher performance than other non-adaptive methods.

Declaration of Originality

I hereby declare that the research recorded in this thesis and the thesis itself was composed and originated entirely by myself in the school of engineering at The University of Edinburgh.

Sultan Alshirah, July 2020

Acknowledgements

All praise and thanks to Allah for everything I was, everything I am now and everything I will be. For him alone, every misfortune becomes a blessing and every obstacle becomes an opportunity. Thanks to Allah for giving me everything that made this thesis possible.

Am thankful to Allah for the loving and supporting parents, my father Zuhair and my mother Hind. This thesis would not have been possible without the unconditional love and support you showered me through the years. Thank you.

Am thankful to Allah for my wife who spent her honeymoon supporting me while am studying here in Edinburgh. Your support and patience were always available when I needed them. Thank you, Nora, for everything.

I would also like to thank my supervisor Prof Bernie Mulgrew. I have been very lucky to have him as my supervisor in my MSc and PhD studies. His knowledge, guidance and attitude fuelled my research and will always inspire me in my way forward. Thank you, Prof Mulgrew.

I would like to express my gratitude for Dr Shahzad Gishkori for all the feedback and deep conversations we had that improved the work presented in thesis and contributed to the publications. Thank you, Dr Gishkori.

Finally, I would like to express my great appreciation to the government of Saudi Arabia and King Abdulaziz City for Science and Technology (KACST) for their financial support and for giving me this opportunity to complete my PhD.

Contents

List of figures

List of tables

List of Algorithms

Acronyms and abbreviations

AMD	Average Mahalanobis Distance
CV	Civilian Vehicle
DFT	discrete Fourier transform
EM	Electromagnetic
ESD	energy spectral density
EVR	Eigenvalues ratio
LDA	Linear discriminant Analysis
LELC	low SNR/energy and low covariance
MIMO	Multi-input multi-output
MISO	Multi-input single-output
PRI	Pulse repetition interval
PRF	Pulse repetition frequency
PSD	Power spectral densities
PWSV	Probability-weighted spectral variance
PWE	Probability-weighted energy
RCS	Radar cross-section
RF	Radio frequency
SAR	Synthetic aperture radars
SCNR	Signal-to-clutter-and-noise ratio
SIMO	Single-input multi-output
SINR	Signal-to-interference-and-noise ratio
SISO	Single-input multi-output
SNR	Signal-to-noise ratio
TFR	Target frequency response
TIR	Target impulse response

List of Symbols

a	lowercase denotes a scalar
$\mathbf{a}$	bold lowercase denotes a vector
$\mathbf{A}$	bold uppercase denotes a matrix
t	time
ϵ_x	time-domain waveform energy
σ_n^2	noise variance
P_{cc}	probability of correct classification
P_{mc}	probability of misclassification
$\mathbf{x}$	time-domain waveform vector
$\mathbf{r}$	extended target impulse response vector
$\mathbf{n}$	time-domain noise vector
$\mathbf{c}$	time-domain clutter vector
$\mathbf{y}$	time-domain received radar return vector
$\mathbf{w}$	projection vector
X	frequency-domain waveform vector
R	extended target frequency response vector
N	frequency-domain noise vector
C	frequency-domain clutter vector
Y	frequency-domain received radar return vector
$\mathbf{\Omega}_X$	diagonal matrix with X on it diagonal
$\mathbf{\Sigma}$	Covariance matrix
$\mathbf{S}$	Scatter matrix
$\mathbf{W}$	projection matrix

Chapter 1
Introduction

Signal processing plays a key role in shaping the performance of radar sensing systems. For example, two radar systems equipped with identical hardware can have substantial difference in performance depending on which waveform they transmit and how they process returns. As radars have various applications and different related performance metrics, many of the signal processing techniques are application-based and designed for specific performance objectives. In this thesis, we investigate maximising target identification and classification performance using both radar waveform and receiver design.

1.1 Motivation for the work

A great body of the literature recognises the importance of radar pulse/waveform design in determining the performance of active remote sensing systems. The probing signal of the radar is an important part of how the radar can contribute to the return signal quality and the sensing performance. Note that a significant part of the performance gain achieved with signal processing is obtained in the receiver. Techniques such as pulse compression, space-time adaptive processing (STAP), Doppler estimation and pulse integration are examples of techniques that enhances the performance without special transmitter design. However, with radar waveform design, the contribution of the radar to the return signal can be shaped to obtain the desired results.

Many of the radar signal processing techniques are application- and performance-based including waveform, transmitter and receiver design. As radars are diverse in functionality and application, the performance metrics and objectives are expected to be different and diverse. For example, while maximising signal-to-noise ratio (SNR) of radar return signals is expected to improve the performance in general by improving signal quality, it does not maximise information gain [1, 2].

Over the last decade, a great body of research has explored radar *detection* performance and how the different methods of radar waveform and receiver design can improve that performance in various scenarios and under different practical constraints [3–9].

Typical practical constraints are that the waveforms have constant envelop in the time-domain or have low peak-to-average-power ratio (PAPR). These are to ensure efficient transmission of radar power and that the power amplifier is operating in the region where the power is amplified efficiently [2]. However, the recent advances in linear power amplifier design allow for sophisticated pulse shaping and waveform designs where these constraints could be relaxed without distorting the radar signal [10, 11]. Conversely, in the literature, designing waveforms to improve target identification performance generally does not cover the evaluation of detection performance. Therefore, aspects relating to constant modulus or PAPR are not included here. However, our design process does offer the flexibility to include such constraints and future work may consider them.

In remote sensing applications, classification can be as important as detection and often the former follows the latter. Both objectives have many applications related to security and emergency services. For example, in a scenario where a remote target could be either a tank or a civilian vehicle, classification is of high importance along with detection. For both objectives, control of the transmitted waveform provides an additional degree of freedom to maximize the performance.

For classification, two strategies have emerged: adaptive and non-adaptive waveform design. Adaptive waveform design procedures operate by continuously updating the transmit waveform design by using the information acquired from received signals. For example, an adaptive procedure can start by transmitting an arbitrary waveform (e.g. a chirp) and then wait for the return signal and use its content to design the next waveform to be transmitted. Then, it waits for the return from the new waveform and design the next waveform using all the signals received so far. Non-adaptive waveform design, on the other hand, is done without feedback from radar returns after deployment. This means that adaptive waveform designs need to be implemented and automated in the radar system to systematically design radar waveforms after deployment. Non-adaptive waveform design can be done offline before radar deployment as no radar return is required in the design process.

In this thesis, it is helpful to explore the different approaches where target identification performance is enhanced using waveform and receiver design. By evaluating the requirements and performance gain of every approach, the difference between the approaches becomes vivid and a new approach that is optimal in all criteria becomes feasible. Also, the investigation of the signal models and the assumptions about the target and radar surroundings is an essential part of this thesis. This will allow for a clear vision of what methods are more practical and which performs better for specific systems.

The thesis investigates the introduction of Fisher discriminant analysis to target identification optimisation using waveform design. To the best of the author's knowledge, Fisher discriminant analysis were never applied to radar waveform design problems especially for target identification applications.

In addition to the operational requirements for the target identification methods, the waveform and receiver design also demands additional computations. The waveform and receiver design usually demands more computations than the target identification processes found in the literature. Also, while most studies assumes a signal model based on the time-domain, a great body of target data are frequency-based data (especially data collected with a synthetic aperture radar (SAR)). Additionally, frequency-based data also provides computational advantages that are yet to be exploited. In this thesis, deriving an optimal waveform strategy in terms of design computational requirements is one of the main aims of this thesis.

1.2 Thesis contribution

The thesis proposes new non-adaptive waveform design procedures for optimal classification, one is inspired by 2-class Fisher discriminant analysis and the other in inspired by the multiclass analysis. The waveform, in both procedures, is designed to maximise either 2-class or multiclass multivariate Fisher separability function under constant waveform energy constraint. The general solutions can be obtained using general optimisation solvers. Also, two closed-form solutions (one for each scenario) to the waveform design optimisation problems are derived under low SNR/energy and low covariance (LELC) assumption. The results show that the proposed classification schemes and waveform designs outperform the non-adaptive

methods proposed in [12–15] in most scenarios and especially in high SNR regions. These contributions are presented in chapter 3.

Chapter 4 expands on chapter 3 with three main contributions. 1) Introduction of signal-dependent interference and clutter to the signal model for the two cases: i) when the target classes share the same covariance matrix ii) when they have different matrices 2) formulation of the waveform design problem based on the new signal model for both cases 3) derivation of a frequency-based closed-form solution for radar waveform design problem. The thesis tests the closed-form solution against flat spectrum wideband waveform, optimised waveforms obtained from the optimisation algorithms and extreme energy waveforms such as low and high energy waveforms.

1.3 Thesis organisation

The thesis is organised as follows:

In chapter 2, a background of the thesis-related theories and concepts is presented. The chapter starts by summarising the basics of radars, its applications, waveform design and a brief summary of classification, linear and Fisher discriminant analysis. Also, an overview of the literature of waveform design for target identification applications is presented. The overview covers the main trends in the field of interest and the notable advances in the areas of research related to the thesis.

Chapter 3 presents the first non-adaptive waveform design procedures and scenarios. The signal model, waveform and classifier design for the clutter-free 2-class and multiclass scenarios are introduced. The waveform is designed to maximise Fisher's separability between target classes. The full derivation of the multiclass waveform design is presented in this chapter while details on the derivation of the 2-class scenario are given in the appendix. By using Fisher's separability as the objective function for the optimisation problem, the optimal waveform can be obtained using a general optimisation solver software. The chapter also summaries the simulation setup and present the results showing the performance of the waveform and receiver derived and compare its results against other waveforms in the literature.

This material form the basis of journal paper in [16].

Chapter 4 expands on 2-class scenario by 1) introducing signal-independent interference to the signal model used in the derivation 2) updating design procedures and results with the new signal model 3) deriving frequency-based closed-form solution for the waveform design problem using Lagrangian multipliers. The results presented in this chapter compare the closed-form solution performance to the optimal waveform obtained by solving the optimisation problem using the solver software. The contributions were primarily presented and published in ICASSP [17] and the results presented in this chapter will form the basis of a journal submission.

Chapter 5 concludes the thesis and summaries it in addition to hinting on the possible future work.

1.4 Publications

- S. Z. Alshirah and B. Mulgrew, "Improved 2-class target classification performance using radar waveform design," 2018 *IEEE Radar Conference (RadarConf18)*, Oklahoma City, OK, 2018, pp. 0458-0461.

- S. Z. Alshirah, S. Gishkori and B. Mulgrew, "Frequency-domain Based Waveform Design for Binary Extended-target Classification," *ICASSP 2019 - 2019 IEEE International Conference on Acoustics, Speech and Signal Processing (ICASSP)*, Brighton, United Kingdom, 2019, pp. 4450-4453.

- S. Z. Alshirah, S. Gishkori and B. Mulgrew, "Frequency-Based Optimal Radar Waveform Design for Classification Performance Maximization Using Multiclass Fisher Analysis," in *IEEE Transactions on Geoscience and Remote Sensing*, 2020, doi: 10.1109/TGRS.2020.3008562.

- S. Z. Alshirah, S. Gishkori, and B. Mulgrew, "Optimal Target Classification Using Frequency-Based Radar Waveform Design ," *IEEE Transactions on Geoscience and Remote Sensing*, 2020, undergoing review.

Chapter 2
Background and Literature Review

In this chapter, we review the basic concepts and theories in radar waveform design and target identification that are related to this thesis. Also, we present the relevant literature and research findings that are essential to waveform design and target identification performance maximisation. Additionally, we cover the concepts that are necessary for understanding the relevant literature and its results.

This thesis presents methods and design strategy to improve target identification performance using radar waveform and classifier design. The methods are inspired by Fisher discriminant analysis and Fisher's separability functions. Thus, this chapter will briefly cover 1) radar basics 2) radar waveform design and its literature 3) linear classification and Fisher discriminant analysis.

The methods presented in this thesis are focused on non-adaptive waveform design techniques. This is sometimes referred to as single illumination design methods [18]. In non-adaptive waveform design method, the waveform is designed, deployed and the identification decision is made from single illumination return without changing the waveform design. Differences between adaptive and non-adaptive designs are presented in this chapter.

Waveform design can also be used to improve other performance metrics and objective in modern radar systems. For example, designing radar waveforms to maximise target detection performance is the focus of a majority of the research in the field of radar waveform design [2–9]. However, the focus in this thesis is on target identification optimisation and how it can be improved using waveform design and Fisher discriminant analysis.

The chapter is divided as follows. The first section is an overview of radar basics and the concepts that are essential for understanding the relevant literature and thesis contributions. The second section is focused on radar waveforms, their literature and the materials related

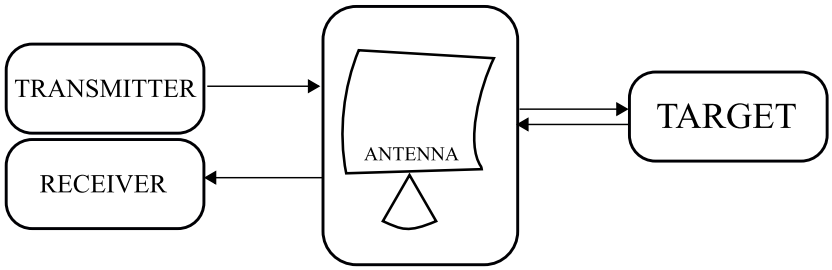

Figure 2.1: *Simplified diagram of a primary radar*

to the derivations and signal models. The third section presents a summary of the linear classification concepts and Fisher discriminant analysis.

2.1 Radar

Radar is an active sensing device that utilise radio waves to detect and range remote targets. Target detection and ranging is achieved using electromagnetic (EM) pulses transmitted from the radar usually at radio frequency (RF) (The RF range is from around 20 kHz to around 300 GHz). The radar pulse travels maximally at the speed of light, depending on the medium, allowing the radar system to sense the surrounding environment and remote targets by receiving and processing radar pulse returns. A simplified diagram of a primary radar is shown in Figure 2.1.

The radar returns can be used to obtain information about remote targets. For example, the returns can be processed to extract target delay, range, speed, angle or arrival, its physical extent and the complexity of its structure. This can be used to detect the target, track its movement, predict its path and identify its class to help radar operators in making the correct decision on how to react to its presence [19].

Radar returns can be used also to capture the environmental surroundings of the radar in its line of sight where the radar forms a synthetic aperture of points the radar passes through in space while focussing on the area of interest in the ground. This results in high-resolution imaging of the area of interest that cannot be blocked by cloud or mist. This is known as synthetic aperture radar (SAR) imaging [20, 21].

Radars can also use returns not generated by their hardware. Instead radars can use the signals propagating around them to sense targets. This type of radars is known as passive radars. On the other hand, a radar that sense targets by pulses generated by its hardware is called an active radar.

The radar system mainly consists of:

- a transmitter that transmits the radar waveform. Some transmitters are designed to transmit continuously and the others are designed to transmit periodically. For example, gun radars transmit continuously when triggered to measure vehicle speed.
- a receiver that receives the return from the EM pulses and converts them into processable data delivered to the radar processor.
- a processor that extracts the useful information from the received data and make them available for manual or automatic decision making. The radar can also be used for timing and control of the transmitter and receiver.

2.1.1 Radar Applications and Basic Functionality

Radars are used for many application related to remote sensing. Some radars can be used for multiple applications where the radar is able to change its functionality in what we call radar mode. The main radar functions are as follows:

- target detection: where the radar make use of its probing EM waves and electromagnetic properties of the conductive properties of the body of the target to range and detect the presence of targets and extract their information.
- Target tracking: where the radar keep track of the target, its speed, and its path.
- target identification: where the target is assigned to a class of targets with common features of interest to the radar operator
- Imaging: where the radar forms images of the terrain and targets seen in a given interval

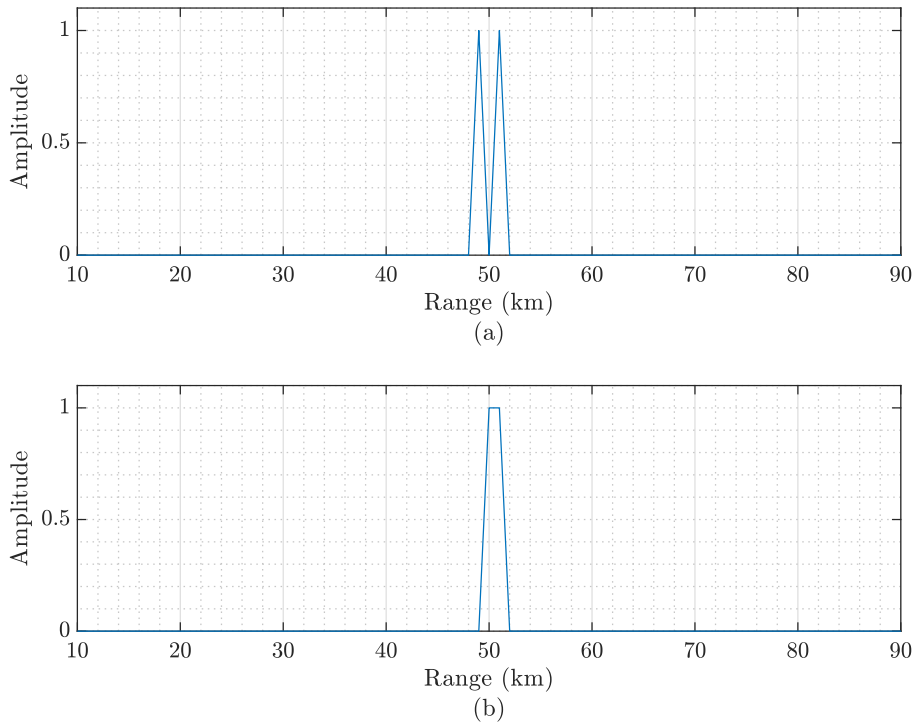

Figure 2.2: *A simplified representation of radar return vs range in two scenarios where (a) the distance between two targets is larger than range resolution and (b) where the distance is lower than the range resolution*

2.1.2 Range Resolution

Ranging remote targets is one of the basic applications of radar systems. In practical scenarios, two or more targets can be on the same line-of-sight where the radar is pointing and in close distance from each other. Range resolution is defined as the minimum distance between targets in which the radar can see them as separate targets in the range axis. When radars used to send high power impulses as their waveform, the best range resolution achieved is limited by the impulse width which theoretically is zero but practically is not. However, techniques like pulse compression allows the radar to have finer and better range resolution that is determined by the bandwidth of the radar waveform [21].

Fig 2.2 shows two scenarios where the radar has a range resolution of around 2 km (i.e. $\Delta r = 2$ km). In the first scenario in the plot (a) in Fig 2.2, the distance between the targets Δd equals Δr and hence the radar can see them as two individual targets at the receiver. In

the plot (b) from the same figure, the targets are closer to each other and the distance Δd is less than Δr which means the radar can only see them as one target at that moment.

2.1.3 Point Target Model vs Extended Target Model

Accurate target modelling is a requirement for a good approximation of the practical aspects of the radar operation. This requirement becomes more important when the main task of the modelling is to study target identification performance.

A great body of research models remote targets as single-point reflectors which only attenuate the radar pulse and delay it with a delay determined by the range of the target. This model is known as point target model [2]. The model is usually assumed in a wide range of research where it is accurate enough to be used practically in many detection or tracking scenarios.

When the system bandwidth of the radar is narrow such that target extent is smaller than the radar range resolution, the point target model can approximate the realistic target behaviour observed in practice. However, if 1) the target physical extent is larger than the range resolution or 2) if the radar was equipped with hardware allowing for wideband operation, then the range resolution can become comparable or smaller than the target extent. The extended target model, in this case, will be more accurate than the point target model. Consequently, the point target model should not be used in representing target response [2].

Figure 2.3 shows an example of the difference between what the radar sees a target with large physical extent in a system (a) with $\Delta r = 10$ m and another (b) with $\Delta r = 1$ m. Extended target model captures the target behaviour in an impulse response generated from the reflection of the different reflectors on the target which can attenuate the radar pulse differently and can delay it according to its position on the target.

The target impulse response (TIR) can be used as a distinct feature for every class of targets. The uniqueness of a TIR of a class of targets can be exploited to improve classification performance. This is also was shown to be useful in improving target detection and other radar applications [2]. Alternatively, the frequency transform of the TIR can be used to distinguish targets. Many of datasets, especially data collected with SAR imaging, consist of target

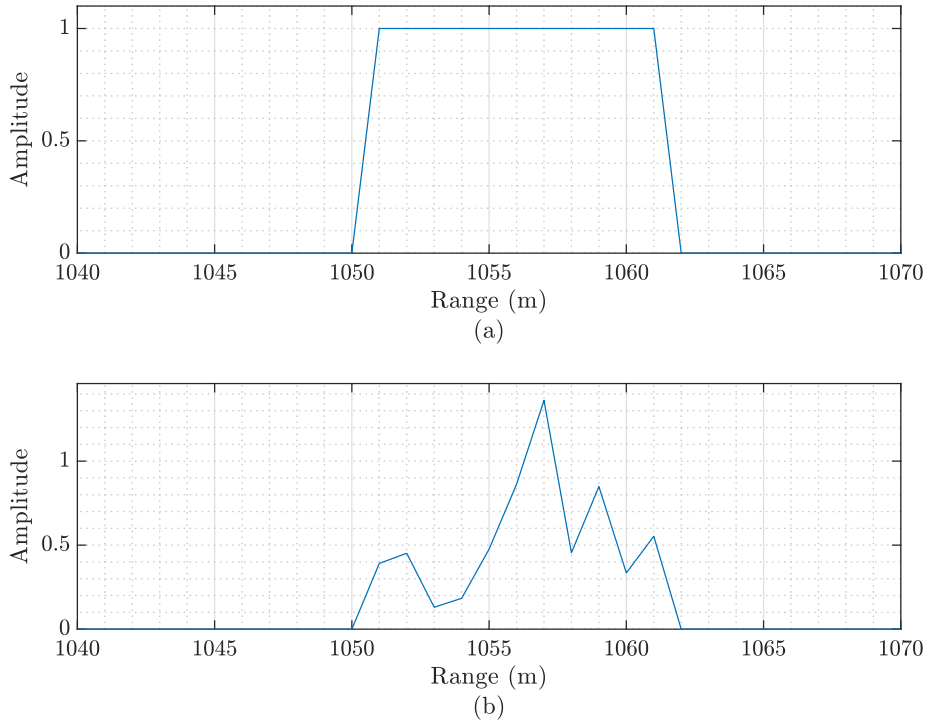

Figure 2.3: *A simplified representation of radar return vs range for (a) narrow band radar system where the target is seen like a point reflector (b) wideband radar where the target has a detailed extended impulse/frequency response*

frequency responses (TFRs) taken at different target orientations like MSTAR CVS data [22].

Many man-made vehicles and especially military targets are not symmetric on every illumination angle. Therefore, these targets are expected to behave differently if illuminated from various angles and orientations. This difference is not expected to be clear when targets are modelled using point target model. Assuming the radar can observe the TIR, the various delays from the target illuminated surface at different angles will result in different TIRs. An illustration is shown in Figure 2.4 where an airborne radar observe a civilian vehicle from different angles resulting in dissimilar observed extended responses. Targets with radar cross-sections (RCSs) and TIRs that are rapidly changing with angle are known as high-fidelity targets. RCS fluctuation can also be caused by the change in target range.

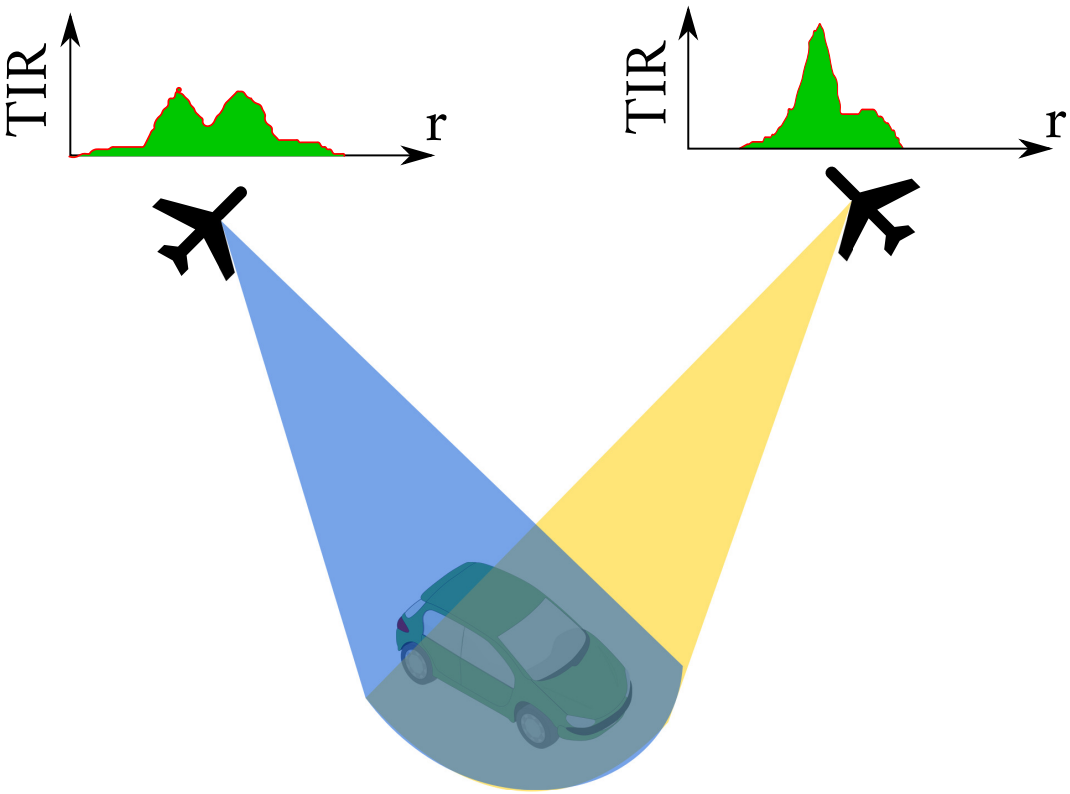

Figure 2.4: *Radars observe different TIRs if the target is viewed from different radar-target orientations*

2.1.4 Radar Types

There are many categories that can be used to distinguish radars from each other. In this section, the types of radar that are related to this thesis are presented here to distinguish them from the ones that are not of interest.

2.1.4.1 Radar Types Based On Transmission Strategy

Pulsed Radars

Pulsed radar is one of the earliest types of radars where the radar actively transmits a probing pulse to sense remote objects using pulse returns [21]. Radar pulses are transmitted periodically then a listening period, where the radar only receive pulse returns, follows each pulse transmitted. The interval of time between radar pulses is known as pulse repetition interval (PRI). The multiplicative inverse of the PRI is the pulse repetition frequency (PRF) (i.e. $PRF = \frac{1}{PRI}$) which is more widely used than the PRI value.

Pulse-Doppler Radars

Pulse-Doppler radars are pulsed radar that also can measure the speed of targets by observing the Doppler frequency in radar returns due to Doppler effect [21]. Doppler information can be used in tracking and clutter suppression and also classification.

Pulse Doppler radars can have: i) low PRF waveforms with typical values of PRF between 0.3–2 kHz; ii) high PRF waveforms (100–300kHz) or iii) medium PRF waveforms with PRF between 5–30 kHz in an X-band airborne pulse-Doppler radar [23].

Differentiating between these types of PRFs is dependent on the maximum unambiguous radar range and the speed it can measure unambiguously.

Continuous-Wave (CW) Radars

CW radar transmits and receives radar signals continuously unlike pulsed radars. CW radars are usually used for speed measurement (e.g. speed gun radars). However, by using frequency-

modulated waveforms that are periodically swept between two frequencies, the radar can range and detect targets in addition to observing the speed of the target by Doppler measurement. This type of radar are known as FMCW radar where the FM is short for frequency modulated [21].

2.1.4.2 Radar Types Based On Transmitter and Receiver Locations

Monostatic Radars

Radars with common RF system for the transmitter and the receiver are known as monostatic radar. In order for monostatic radars to utilise common RF channel for both transmission and reception of radar signal, a duplexer is used. However, the isolation of the transmitted pulse from leaking and interfering with the received signal is a challenging problem that can result in blocking the vision of some target due to the high power of the leakage.

Bistatic Radars

Radar transmitter and receiver do not have to share the same RF system or be colocated for the radar to operate correctly. Bistatic radars are radars where the transmitter and receiver are not colocated and are separated by an appropriate distance. Naturally, it is expected that bistatic radars would cost more than monostatic radars as they require two RF systems for it to operate in addition to a way for the transmitter and receiver to communicate and be controlled and synced if necessary. The costs of bistatic radars are also influenced by whether the transmitter is from a third party or not which can also influence the lightness and compactness of the receiver and the communication channel between the transmitter and receiver if needed. Bistatic radars provide advantages such as enhanced target RCS perception, improved aspect angle diversity and tracking accuracy [24].

Multistatic Radars

Multistatic radars have similar configuration to that of bistatic radar where the transmitter and receiver are separated. However, more than one transmitter or more than one receiver

can be employed. For example, a multistatic radar could have one transmitter and two or more receivers distributed in different locations. Also, a multistatic radar could have two or more transmitters and one receiver. Multistatic radars could also have multiple transmitter and receivers at in the system and can also be separated spatially.

2.2 Radar Waveforms and Radar Waveform Design

Advances in radar hardware enabled huge improvement to the capabilities of modern radars. For example, radar processors became faster, lighter, more compact and reliable. This allows for more sophisticated and complicated computations executed by the radar processor while the radar is deployed. Also, linear power amplifiers became more reliable and more capable of amplifying arbitrary radar probing signals without significant distortion to its amplitude or phase. Power amplifiers can be divided into two different categories, namely, linear and nonlinear power amplifiers. Linear power amplifiers maintain the amplification gain across all input signal amplitudes. In contrary, the amplification gain in nonlinear power amplifiers depends on the amplitude of the input signal. As a result, a radar signal with non-constant envelope is distorted when it is amplified by a nonlinear amplifier. On the other hand, the linear power amplifier does not distort signals with varying envelops. Nonlinear power amplifiers cost less and are more efficient than linear amplifiers [25].

With advanced linear amplifiers in addition to having a radar processor capable of arbitrary radar waveform design, modern radar systems can exploit significant number of degrees of freedom with radar waveform and receiver design to achieve new levels of efficiency and performance [11]. The term arbitrary waveform is used for waveforms with no assumed parametric structure. The waveform will still be constrained by the radar hardware restrictions.

2.2.0.1 Waveform Design Methodology-based Taxonomy

Waveform design can be divided based on the design methodology which can be used in adaptive or non-adaptive design procedures. We list the types of design methodologies from

the one with least degrees of freedom to the most as presented in [11]:

- Waveform selection: where the radar can only choose a waveform from a finite library of pre-defined waveforms to select from.
- Parameter Selection: where the waveform is defined with pre-determined parameters with limited number of values to select.
- Parameter Design: where the waveform has a structure based on a set of parameters and the number of possible values of the parameters can be virtually infinite.
- Suboptimal Arbitrary Waveform Design: where the waveform is designed achieves suboptimal performance despite having almost no constraints on its structure.
- Constrained Optimal Waveform Design: The waveform is designed to achieve optimal performance while satisfying one or multiple constraints.
- Unconstrained Optimal Waveform Design: The waveform is designed to achieve optimal performance under no constraints.

2.2.1 Radar Waveform Design for Target Identification

Radar waveform design is a major area of interest in the field of radar signal processing [26]. Although waveform design in radars is a long time interest, the new trends in designing an application-based waveforms can be dated back to the publication of [2]. The author agreed with P. M. Woodward and I. L. Davies [1], that maximising output signal-to-noise ratio (SNR) at the radar receiver does not necessarily maximises information gain. Therefore, when the radar performance is dependent on information gain, maximising system SNR using waveform design does not necessarily lead to maximising the performance.

In [2], the author showed how prior knowledge about the target can be used to improve radar performance. The prior knowledge was in the form of known properties about the extended target response and its statistics which has been shown to be exploitable and lead to closed-form solutions to the waveform design problem. The two main scenarios presented are:

- the scenario where an extended target with known deterministic TIR is to be detected and an optimal detection waveform is to be designed
- a TIR estimating scenario where the target has probabilistic TIR characterised by known spectral variance and the problem is to design an optimal waveform for maximum information gain

The first problem was solved by designing a waveform that maximises the SNR at the receiver by exploiting the prior knowledge about the target TIR (which in this scenario assumed deterministic) in addition to knowledge about noise spectrum. The optimal detection waveform is then found to be the eigenfunction that maximises an integration expressed using the available prior knowledge.

The estimation waveform is designed by using the mutual information (MI) between the target ensemble and the received signal as the objective function and find the waveform that maximises it. The optimal estimation waveform was found to be a water filling solution where waveform energy is allocated to frequency bands where the target spectral variance is higher than that of the noise. In terms of classification, however, the author shows that maximising MI is expected to improve the probability of correct classification (P_{cc}). This, however, does not guarantee that maximum P_{cc} is attained at maximum MI [2].

The author also expected that these solutions to be impractical as radar systems of that era required constant envelope/modulus waveform so it can be used in saturated transmitters amplifiers [2]. Constant envelop does not require the waveform to have fixed amplitude but to have a constant outline of extreme waveforms amplitudes. The chirp and sinusoidal signals are examples of constant envelop waveforms. This ensures that the radar amplifier is operating in the region where the signal is not distorted. This is also to ensure efficient transmission of power. The other constraints include low peak-to-average-power ratio, impulse-like autocorrelation function and continuous phase.

In this section, we highlight the various approaches to classification maximisation in radar systems using waveform design. The section is divided into two main subsections: Adaptive and non-adaptive waveform design. We start with the later as it was developed before the earlier.

2.2.2 Non-Adaptive Waveform Design

The literature refers to designs that do not require to be updated after deployment as non-adaptive designs or single illumination waveform designs [18]. This means that the radar waveform and receiver can be designed off-line without involving the radar processor in the design process. Also, a decision is usually made on what class to assign the target to from single illumination. Prior knowledge about the operational conditions and the classes of target to be classified is often a requirement for this type of design. The design in both adaptive and non-adaptive technique involves designing the optimal classifier and receiver for the resulted waveforms. We start here with non-adaptive waveform design to follow the chronological order in which these techniques were developed.

2.2.2.1 Classification Of Targets With Deterministic TIRs Under No Angular Uncertainty

In [13], the general problem of classifying a target with a deterministic known TIR was formulated in its continuous. The radar is to classify the target detected into one of two classes (no specific classes were considered) using its continuous TIR. The target is to be classified in the presence of signal-independent AWGN. The authors explored if it is possible to jointly design radar waveform and receiver in order to maximise target identification performance. The proposed solution was to maximise the classification performance where to two targets with deterministic known TIRs in AWGN noise and later for coloured noise [12].

The objective function chosen for classification performance maximisation is based on the L^2 norm between signals corresponding to different targets. An extension to the two targets problem into the more general case where more than two targets are to be classified, was also presented in [12] and was described as relatively straightforward. The extension to multi-class [12] is accomplished with average (or weighted average) separation objective function which on average improves the overall P_{cc}. This extension helps provide a good solution for the impracticality of assuming targets TIRs known and deterministic as many unequal TIRs can belong to the same class of targets but from different viewing angle.

In [14], the same problem is vectorised and signal-dependent interference is also considered

in addition to coloured noise. The objective function was changed to be the Mahalanobis distance between the target responses. The waveform design solutions depends on whether a signal-dependent interference (clutter) is present or not. If no clutter is present, the solution is what later was coined as the eigensolution or the eigenwaveform where waveform is expressed by the eigenvector (the eigenfunction in the continuous scenario) of a matrix that correspond to its maximum eigenvalue. In this paper the matrix is named the target difference auto-correlation matrix and is dependent on the difference between targets TIRs and the auto-correlation matrix of interference. If the clutter is present however, the iterative procedure presented before in [13] is used with some adjustment to find the optimal waveform.

Later in [27] the author included Full-polarisation design of the waveform for full-polarisation data. Finally, in [28, 29] the author developed a waveform design procedure for SIMO radars where banks of receiver can be designed for optimal performance. Although [29], explores the idea for the design procedure for a MIMO radar system, there is no actual design of multiple orthogonal transmitted waveforms that accomplish the benefits of MIMO radars.

2.2.2.2 Classification Of Targets With Deterministic TIRs Under Angular Uncertainty

Practical targets with sophisticated man-made structures are not expected to have the same fixed TIR if viewed from different angles. When angular uncertainty in accounted for is radar design, modelling the target with deterministic known TIR results in significant drop in performance in practice. Although the extension to multi-class problem to account for angular uncertainty is a viable option that could improve classification performance, the number of possible different TIRs can skyrocket easily with the complexity of the target physical structure. In [15], the angular/aspect uncertainty problem addressed. When radar-target orientation is known to be within certain interval of angles, to assume target TIR is deterministic should lead to degradation in the performance due to the mismatch between the expected TIR and the actual TIR. The targets considered in [15] are the “T-72 and M1 main battle tanks”. They modelled TIRs changing with possible azimuth angles as a Gaussian density with mean and variance.

When no signal-dependent interference (clutter) is present, the author suggest finding the

aspect-averaged autocorrelation kernel (aspect-averaged autocorrelation matrix in the vectorised scenario). By including the aspect-averaged autocorrelation matrix $\bar{\mathbf{\Omega}}$ in the Mahalanobis distance maximisation procedure, the waveform is optimised to improve P_{cc} on average as well. The results in [15] presented an enhanced performance compared to chirped pulse in terms the Mahalanobis distance. The performance in terms of P_{cc} was not displayed but it is assumed that P_{cc} is monotonically increasing with the Mahalanobis distance. The simulations also showed that the aspect-uncertainty variance is dependent on the carrier frequency of the radar transmitter. Radars with X-band frequencies, for example, perform poorly with degraded improvement over a variance of 0.5° in compare to VHF-band. VHF system were still robust at a variance of 10°.

We refer to the approach developed in [12–15, 27–29] as the Average Mahalanobis Distance (AMD) approach. AMD design is, to the best of our knowledge, the latest and most advanced off-line non-adaptive radar waveform and receiver design procedure that maximises target identification performance without utilising previous received data or adaptively designing the waveform online on-the-fly.

2.2.3 Adaptive Waveform Design

Radars with adaptive transmitter and receiver are known by the name "Cognitive Radars" [19, 30]. Not to be confused with "Adaptive Radars", which is equipped with an adaptive receiver that can utilise received data to improve radar performance. Cognitive radars have an established link between the receiver and the transmitter that allows for the joint design of the transmitted waveform and receiver using previous radar returns [30]. Radars designed with radar modes can still choose from a set of modes with pre-defined transmitter and receiver configurations depending on the best mode for the radar task.

In [19], the author states three main "ingredients" for any cognitive radar, it is mainly:

- a system that keeps and preserve useful information acquired from previous returns
- a feedback link from the receiver to the transmitter enabling the utilisation of available knowledge in controlling the transmitter and designing waveforms

- an intelligent signal processing, which allows for the use of prior knowledge, acquired in operation, in improving radar performance

and the last ingredient is the most important here as it is where most joint receiver and waveform design happens.

The concept of cognitive radars inspired a lot of adaptive waveform design literature directly and indirectly. However, the early adaptive waveform design research was inspired with the work of [31] where sequential hypothesis testing and sequential probability ratio tests were popularised.

2.2.3.1 SISO Adaptive Waveform Design

Adaptive waveform designs are enabled by the ability to make use of radar returns received previously in designing the next waveform. The waveform is usually redesigned on pulse-by-pulse basis until a certain condition is met and a decision is made. The goal is usually to arrive at a decision with given probability of classification in mind using the lowest possible number of transmissions.

The iterative scheme proposed in [18] uses the sequential multi-hypotheses testing procedure introduced in [2] and [14] to design the next optimal waveform. At every iteration, the next waveform is designed until the desired classification performance is achieved (the desired fixed probability of misclassification) in the lowest possible number of iterations. No signal-dependent interference is present. The noise is assumed to be AWGN and the waveform is adapted and designed from pulse-to-pulse.

In order to minimise the number of iterations, maximum information gain is required and hence the best waveform to be designed in this scenario is the waterfilling waveform which maximises the mutual information between target ensemble in AWGN and the received radar signal. At each iteration,

- the likelihood for every hypothesis is calculated using know targets information and all received signals from every previous iteration

- the likelihoods are used to update the prior probability of every hypothesis
- the likelihood ratios of all pairs of hypothesis are calculated
- all likelihood ratios are compared to thresholds determined by the desired P_{cc}
- the spectral variance of the target ensemble is calculated and used in waterfilling design
- MI maximisation waveform (waterfilling waveform) is designed and used as the next waveform to be transmitted. A waterfilling waveform is a waveform designed with most of its energy is allocated in frequency bands where the receive signal is expected to have SNR greater than 0 dB [32].

if likelihood ratios exceed the thresholds in favour of one of the hypothesis, the iterative process terminates and a decision is made to declare the target assigned to the output class from the process.

Note that to design the MI maximisation waveform, a spectral variance for the target ensemble is required to be computed at each iteration. The spectral variance at any iteration is computed using known target spectral variances and prior probabilities. This spectral variance is refer to as probability weighted spectral variance.

On the other hand, the authors updated the eigenwaveforms introduced in [12–15, 27–29] by introducing some form of adaptivity in their definition where the weighted average Mahalanobis distance is redefined so that its weights are the product of the probabilities of every pair of classes.

The results shows that the iterative scheme with waterfilling waveforms fails to outperform the eigenwaveform when the number of target classes is limited to two. However, in the multi-class scenario, the waterfilling waveforms outperform eigenwaveforms in both error rate and the average number of iterations.

In [33, 34], the authors build on their previous work and explicitly mention the importance of this work to closed-loops in cognitive radars. Classes of targets while characterised by TIRs, also have known spectral variances. Later in [35], they also talk about the framework

developed in University of Arizona where they show that spatial adaptation of the waveforms is also possible.

The extension to the scenario where clutter is present was presented in [36, 37] where signal-dependent interference is added to signal model and the derivations.

One of the common constraints in most waveform design problems is to constraint the waveform energy to be constant for any waveform designed. However, as mentioned in [2], the practicality of waveforms have been always linked to its modulus being constant. While modern radar system are becoming less demanding for this constraint [11], it is still desirable for radar waveforms to have constant envelop. In [38], the author apply constant modulus constraint on adaptive waterfilling waveform design problem instead of the constant energy to study how this can affect the performance. Two approaches were investigated: constant modulus and maximum modulus normalization. The results show that maximum modulus normalization result in high error rate while the constant modulus waveform performs slightly less the waveforms design without constraining their modulus [38].

2.2.3.2 MIMO Adaptive Waveform Design

All the adaptive design presented above are based on single-input single-output (SISO) radar configuration where the radar is equipped single transmitter and receiver that can be colocated or separated.SISO is the standard radar configuration where single transmitter and receiver in the same radar are used. This configuration is optimal in terms of simplicity, cost, and size. SISO can be monostatic or bistatic depending on the separation of the transmitter and receiver. The other main configurations are SIMO, MISO and MIMO.

SIMO is the configuration where multiple receivers capture the radar signal transmitted by a single transmitter. In communication systems, SIMO provide an advantage in combating fading but in terms of detection and classification in radar system, SIMO provides diverse receiving channels with banks of filters allowing for different features of the target to be processed simultaneously like polarisations for example. Although the receivers in SIMO radars do not have to be co-located, they have to be linked in order to achieve performance gain.

MISO radar are radars equipped with multiple transmitters and one receiver. The advantage of employing MISO configuration is improved angular resolution in addition to RCS diversity where the radar will observe the target from different perspectives [39].

Diversifying the number of outputs/transmitters and input/receivers of radar systems can bring several advantages to their performance. MIMO radars provide improved spatial resolution and enhanced target range and speed measurement [40]. With radar returns observing the target from multiple illumination angles, widely-distributed MIMO configuration can also provide diverse RCS measurements with improved SNR and SINR. MIMO radars can have the advantages of SIMO and MISO radar where transmitters and receivers diversity is combined. Improved spatial/angular and Doppler resolution are some of the advantages of MIMO radars. There are two types of MIMO radars: colocated MIMO radars and widely separated MIMO radars. Colocated MIMO radars have the transmitters and receivers in close distance from each other on the same platform. On the other hand, widely separated MIMO position the transmitters and receiver away from each other to allow for spatial diversity in transmission and observing targets RCS.

In order to gain the advantages of having multiple transmitters in MIMO radars, MIMO waveforms must be designed so that they are mutually orthogonal. This allows for simultaneous reception of the radar returns with multiple delays and attenuations without causing and inter-pulse interference between the returns. For example, waveforms with non-overlapping spectra are often used in MIMO as their orthogonality can be achieved with guard bands and non overlapping spectra.

While most of the research we presented so far are SISO-based, it is possible to extend the adaptive waveform design in cognitive radar systems from SISO to mulit-input multi-output (MIMO) configuration as presented in [41].

The MIMO waveform is designed to maximise MI. The solution resulted from the derivation was shown to be also a waterfilling waveform design. The waveform formulation was chosen to be in the frequency-domain. This allows for an orthogonal design of MIMO waveforms to achieve the full potential gain of MIMO radar configuration. Two types of energy constraints were tested : 1) to give every transmitter equal constant waveform energy 2) to set the total

waveform energy for all transmitters combined to be constant.

These models are not, however, necessarily good for representing high fidelity targets. These target have very high variability of TIRs with angles in comparison to low fidelity targets.

As for the target classes, they model targets mainly using two different models:

- with deterministic hypothesis from a scattering centre model (deterministic TIR at each angle computed from a scattering centre model)
- with random target model defined by a set of power spectral densities (PSD)

The different waveform designs tested are as follows:

i. MIMO waterfilling waveforms with constant total waveform energy
ii. MIMO waterfilling waveforms with independent transmitters (waveform energy per transmitter are constant and identical)
iii. MIMO Gaussian approximation
iv. Gaussian approximation (SIMO)
v. Non-adaptive

where the Gaussian approximation waveforms are designed by approximating the target as a Gaussian process.

When the deterministic target model is assumed, all waveforms achieved the best performance in terms of average number of iterations to make decision except for the non-adaptive waveform and the SIMO waveform. All waveforms that achieved the best performance among all the waveforms are all MIMO waveforms. However, the results also showed that when the random target model was considered, all the waveforms except the non-adaptive waveform achieved similar performance. This can be interpreted that in practice, MIMO radars may not attend better performance than SIMO radars if the design procedures in [41]

were used. The results also shows that in terms of the classification error rate, the MIMO waveform with Gaussian approximation performs better than all waveforms.

In [42, 43], the problem of MIMO waveform design for classification performance maximisation was extended from co-located scenario to a scenario where the radar transmitters and receiver are spatially separated (widely separated MIMO radar). The paper studied the two-transmitters-two-receivers MIMO radar scenario. Because waveforms orthogonality is mandatory condition for MIMO waveform design and because constant modulus can cause spectral leakage, adaptive MIMO waveforms must be managed to insure an acceptable levels of orthogonality between the waveforms while also maintaining a constant modulus in the time domain. Luckily, waterfilling waveforms, resulting from MI maximisation, tend to have sparse spectra which allows for better waveform orthogonality and reduced interference [42].

In [42, 43], instead of the scattering centres and PSD based models, they used XFdtd software to generate TIRs for the widely separated MIMO scenario where the two receiver should observe the same target from different angles. Because the targets generated from the software should be more close to practical targets, the targets are expected to be high fidelity targets. Thus, limiting the viewing angle of the target was essential to achieve good performance gain [44]. This is why they limited the viewing angle of the target to 2° where every 1° is assumed to be one hypothesis. There are only four hypotheses to choose from in this scenario. The results showed clear advantage for the MIMO waveform over flat-spectrum wideband waveform.

2.2.4 Probability Weighted Energy Waveforms

It is common for waveform design techniques to be matched to a single target and its features [45]. Therefore, for extended target detection, using these techniques is straightforward. This is achieved by only using that target deterministic or stochastic response, depending on the techniques and its assumptions, to design optimal detection waveform. However, when the objective is target identification, every target is assumed to have different response and all of them are to be considered when designing optimal waveforms.

The proposed solution for this problem is to create a weighted sum of target ensembles where

the weights can be, for example, the prior probabilities of the every target. In [36], the authors presented an MI-based waveform design strategy where single spectral variance of one target is used to design the optimal waveform in presence of signal-dependent interference. In order to apply that design procedure for multiple target identification problem, they suggested what they coined as probability-weighted spectral variance (PWSV) where the spectral variance of all target classes are weighted-summed using their prior probabilities which is updated at every design iteration assuming Bayesian representation of the channel and using an update rule.

PWSV estimation requires both calculation of an effective PSD and a costly search algorithm to generate a transmit waveform for each iteration [45]. After updating the prior probabilities, the PWSV is calculated using the estimated prior probabilities, which have to sum up to one if it is not [45], and using every spectral variance of target classes. Prior probabilities are estimated from the likelihood function of every hypothesis individually and then used to estimate the prior probability of every hypothesis. PWSV is then used as the single spectral variance which is required for obtaining optimal waveforms. After every transmission, the prior probabilities are updated and a new PWSV is expected calculated and used in designing the next adapted waveform.

The Probability-weighted energy (PWE) method on the other hand, computes the optimal waveform energy spectral density (ESD) function for each target ensemble and weight-sum the waveforms. The ESD of the optimal waveform at each iteration is the weighted sum of all energy density functions. This allows for every class ESD to be calculated in advance. Also, PWSV calculations require significantly more computations than ESD calculation as no mean ensemble is computed or subtracted from every class ensemble [37].

The new approach can also be applied to SNR-maximisation approach which in this case can be used to improve classification performance. In this approach (SNR-PWE), eigen-waveforms are designed based on every target ensemble and the optimal eigenwaveform at each iteration is the weighed sum of all eigenwaveforms of all classes. While eigenwave-forms are originally developed for maximising detection performance, the SNR-PWE (as the this approach is called) was shown to achieve better classification performance than all other techniques in high waveform energy regions[45].

In [46], the author used high fidelity target CAD models in the EM modelling software CST to generate practical target signatures and extended TFRs. The responses were used to test PWE techniques and its performance under angular uncertainty or without it against the performance of wideband waveform (WI). The PWE performance was shown to vary from passably to significantly better performance than WI waveform. The performance also varied with angle while PWE techniques performing better than WI in general. The results also showed that SNR-PWE sometime outperform MI-PWE and vice-versa. Finally, it was shown than PWSV performs better than PWE in some scenarios while requiring considerably more delay, between transmissions, for waveform design and updating probabilities in comparison to PWE.

The SNR-PWE in addition to MI-PWE were also shown to be useful in jammer nulling waveform design for high fidelity aircraft RCS responses. In [47], the author studied the sweep and base jammers and how PWE technique can be used to improve the target recognition performance in their presence. The results showed that jammer nulling PWE waveforms outperforms the other waveforms that does not null jamming interference while also outperforming WI. They also showed that the improvement varies and depend on properties of the jamming signal like its relative magnitude and the magnitude of the frequency response of the jammer. [47].

In [48], the authors applied the PWE in an automotive cognitive radar in a closed-loop adaptive framework. The application is for ground target identification in a forward-looking radar to identify vehicles autonomously. Two main cases were considered: i) to recognise target with deterministic TIR ii) to identify target class when angular uncertainty is present. PWE techniques were shown to outperform WI in the first case. Under angular uncertainty, however, the authors suggested an improved PWE techniques where the probability distribution of angular uncertainty are exploited for improved performance. TIRs, generated by CST (the computational electromagnetic tool) from high fidelity target CAD models, were also used here to validate results at two main frequency bands: 24-25 and 76-77 GHz. PWE in general performed better than WI in both main scenarios. The newly introduced waveform that exploit the knowledge about angular uncertainty were shown to vary in performance from being moderately to considerably better than WI [48].

2.2.4.1 Waveform Energy

Constraining the radar waveform energy to be constant is a common practice in a majority of the papers mentioned here or in the literature. It is also the main constraint used in this thesis.

In signals and systems theory, energy signals are signals with finite time and finite energy. The energy is given by:

$$\epsilon_x = \int_{-\infty}^{\infty} |x(t)|^2 \cdot dt \tag{2.1}$$

for the continuous-time signal $x(t)$ and by:

$$\epsilon_x = \sum_{n=-\infty}^{\infty} |x[n]|^2 \tag{2.2}$$

if $x[n]$ is a discrete-time signal.

If the discrete-time signal $x[n]$ is frequency transformed by discrete Fourier transform (DFT), then according to Parseval's theorem:

$$\sum_{n=0}^{m-1} |x[n]|^2 = \frac{1}{m} \sum_{k=0}^{l-1} |X[k]|^2 \tag{2.3}$$

where m is the number of length of the vector $\mathbf{x}$ containing the elements of $x[n]$, $X[k]$ is the DFT of $\mathbf{x}$ and l is the length of the DFT.

From (2.3), the energy of the vector X equals $m \times \epsilon_x$.

2.3 Linear and Fisher's Discriminant Analysis

In this section we outline some of the basic concepts of classification relevant to target identification in radars and the contributions presented in this thesis. target identification is about identifying the features that cluster targets into classes and then assign any target detected by the radar into the correct class of targets.

In the context of radars, discrimination is about identifying the level of interest of the target while classification is focused on threat category while identification is more specific in what the target is such as being a tank or an aircraft with specific model for example [49].

2.3.1 Linear Discriminant Analysis

Linear discriminant Analysis (LDA) is used when linear combinations of the data features can be used to separate two or more classes. By using TIRs and TFRs as the features of the target to be classified, we can:

- use LDA to design a linear classifier that assigns the target, based on its response, into the correct class
- study the classification performance for the proposed radar waveforms
- synthesize a design procedure to design the optimal waveform

LDA is perfect for classifying a data point into one of two Gaussian distributions with different mean vectors but with identical covariance matrices [17, 50]. In [17], we showed how the probability of misclassification can be expressed and directly minimised using LDA when the the two classes of targets share the same covariance matrix.

2.3.2 2-class Fisher Discriminant Analysis

When the mean vectors of two multivariate Gaussian distributions, of two classes of targets, are not identical especially when the covariance matrices are unequal, Fisher discriminant analysis is used to find the optimal projection for maximum classes mean separation and minimum class variance.

Fisher defined a classification separability function that captures how much separation between two multivariate Gaussian populations/distributions can be achieved and how classes variances can be decreased using the linear projection vector $\mathbf{w}$. The data is projected by $\mathbf{w}$ to a subspace where the classes have maximum Fisher separability.

Fisher formulated an optimisation problem to find the optimal linear projection vector $\mathbf{w}_{opt}$ that maximises the separability function while is well known and is dependent on the statistical properties of the two Gaussian distributions [50].

Maximising Fisher's separability should improve the classification performance as misclassification events is expected to become less probable as Fisher's separability increase. However, maximising Fisher's separability function does not guarantee minimum probability of misclassification. It can however, achieve higher classification performance than LDA in the different covariance matrices scenario.

Given two classes $\mathcal{H}_1$ and $\mathcal{H}_2$, two important covariance matrices are to be computed. $\mathbf{S}_W$ and $\mathbf{S}_B$ are the within-class and between-class scatter matrices respectively and are defined as follows:

$$\mathbf{S}_W = \sum_{k=1}^{2} \sum_{\mathbf{z} \in \mathcal{H}_k} (\mathbf{z} - \mathbf{m}_k)(\mathbf{z} - \mathbf{m}_k)^H \tag{2.4}$$

$$\mathbf{S}_B = (\mathbf{m}_1 - \mathbf{m_2})(\mathbf{m}_1 - \mathbf{m_2})^H \tag{2.5}$$

where:

$$\mathbf{m}_k = \frac{1}{n_k} \sum_{\mathbf{z} \in \mathcal{H}_k} \mathbf{z} \tag{2.6}$$

Fisher's separability is then given by:

$$\frac{\mathbf{w}^H \mathbf{S}_B \mathbf{w}}{\mathbf{w}^H \mathbf{S}_W \mathbf{w}} \tag{2.7}$$

The optimal $\mathbf{w}$ that maximises Fisher's separability is given by:

$$\mathbf{w} = (\mathbf{S}_W)^{-1}(\mathbf{m_1} - \mathbf{m_2}) \tag{2.8}$$

The new input $\mathbf{y}_{new}$ is then assigned to the class with the mean closest to $\mathbf{y}_{new}$ [50].

2.3.3 Multiclass Fisher Discriminant Analysis

When more than two classes with multivariate Gaussian distributions (with different mean vectors) are considered, projection the data into one dimensional subspace is not guaranteed to achieve the same performance as projecting the data in a multidimensional subspace [50].

In this scenario, an extended definition of Fisher separability is needed and the projection needs to be a projection to a subspace with dimensions at least greater than one. Thus, the projection vector is replaced with a projection matrix $\mathbf{W}$. The data is projected by $\mathbf{W}$ into a subspace where Fisher's separability is maximised. The dimensions of the subspace is determined by the prior knowledge about classes distributions and the number of subspaces is maximally less than the number of classes by one [50].

Classes separability can be estimated and by increasing the separability, the classification performance can be improved. Fisher separability, which inspired our objective function, utilises distances between means in addition to the confinement of every class's variance as the basis of its separability measure [50].

We denote each class by $\mathcal{H}_k$ where $k = 1, 2, ..., c$ and c is the number of classes. To define Fisher's function, two important matrices $\mathbf{S}_W$ and $\mathbf{S}_B$ should be defined first. Following the naming in [50], $\mathbf{S}_W$ and $\mathbf{S}_B$ are the within-class and between-class scatter matrices respectively and are defined as follows:

$$\mathbf{S}_W = \sum_{k=1}^{c} \sum_{\mathbf{z} \in \mathcal{H}_k} (\mathbf{z} - \mathbf{m}_k)(\mathbf{z} - \mathbf{m}_k)^H \tag{2.9}$$

$$\mathbf{S}_B = \sum_{k=1}^{c} n_k (\mathbf{m}_{k_i} - \mathbf{m})(\mathbf{m}_{k_i} - \mathbf{m})^H \tag{2.10}$$

where $\mathbf{z}$ is a data samples,

$$\mathbf{m}_k = \frac{1}{n_k} \sum_{\mathbf{z} \in \mathcal{H}_k} \mathbf{z} \tag{2.11}$$

$$\mathbf{m} = \frac{1}{c}\sum_{k=1}^{c}\mathbf{m}_k \tag{2.12}$$

where $\mathbf{m}_k$ is the sample mean vector of $\mathcal{H}_k$, $\mathbf{m}$ is the total sample mean vector of all classes, n_k is the number of data points from the class $\mathcal{H}_k$ while n_{total} is the total number of data samples.

Fisher's separability is then defined as follows:

$$\frac{|\mathbf{W}^H \mathbf{S}_B \mathbf{W}|}{|\mathbf{W}^H \mathbf{S}_W \mathbf{W}|} \tag{2.13}$$

where $\mathbf{W}$ is a transformation matrix which is designed to maximise the separability function The transformation matrix projects the random vector into a space where the means and covariances are different. For maximum separability, $\mathbf{W}$ is designed to project to a space where distances between all means are as large as possible and the covariances the lowest possible at the same time.

The matrix $\mathbf{W}$ is dependent on $\mathbf{S}_B$ and $\mathbf{S}_W$, both of which are dependent on the radar waveform in $\mathbf{\Omega}_X$. $\mathbf{W}$ is also dependent on the statistical properties of the target classes and subclasses which are known a priori.

Fisher's separability function is also extended to maximise the determinant of the projected between-class scatter matrix and minimise the determinant of the projected within-class scatter matrix. Scatter matrices can be replaced with the covariance matrices if known. Scatter matrices are an estimate of covariance matrices which are calculated form the data whenever covariance matrices are not available. Otherwise, scatter matrices can be calculated from data points. The projection matrix $\mathbf{W}$ is also a function of the between-class and within-class scatter matrices.

2.4 Signal model

Consider a scenario where a pulsed radar must assign a target, that has already been detected and hence its range and speed are known, into one of two classes based on its extended

response [2] using single pulse with an arbitrary radar waveform.

If the radar waveform is captured in the vector $\mathbf{x}$, the target extended impulse response is $\mathbf{r}$, the additive noise in the receiver is $\mathbf{n}$ while $\mathbf{c}$ is the clutter response signal; then the received complex signal $\mathbf{y}$ is given by:

$$\mathbf{y} = \mathbf{x} * \mathbf{r} + \mathbf{x} * \mathbf{c} + \mathbf{n} \tag{2.14}$$

where the length of $\mathbf{x}$ and $\mathbf{r}$ is m, the length of $\mathbf{n}$ is $2m-1$ and $*$ denotes the one-dimensional linear convolution operator.

By assuming the frequency snapshot model where we deal with all variables in the frequency domain [17, 32, 51], (2.14) will be given by:

$$Y = \mathbf{\Omega}_X R + \mathbf{\Omega}_X C + N + N \tag{2.15}$$

where R is the extended frequency response of the target; N is the frequency transformed noise vector; C is the frequency transformed clutter vector and $\Omega_X = \mathrm{diag}(X)$ is the diagonal matrix with the frequency transform of the radar waveform on its diagonal while Y, X, R, C and N are all $n_f \times 1$ vectors. n_f is the length of the frequency domain vectors.

Note, a frequency domain based processing is adopted here because from the point of view of mathematical derivations, it is easier to deal with diagonal matrices (especially for non-adaptive design scenarios), as in (2.15), than to deal with convolution matrices [14], e.g., in order to obtain closed-form expressions.

2.5 Summary

The chapter presented a review of radars and radar waveform design basics in addition to the literature of optimal radar waveform design for target identification and the relevant research. The chapter also reviewed relevant classification concepts like LDA and (Fisher discriminant analysis) FDA.

From this chapter, we concluded that the two main trends in the literature are to either design

waveforms adaptively or non-adaptively for optimal target identification. The chapter presented the differences between the two trends and the literature of both. We also concluded that angular uncertainty can cause significant drop in the classification performance and that waveform design methods should account for angular uncertainty. Finally, we presented the signal model adopted in the rest of the thesis.

The aim was to supplement the reader with the necessary background for clear understanding of the following chapters. The following technical chapters are focused on optimal non-adaptive frequency-based waveform design for target identification using Fisher discriminant analysis where angular uncertainty is present.

Chapter 3

Target Identification Using Optimised Waveform design in Noisy Environment

In this chapter, we consider the scenario where the radar system is designed to maximise target identification performance in the presence of noise and with no signal-dependent interference nor clutter present. We study the two main cases where the target class is to be identified from two or multiple classes. The chapter covers the non-adaptive radar waveform and receiver design for optimal target classification under angular uncertainty using extended target responses and the theory of Fisher discriminant analysis.

In this chapter, we propose new waveform design procedures and classification schemes to improve target identification performance non-adaptively in radar systems. The new designs and schemes are all inspired by 2-class and multiclass Fisher discriminant analysis. The 2-class scenario provide a simpler design procedure than the multiclass scenario especially when the number of classes is exactly two and accurate knowledge about target orientation is available.

The proposed system does not require as much computational capability as adaptive waveform design systems while also overcoming 1) angular uncertainty in classifying high fidelity targets and 2) drops in performance experienced by non-adaptive systems when classification is extended to more than two targets. The waveform design procedure is based on an optimization problem to find the waveform that maximises the objective function inspired by Fisher analysis under constant energy constraint. We also derive two closed-form solutions for the optimization problems under certain conditions for the 2-class and multiclass cases. All the methods are tested using synthetic and real data to show the performance of the proposed methods against the average Mahalanobis distance (AMD) non-adaptive waveform design and classifier. The results shown in this chapter were published in [16].

The chapter is divided as follows. In the first section, we define the frequency-based signal model and define and derive the expected statistical distributions of radar returns based on the signal model. In the second section, 1) we cover dividing target classes into angle-dependent subclasses for scenarios with large angular uncertainty 2) we derive the optimisation problem for radar waveform in the multiclass and 2-class scenarios using Fisher discriminant analysis 3) we derive optimal classifier for both scenarios 4) we derive closed-form solutions for extreme waveform energy scenario where expressing a closed-form solution for the optimisation problem is possible. Results and discussions are presented in the fourth section. Finally, in the last section, we summaries the chapter and conclude its contributions.

3.0.1 Statistical properties of Y

Assuming $R \sim \mathcal{CN}(M_k, \mathbf{\Sigma}_k)$ and $N \sim \mathcal{CN}(M_N, \mathbf{\Sigma}_N)$ and then: $Y \sim \mathcal{CN}(M_{Y_k}, \mathbf{\Sigma}_{Y_k})$ where:

$$M_{Y_k} = \mathrm{E}\{Y_k\} = \mathbf{\Omega}_X \mathrm{E}\{R_k\} + \mathrm{E}\{N\} = \mathbf{\Omega}_X M_k + M_N \tag{3.1}$$

$$\begin{aligned}
\mathbf{\Sigma}_{Y_k} &= \mathrm{E}\{(Y_k - \mathrm{E}\{Y_k\})(Y_k - \mathrm{E}\{Y_k\})^H\} \\
&= \mathrm{E}\{(\mathbf{\Omega}_X(R - M_k) + (N - M_N))(\mathbf{\Omega}_X(R - M_k) + (N - M_N))^H\} \\
&= \mathrm{E}\{\mathbf{\Omega}_X(R - M_k)(R - M_k)^H \mathbf{\Omega}_X^H + (N - M_N)(R - M_k)^H \mathbf{\Omega}_X^H \\
&\quad + \mathbf{\Omega}_X(R - M_k)(N - M_N)^H + (N - M_N)(N - M_N)^H\}
\end{aligned} \tag{3.2}$$

assuming R and N are uncorrelated, (3.2) becomes:

$$\begin{aligned}
\mathbf{\Sigma}_{Y_k} =& \mathbf{\Omega}_X \mathrm{E}\{(R - M_k)(R - M_k)^H\} \mathbf{\Omega}_X^H \\
&+ \mathrm{E}\{(N - M_N)(N - M_N)^H\} \\
=& \mathbf{\Omega}_X \mathbf{\Sigma}_k \mathbf{\Omega}_X^H + \mathbf{\Sigma}_N
\end{aligned} \tag{3.3}$$

where $\mathrm{E}\{\cdot\}$ is the expectation operator.

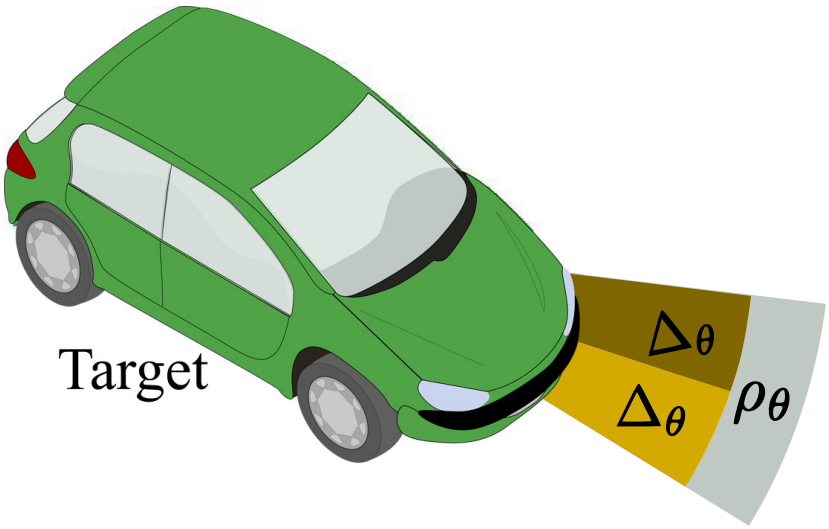

Figure 3.1: *Illustration of the total viewing angle range ρ_θ and subsectors width Δ_θ of a target (a car)*

3.1 Classes and Sub-Classes of Target Signatures

We assume each class consists of angle-dependent unique subclasses with stationary statistical properties and can be modelled as a complex Gaussian random vector. We then proceed to formulate the optimisation objective function for a multi-class problem. The objective function is then used to find the radar waveform that improves the classification performance while satisfying the energy constraint.

Assuming each class $\mathcal{H}_k$ is made up of subclasses $\mathcal{H}_{k_i}$ with $k = 1, 2, ..., c$ and $i = 1, 2, ..., l$ where i is the subclass number respectively. Every unique angular sector of a class is assigned to a subclass. Each sector is Δ_θ in width while the width of the combined sectors of a target is ρ_θ. see Fig. 3.1 for illustration. The total number of subclasses of all classes is $c \times l$.

Classes separability can be estimated and by increasing the separability, the classification performance can be improved. Fisher separability, which inspired our objective function, utilises distances between means in addition to the confinement of every class's variance as the basis of its separability measure [50].

To define Fisher's function, two important matrices $\mathbf{S}_W$ and $\mathbf{S}_B$ should be defined first. Following the naming in [50], $\mathbf{S}_W$ and $\mathbf{S}_B$ are the within-class and between-class scatter matrices

respectively and are defined as follows:

$$\mathbf{S}_W = \sum_{k=1}^{c} \sum_{i=1}^{l} \sum_{\mathbf{z} \in \mathcal{H}_{k_i}} (\mathbf{z} - \mathbf{m}_{k_i})(\mathbf{z} - \mathbf{m}_{k_i})^H \tag{3.4}$$

$$\mathbf{S}_B = \sum_{k=1}^{c} \sum_{i=1}^{l} n_{k_i} (\mathbf{m}_{k_i} - \mathbf{m})(\mathbf{m}_{k_i} - \mathbf{m})^H \tag{3.5}$$

where $\mathbf{z}$ is a data samples,

$$\mathbf{m}_{k_i} = \frac{1}{n_{k_i}} \sum_{\mathbf{z} \in \mathcal{H}_{1i}} \mathbf{z} \tag{3.6}$$

$$\mathbf{m} = \frac{1}{c \times l} \sum_{k=1}^{c} \sum_{i=1}^{l} \mathbf{m}_{k_i} \tag{3.7}$$

where n_{k_i} is the number of data points from the subclass $\mathcal{H}_{k_i}$ while n_{total} is the total number of data samples.

The objective function is then defined as follows:

$$\mathrm{f}(\mathbf{W}) = \frac{|\mathbf{W}^H \mathbf{S}_B \mathbf{W}|}{|\mathbf{W}^H \mathbf{S}_W \mathbf{W}|} \tag{3.8}$$

where $\mathbf{W}$ is a transformation matrix which is designed to maximise the objective function $\mathrm{f}(\mathbf{W})$. The transformation matrix projects the random vector into a space where the means and covariances are different. For maximum separability, $\mathbf{W}$ is designed to project to a space where distances between all means are as large as possible and the covariances the lowest possible at the same time.

The matrix $\mathbf{W}$ is dependent on $\mathbf{S}_B$ and $\mathbf{S}_W$, both of which are dependent on the radar waveform in $\mathbf{\Omega}_X$. $\mathbf{W}$ is also dependent on the statistical properties of the target classes and subclasses which are known a priori.

3.1.1 Derivation of The Objective Function for Multiple Classes ($c >= 2$) Problem

3.1.1.1 General solution

The within-class scatter matrix $\mathbf{S}_W$ is the sum of scatter matrices of all subclasses for all classes. For the objective function, we replace the scatter matrices with the covariance matrix of each subclass to get:

$$\begin{aligned}\mathbf{S}_W =& \sum_{k=1}^{c}\sum_{i=1}^{l}\left(\mathbf{\Omega}_X\mathbf{\Sigma}_{\mathcal{H}_{k_i}}\mathbf{\Omega}_X^H + \mathbf{\Sigma}_N\right) \\ =& \mathbf{\Omega}_X\left(\sum_{k=1}^{c}\sum_{i=1}^{l}\left(\mathbf{\Sigma}_{\mathcal{H}_{k_i}}\right)\right)\mathbf{\Omega}_X^H + (cl)\mathbf{\Sigma}_N\end{aligned} \tag{3.9}$$

The between-class scatter matrix $\mathbf{S}_B$ is dependent only on the waveform and the means of all subclasses. The mean of Y_{k_i}, assuming the noise mean M_N equals the zero vector, is $M_{Y_{k_i}}$ and is given by:

$$M_{Y_{k_i}} = \mathbf{\Omega}_X M_{k_i} \tag{3.10}$$

If we assume all subclasses are equiprobable, then:

$$\begin{aligned}\mathbf{S}_B =& \sum_{k=1}^{c}\sum_{i=1}^{l}(M_{Y_{k_i}} - M_A)(M_{Y_{k_i}} - M_A)^H \\ =& \sum_{k=1}^{c}\sum_{i=1}^{l}\mathbf{\Omega}_X(M_{k_i} - M_A)(M_{k_i} - M_A)^H\mathbf{\Omega}_X^H \\ =& \mathbf{\Omega}_X\mathbf{B}\mathbf{\Omega}_X^H\end{aligned} \tag{3.11}$$

where:

$$\mathbf{B} = \sum_{k=1}^{c}\sum_{i=1}^{l}(M_{k_i} - M_A)(M_{k_i} - M_A)^H \tag{3.12}$$

and

$$M_A = \mathbf{\Omega}_X M = \frac{1}{n_{total}} \sum_{k=1}^{c} \sum_{i=1}^{l} M_{Y_{ki}} \tag{3.13}$$

In order to formulate the objective function to be variable only in $\mathbf{\Omega}_X$, we need to find the optimal $\mathbf{W}$ that maximises the objective function in (3.8) which is also variable only in $\mathbf{\Omega}_X$. The optimal $\mathbf{W}$ is found first by finding generalised eigenvectors $\mathbf{v}_i$ corresponding to the non-zero eigenvalues of:

$$\mathbf{S}_W \mathbf{v}_i = \lambda_i \mathbf{S}_B \mathbf{v}_i \tag{3.14}$$

for $i = 0, 1, ..., n_\lambda - 1$ where n_λ is the number of the non-zero eigenvalues. The optimal $\mathbf{W}$ is then formed by arranging all the generalised eigenvectors as the columns of $\mathbf{W}$ as follows:

$$\begin{array}{ccccccc} \mathbf{W} & = & [& \mathbf{v}_0 & \mathbf{v}_1 & \cdots & \mathbf{v}_{n_\lambda - 1} \quad] \\ n_f \times n_\lambda & & & n_f \times 1 & n_f \times 1 & & n_f \times 1 \end{array} \tag{3.15}$$

the size of the rectangular optimal projection matrix $\mathbf{W}$ is then given by $n_f \times n_\lambda$ as shown in (3.15) while the size of $\mathbf{S}_W$ and $\mathbf{S}_B$ is $n_f \times n_f$ and n_f is the length of every data point. Note that if the matrix $\mathbf{S}_W$ is not singular, then the eigenvectors are conventional eigenvectors of the matrix $\mathbf{S}_W^{-1}\mathbf{S}_B$ and $n_\lambda = \mathrm{rank}\{\mathbf{S}_B\}$ [50]. All eigenvectors are orthogonal with unity energy (i.e. orthonormal)

The objective function $\mathrm{f}(\mathbf{W})$ can then be expressed in terms of waveform matrix $\mathbf{\Omega}_X$ (and other matrices that are constant) to become $\mathrm{g}(\mathbf{\Omega}_X)$ where:

$$\mathrm{g}(\mathbf{\Omega}_X) = \mathrm{f}(\mathbf{W})_{|\mathbf{W}=\mathbf{W}_{opt}(\mathbf{\Omega}_X)} \tag{3.16}$$

The constant energy constraint on the time-domain waveform is the optimisation constraints of choice. Its tractability is the main reason of choosing it.

The optimisation problem is then:

$$\begin{array}{ll} \underset{\mathbf{\Omega}_X}{\arg\max} & \mathrm{g}(\mathbf{\Omega}_X) \\ \mathrm{s.t.} & \mathrm{tr}(\mathbf{\Omega}_X \mathbf{\Omega}_X^H) = m\epsilon_x \end{array} \tag{3.17}$$

The waveform then can be designed by solving the optimisation problem. The solution is obtained using general optimisation solvers. In this thesis, the optimisation solver of choice is Mathwork's MATLAB global optimisation toolbox.

Algorithm 1 shows how to calculate $\mathrm{g}(\mathbf{\Omega}_X)$ from $\mathbf{\Omega}_X$ and $\mathbf{\Sigma}_N$. It is clear that the object function is dependent on many input that can affect the difficulty of the optimisation problem and the best optimisation algorithm to solve it. In this chapter, the optimisation software of choice is MathWorks's MATLAB using its Global Optimisation Toolbox and the algorithm of choice is Simulated Annealing. This will be discussed in details in section 3.2.

Algorithm 1 Calculate $\mathrm{g}(\mathbf{\Omega}_X)$ in multiclass scenario

Require: $\mathbf{\Omega}_X$ and $\mathbf{\Sigma}_N$ in addition to all classes mean vectors, covariance matrices
  Calculate $\mathbf{S}_W$ using equation (3.9)
  Calculate $\mathbf{S}_B$ using equation (3.11)
  $n_\lambda \Leftarrow \mathrm{rank}\{\mathbf{S}_B\}$
  if $\mathbf{S}_W$ is singular **then**
    $\mathbf{v}_0, \mathbf{v}_1, ..., \mathbf{v}_{n_\lambda} \Leftarrow$ the generalised eigenvectors $\mathbf{v}_i$ corresponding to the non-zero eigenvalues of equation (3.14)
  else
    $\mathbf{v}_0, \mathbf{v}_1, ..., \mathbf{v}_{n_\lambda} \Leftarrow$ the eigenvectors of the matrix expressed by $\mathbf{S}_W^{-1}\mathbf{S}_B$ corresponding to its non-zero eigenvalues.
  end if
  $\mathbf{W} \Leftarrow$ a matrix with $\mathbf{v}_0, \mathbf{v}_1, ..., \mathbf{v}_{n_\lambda}$ as its columns.
  $\mathrm{g}(\mathbf{\Omega}_X) \Leftarrow \dfrac{|\mathbf{W}^H \mathbf{S}_B \mathbf{W}|}{|\mathbf{W}^H \mathbf{S}_W \mathbf{W}|}$

3.1.1.2 Low SNR/Energy and Low Covariance (LELC) Solution Under AWGN

The general solution has a structure that implies that the optimisation problem is nonconvex. Also, the numerator and denominator of $\mathrm{g}(\mathbf{\Omega}_X)$ may both approach zero (in some scenarios) resulting in discontinuities in $\mathrm{g}(\mathbf{\Omega}_X)$ where the value of the objective function will be undefined. This necessitates the need for iterative methods to find the solution to the optimisation problem as no closed-form solution is expected. However, the objective function also implies that relation between $\mathbf{\Omega}_X(\sum_{k=1}^{c}\sum_{i=1}^{l}\mathbf{\Sigma}_{\mathcal{H}_{ki}})\mathbf{\Omega}_X^H$ and $(cl)\mathbf{\Sigma}_N$ influences the shape and behaviour of the multidimensional surface of $\mathrm{g}(\mathbf{\Omega}_X)$.

The low SNR/energy and low covariance (LELC) solution is derived for the case where the magnitude of every element in the signal term matrix $\mathbf{\Omega}_X(\sum_{k=1}^{c}\sum_{i=1}^{l}\mathbf{\Sigma}_{\mathcal{H}_{ki}})\mathbf{\Omega}_X^H$ is very low compared to the corresponding element in the noise term matrix $(cl)\mathbf{\Sigma}_N$. This is expected in three cases:

- Waveform energy is low
- Target covariance is low compared to noise variance
- All of the above

In other words, the LELC solution is expected to hold when:

$$\mathbf{S}_W \approx (cl)\mathbf{\Sigma}_N \tag{3.18}$$

and under AWGN, the equation becomes:

$$\mathbf{S}_W \approx \sigma_n^2(cl)\mathbf{I}_m \tag{3.19}$$

where σ_n^2 is the spectral noise variance.

Under LELC and AWGN assumptions, the optimal transformation matrix $\mathbf{W}$ will be dependent only on the eigenvectors corresponding to the largest non-zero eigenvalues of $\mathbf{S}_B$ as the matrix $\mathbf{S}_W^{-1}\mathbf{S}_B$ will become just a scaled version of $\mathbf{S}_B$ because of the result in (3.19). This means that the columns of the optimal $\mathbf{W}$ are the eigenvector of the non-zero eigenvalues of $\mathbf{S}_B$. Then, $\mathbf{v}_i$ for $i = 0, .., n_\lambda - 1$ are, in this scenario, the eigenvectors of $\mathbf{S}_B$.

From eigenvalues and eigenvectors theory [52], $\mathbf{S}_B$ can be expressed using its eigenvectors as: $\mathbf{S}_B = \sum_{i=0}^{n_\lambda-1}\lambda_i\mathbf{v}_i\mathbf{v}_i^H$ where λ_i is ith eigenvalue of $\mathbf{S}_B$. From matrix theory [52], every element α_{ij} in the matrix $\mathbf{W}^H\mathbf{S}_B\mathbf{W}$ can be expressed as: $\alpha_{ij} = \mathbf{v}_i^H(\sum_{i=0}^{n_\lambda-1}\lambda_i\mathbf{v}_i\mathbf{v}_i^H)\mathbf{v}_j$. Given that the eigenvectors are orthonormal, then:

$$\alpha_{ij} = \begin{cases} \lambda_i & i = j \\ 0 & i \neq j \end{cases} \tag{3.20}$$

It is clear that the matrix $\mathbf{W}^H\mathbf{S}_B\mathbf{W}$ (i.e. the matrix in the numerator of $\mathrm{g}(\mathbf{\Omega}_X)$ the objective function) is a diagonal matrix with the eigenvalues of $\mathbf{S}_B$ as its diagonal elements. $\mathbf{S}_B$ as shown from (3.11) and (3.12) equals $\mathbf{\Omega}_X\mathbf{B}\mathbf{\Omega}_X^H$.

From matrix theory, the diagonal elements of a diagonal matrix are also its eigenvalues and the determinant of any square matrix equals the product of all its eigenvalues. This mean that maximising the determinant of $\mathbf{S}_B$ will maximise the product of its eigenvalues and will results in maximising the $\mathrm{g}(\mathbf{\Omega}_X)$ which is the objective function.

Using $|\mathbf{\Omega}_X\mathbf{B}\mathbf{\Omega}_X^H| = |\mathbf{\Omega}_X||\mathbf{B}||\mathbf{\Omega}_X^H|$ [52], we can see that maximising $\mathrm{g}(\mathbf{\Omega}_X)$ is independent of B and only dependent on maximising $|\mathbf{\Omega}_X^H\mathbf{\Omega}_X|$ which is achieved by assigning all elements of X values with equal magnitudes regardless of phase. These conditions, of course, are ideally satisfied in the case of LFM or chirp signal.

Finally, the solution should be scaled by $\sqrt{m \times \epsilon_x}/\sqrt{\|X\|^2}$ to match the energy constraint using:

$$X_{scaled} = \sqrt{m \times \epsilon_x}\frac{X}{\sqrt{\|X\|^2}} \tag{3.21}$$

3.1.1.3 The Derivation of the Classifier

The classifiers in Fisher discriminant analysis, especially in multiclass problems, are based on minimum distance classifiers.

In the scenario of multiclass, the classifier should have subclasses' means and covariance matrices already transformed using the $\mathbf{W}_{opt}$ as follows:

$$\tilde{M}_{Y_{ki}} = \mathbf{W}_{opt}^H M_{Y_{ki}} = \mathbf{W}_{opt}^H\mathbf{\Omega}_X M_{k_i} \tag{3.22}$$

$$\begin{aligned}\tilde{\mathbf{\Sigma}}_{Y_{ki}} &= \mathbf{W}_{opt}^H\mathbf{\Sigma}_{Y_{ki}}\mathbf{W}_{opt} \\ &= \mathbf{W}_{opt}^H(\mathbf{\Omega}_X\mathbf{\Sigma}_{ki}\mathbf{\Omega}_X^H + \mathbf{\Sigma}_N)\mathbf{W}_{opt}\end{aligned} \tag{3.23}$$

where $\tilde{M}_{Y_{ki}}$ and $\tilde{\mathbf{\Sigma}}_{Y_{ki}}$ are the transformed subclass means and covariance matrices respectively.

Every received signal Y is transformed with $\mathbf{W}_{opt}^H$ into $\tilde{Y}$ and used to calculate the Maha-

lanobis distance for all classes. The Mahalanobis distance of the subclass i from class k from the received signal Y is then given by:

$$d_{k_i} = \sqrt{(\tilde{M}_{Y_{k_i}} - \tilde{Y})^H \tilde{\mathbf{\Sigma}}_{Y_{k_i}}^{-1} (\tilde{M}_{Y_{k_i}} - \tilde{Y})} \tag{3.24}$$

The subclass with the minimum distance to the received signal is then assigned. The corresponding class is the output decision of the classifier. Algorithm 2 shows in step-by-step how the classifier assign a target to a class from the received signal Y.

Algorithm 2 Identify target class from received signal Y in multiclass scenario

Require: Y, $\mathbf{\Omega}_X$ and $\mathbf{\Sigma}_N$ in addition to all classes mean vectors, covariance matrices
  Calculate $\mathbf{S}_W$ using equation (3.9)
  Calculate $\mathbf{S}_B$ using equation (3.11)
  $n_\lambda \Leftarrow \text{rank}\{\mathbf{S}_B\}$
  if $\mathbf{S}_W$ is singular **then**
    $\mathbf{v}_0, \mathbf{v}_1, ..., \mathbf{v}_{n_\lambda} \Leftarrow$ the generalised eigenvectors $\mathbf{v}_i$ corresponding to the non-zero eigenvalues of equation (3.14)
  else
    $\mathbf{v}_0, \mathbf{v}_1, ..., \mathbf{v}_{n_\lambda} \Leftarrow$ the eigenvectors of the matrix expressed by $\mathbf{S}_W^{-1}\mathbf{S}_B$ corresponding to its non-zero eigenvalues.
  end if
  $\mathbf{W}_{opt} \Leftarrow$ a matrix with $\mathbf{v}_0, \mathbf{v}_1, ..., \mathbf{v}_{n_\lambda}$ as its columns.
  $\tilde{Y} \Leftarrow \mathbf{W}_{opt}^H \mathbf{\Omega}_X Y$
  for $k = 1$ to c **do**
    for $i = 1$ to l **do**
      $\tilde{M}_{Y_{k_i}} \Leftarrow \mathbf{W}_{opt}^H \mathbf{\Omega}_X M_{k_i}$
      $\tilde{\mathbf{\Sigma}}_{Y_{k_i}} \Leftarrow \mathbf{W}_{opt}^H (\mathbf{\Omega}_X \mathbf{\Sigma}_{k_i} \mathbf{\Omega}_X^H + \mathbf{\Sigma}_N) \mathbf{W}_{opt}$
      $d_{k_i} \Leftarrow \sqrt{(\tilde{M}_{Y_{k_i}} - \tilde{Y})^H \tilde{\mathbf{\Sigma}}_{Y_{k_i}}^{-1} (\tilde{M}_{Y_{k_i}} - \tilde{Y})}$
    end for
  end for
  Assign target to the class k corresponding to the minimum d_{k_i}

3.1.2 The Derivation of The Objective Function for Two Classes ($c = 2$) with one subclass (i.e. $\rho_\theta = \Delta_\theta$) design problem

In the special case of applying the same principles to a 2-class problem where knowledge of the radar-target orientation is available (i.e. only one subclass per class), a different formula-

tion which leads to a simpler objective function can be implemented.

When the number of classes is only two, the projection matrix $\mathbf{W}$ is replaced with a projection vector $\mathbf{w}$. The optimal $\mathbf{w}$ is given by:

$$\mathbf{w}_{opt} = (\mathbf{S}_W)^{-1}\mathbf{\Omega}_X \Delta M \tag{3.25}$$

and the objective function is given by:

$$\begin{aligned} &\mathrm{g}(\mathbf{\Omega}_X) = \\ &\Delta M^H \mathbf{\Omega}_X^H \big(\mathbf{\Omega}_X(\mathbf{\Sigma}_{c_1} + \mathbf{\Sigma}_{c_2})\mathbf{\Omega}_X^H + 2\mathbf{\Sigma}_N\big)^{-1}\mathbf{\Omega}_X \Delta M \end{aligned} \tag{3.26}$$

Note, the complete derivation in addition to the derivation of the LELC solution and the classifier design are included in the appendix.

3.2 Results and Discussion

In this section, we present and discuss the simulation results, procedures and parameters used for all scenarios of interest.

3.2.1 The Two Classes Scenario ($c = 2$ and $l = 1$):

For this case, we assume that the knowledge of the radar-target orientation is perfectly available, and classes' means and covariances are known a priori. The waveform and classifier design of the special case of two classes is shown in the appendix.

The means and covariances were generated synthetically while the noise is assumed zero-mean AWGN with unity spectral variance. We used sixty-four frequency bins (i.e. $m = 64$) as the size of all vectors for targets responses and noise realisations. The target mean-vectors are generated arbitrarily. The covariance matrices of the target classes are chosen with eigenvalues ratio (EVR) less than one (i.e. non-isotropic or non-spherical covariance

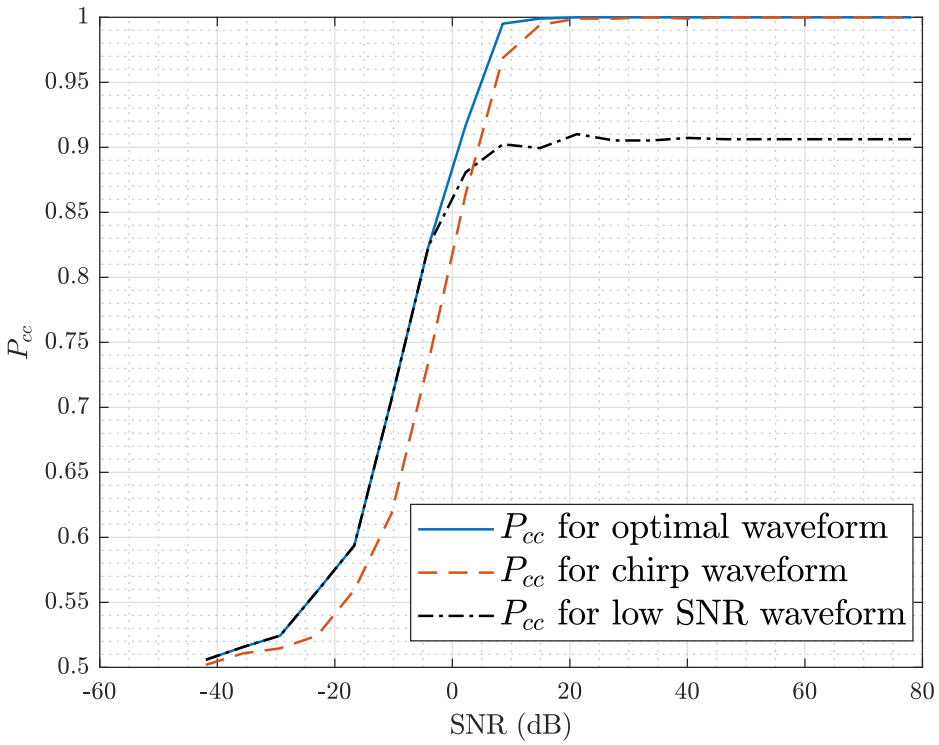

Figure 3.2: *Probability of correct classification vs SNR for Chirp/Wide-Band, low-SNR and optimal waveforms for 2-class scenario using synthetic data with 64 frequency bins target Frequency responses*

matrix) where:

$$\mathrm{EVR}(\mathbf{A}) = \min(\mathrm{eig}(\mathbf{A}))/\max(\mathrm{eig}(\mathbf{A})) \tag{3.27}$$

where $\mathrm{eig}(\mathbf{A})$ is a vector of the eigenvalues of the matrix $\mathbf{A}$. The noise covariance matrix of an AWGN has unity EVR. The performance is obtained using Monte Carlo simulation where at every SNR level, 10000 runs are performed. The SNR of radar returns is measured at the receiver.

The optimisation software of choice is MathWorks's MATLAB using its Global Optimisation Toolbox and the algorithm of choice is Simulated Annealing. This algorithm showed fast convergence through multiple trials. The objective function $\mathrm{g}(\mathbf{\Omega}_X)$ may contain multiple local maxima and may have points where it is undefined (e.g. when its numerator and denominator become zero). This makes it difficult for local optimisation algorithms to find the global maxima where the energy constraint is satisfied as well. Therefore, global optimisation algorithms are required to solve this optimisation problem.

Fig. 3.2 shows the classification performance where the minimum distance classifier is used, and the distance of choice is the Mahalanobis distance. The performance in Fig. 3.2 is for three waveforms vs signal-to-noise ratio (SNR). The waveforms are as follows:

- Proposed waveform obtained from solving the optimisation problem
- Chirp waveform representing wideband flat-spectrum waveforms which is the popular choice
- LELC waveform as derived in the Appendix

The plot shows that for an SNR below certain value (in this case 0 dB) the LELC waveform outperforms the chirp waveform. After that, the performance of LELC waveform saturates while the chirp's performance keeps improving. The figure also shows that the optimal waveform matches the performance of the LELC solution in the LELC region and then it outperforms the performance of the chirp until both waveforms reach perfect classification. This means that at LELC region, it is always better to design the waveform using the LELC solution as it attains the same performance as the optimal waveform with significantly less computational requirements. The LELC solution does not require an optimisation solver.

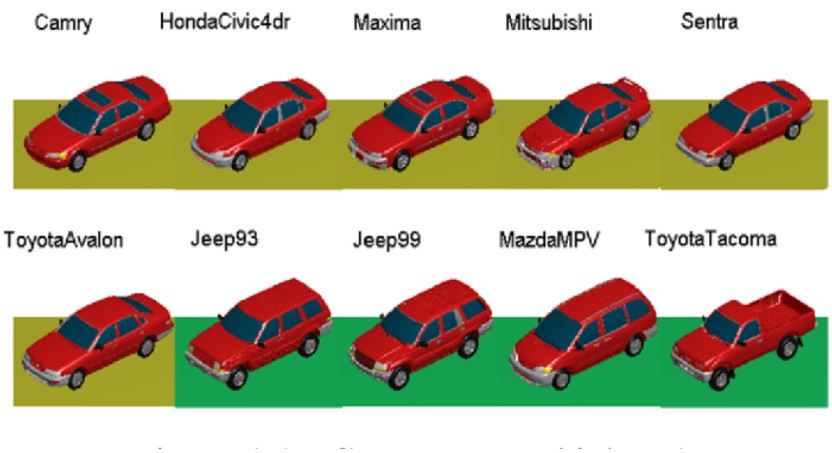

Figure 3.3: *CV domes vehicles [53]*

3.2.2 Multiple Classes Scenarios ($c > 2$):

For the next simulation, we move to the scenarios where more than two subclasses are to be classified. These scenarios include the two possible design problems where: 1) two targets are to be classified but each target is divided into more than one subclasses or 2) when more than two targets (classes) are to be classified. The waveform design and the classifier used in this scenario are based on the derivation in Section 3.1.1.

In this section, the synthetic data is replaced with the MSTAR CSV (civilian vehicles data dome) dataset. The dataset was collected by the Sensors Data Management System of the US Air Force [22]. The dataset contains X-band fully polarised far-field monostatic scattering data as complex TFRs at different azimuth and elevation angles for a total of ten civilian cars. The azimuth angular resolution of the data is setup to have 64 target frequency responses within 4°. The angular difference between target responses equals 0.0625°. The scattering data are frequency-domain based with 512 frequency samples from 6.9226 GHz to 12.2774 GHz. An image of all vehicles models are shown in Fig 3.3 from [53].

Note, the derivations made in this thesis are based on the assumption that TIRs/TFRs can be modelled as complex Gaussian random vectors. When real data such as MSTAR's dataset are used, we can expect some inconsistency to surface between the value of the objective function (classes' Fisher separability) and the corresponding estimated classification performance P_{cc}. This will become apparent in some of the scenarios in this section. In some scenarios, the

objective function of proposed waveforms will be higher than that of the chirp waveform whilst the latter waveform is outperforming the former in terms of P_{cc}.

We compare the solutions, derived in this chapter, to the non-adaptive waveform design and classifier proposed in [12–15, 27]. Throughout this thesis, the waveform suggested in these studies shall be referred to as average Mahalanobis distance (AMD) waveform. The reason behind this naming is because the waveform is designed to maximise the average Mahalanobis distance between classes when more than two classes are considered. The AMD waveform and classifier design provides the best classification performance over the other non-adaptive waveform design techniques found in the literature. It is only outperformed by the adaptive waveform design procedures especially when the number of classes is more than two or when angular uncertainty is assumed [18].

The main deferences between the AMD design and the proposed design are as follows:

- The processing is done in the time domain for the AMD design. The processing in the proposed method is done in the frequency domain
- Under angular uncertainty, AMD averages over all TIRs over multiple angles and designs the waveform as if the TIR is deterministic and its value is the mean vector of all TIRs. The proposed method assumes that the TIR is a realisation from a random vector with known mean vector and covariance matrix
- The proposed method classifier has a dimensionality reduction stage where the projection matrix $\mathbf{W}$ projects the received signal vector into a lower dimension subspace. No dimensionality reduction is done in the AMD classifier design
- The AMD waveform is designed to maximise the average Mahalanobis distance between classes. The proposed method maximises Fisher separability function which maximises the distance between classes while also minimises the within-class variance

Three waveform and receiver designs are to be compared in this section:

- The proposed waveform designed by solving the optimisation problem and the classifier design shown in section 3.1.1

- A chirp waveform while using the same classifier design for the proposed waveform. The chirp is a linear frequency modulated waveform that spans the same bandwidth as the other two waveforms.
- The AMD waveform and classifier design [12–15, 27]

The common simulation parameters and setup are shown in table 3.1.

Parameter	Value
Waveform energy	1
Number of frequency bins m	512
Noise	Complex AWGN with variance adjusted based on SNR
Clutter	No clutter
Number of Monte Carlo runs	1000

Table 3.1: *Table of common simulation parameters and setup*

3.2.2.1 Three targets with $\rho_\theta = 4^\circ$ and $\Delta_\theta = 1^\circ$ at an elevation angle $\theta_{el} = 30^\circ$

In this scenario we consider three targets from the civilian cars in the dataset. Namely, a Toyota Tacoma, a Mazda MPV and a 1999 Jeep. We limit the visible viewing angles of all targets to a 4° divided into 4 subsectors with an angular width of $\Delta_\theta = 1^\circ$. Because of target symmetry, this is equivalent to viewing 8° of each target. In this case, the total number of subclasses $l_{total} = c \times l = 3 \times 4 = 12$. Targets are viewed at an elevation angle of $\theta_{el} = 30^\circ$.

Fig. 3.4 shows the classification performance in terms of the probability of correct classification P_{cc} vs SNR for the three waveforms; the chirp wideband signal (which is also the LELC solution as concluded in Section 3.1.1.2), the proposed waveform in this chapter and the AMD waveform.

In this scenario, we notice none of the waveforms achieves unity P_{cc}. This is because at $\theta_{el} = 30^\circ$, the targets are at their highest possible fidelity in the available data. The proposed waveform while achieving higher objective function values as seen in table **??**, does not outperform that of the chirp waveform while both utilise the similar classifier design. However, the two waveforms appear to perform closely in this scenario unlike some other scenarios to

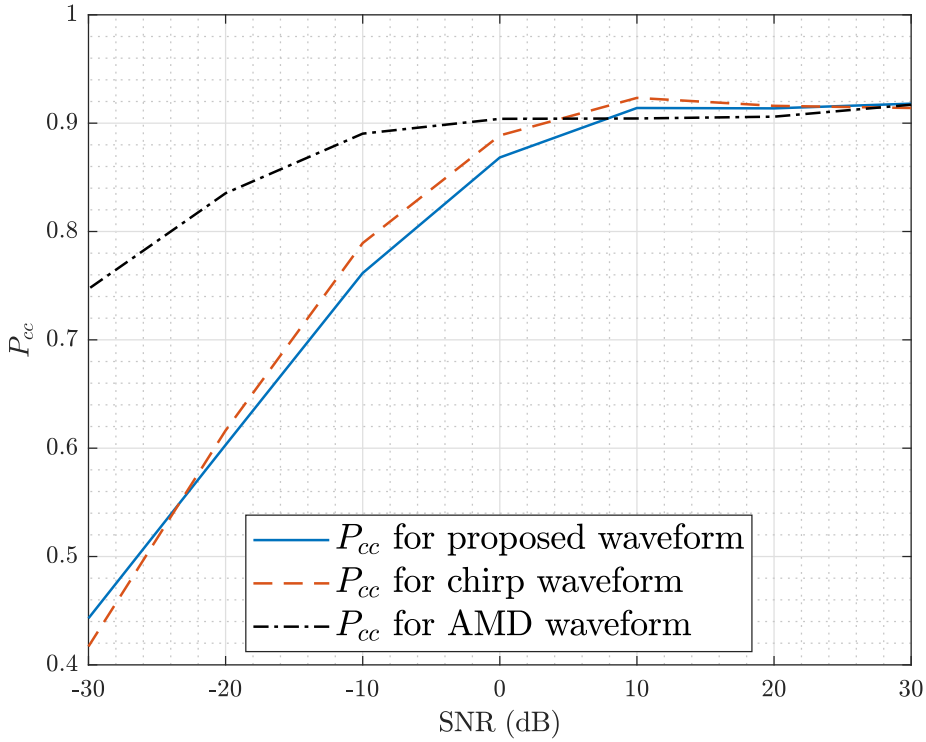

Figure 3.4: *Probability of correct classification P_{cc} vs SNR for three waveforms: The proposed waveform obtained from the optimisation problem in (3.17) in blue, the LFM/Chirp waveform in red, and the AMD waveform in black; for classifying a Toyota Tacoma, a Mazda MPV and a 1999 Jeep with $\rho_\theta = 4^\circ$ and $\Delta_\theta = 1^\circ$ at an elevation angle $\theta_{el} = 30^\circ$*

come. We also notice that, the AMD waveform outperforms the other two waveforms in the lower SNRs region.

In order to understand why AMD performs generally better at lower SNRs, the difference between the classifier required by the AMD strategy and the proposed classifier derived in section III-A3 should be discussed. Both classifiers are minimum distance classifiers. However, the proposed classifier has a dimensionality reduction stage while the AMD classifier does not. The proposed classifier transforms the received signal into a lower-dimensional subspace using $\mathbf{W}_{opt}$. The number of the dimensions (which is also the length of the transformed vectors) is dependent on the rank of the matrix $\mathbf{S}_B$. It is well known that the rank of $\mathbf{S}_B$ maximally equals the number of total subclasses minus one (i.e. $\mathrm{rank}\{\mathbf{S}_B\} \leq l_{total} - 1$). In the current scenario (with $l_{total} = 12$), we expect the rank of $\mathbf{S}_B$ to be less or equal to 11. This also implies that $\tilde{Y}$ and $\tilde{M}_{Y_{ki}}$ vectors would be of length 11 or less. Also, $\tilde{\mathbf{\Sigma}}_{Y_{ki}}$ would be a square matrix with size 11 or less. As the number of degrees of freedom of 11 is low compared to 512 degrees of freedom (time samples) utilised in AMD classification, we expect the maximum performance of the proposed waveform to fall faster than AMD waveform in low SNR regions.

3.2.2.2 Three targets with $\rho_\theta = 4^\circ$ and $\Delta_\theta = 1^\circ$ at an elevation angle $\theta_{el} = 60^\circ$

This scenario is similar to the previous scenario with the difference in the elevation angle changed to $\theta_{el} = 60^\circ$. This allows for a new view of the targets and more coherent responses as more persistent parts of the targets are almost always visible within the azimuth viewing angels.

In Fig. 3.5, P_{cc} vs SNRs of this scenario is shown for the three waveforms. We observe that, unlike the previous scenario, the performance of the proposed and the chirp waveform improved and reached perfect classification at SNRs equal or greater than 10dB. We attribute this improvement to targets realisations within Δ_θ becoming more coherent as you increase the elevation angle between the target and the radar system θ_{el}. The performance of the AMD waveform on the other hand saturates around $P_{cc} = 0.95$ with slight improvement in comparison to the previous scenario.

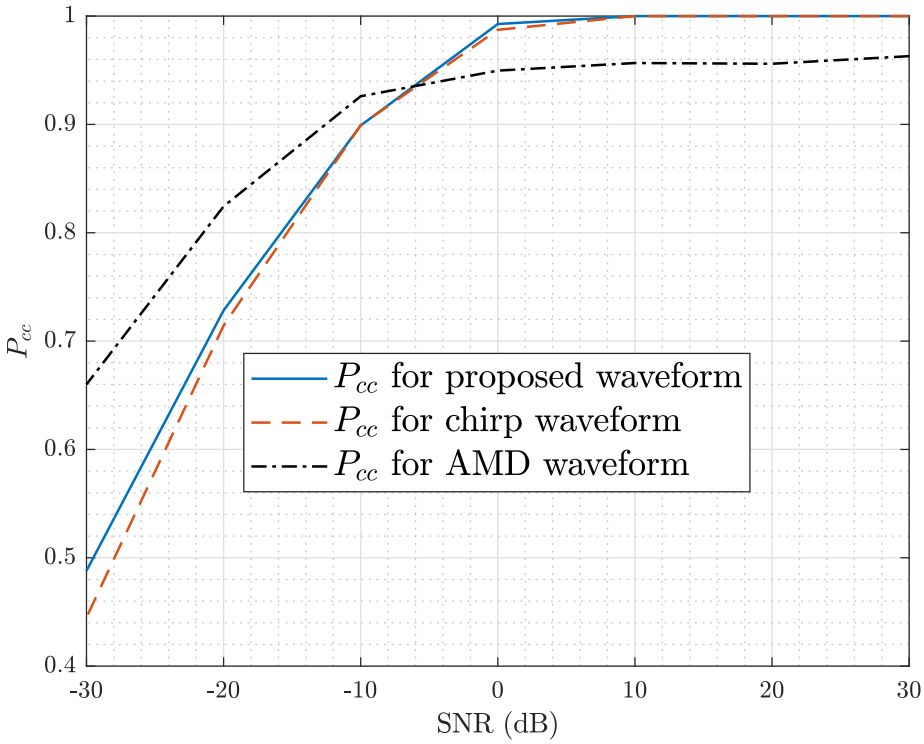

Figure 3.5: *P_{cc} vs SNR for three waveforms: The proposed waveform obtained from the optimisation problem in (3.17) in blue, the LFM/Chirp waveform in red, and the AMD waveform in black; for classifying a Toyota Tacoma, a Mazda MPV and a 1999 Jeep with $\rho_\theta = 4^\circ$ and $\Delta_\theta = 1^\circ$ at an elevation angle $\theta_{el} = 60^\circ$*

3.2.2.3 Three targets with $\rho_\theta = 8^\circ$ and $\Delta_\theta = 1^\circ$ at an elevation angle $\theta_{el} = 30^\circ$

In this scenario, we keep the choice of the targets and Δ_θ the same while increasing the viewing angle ρ_θ to 8° at $\theta_{el} = 30^\circ$. This allows us to observe the benefits of widening ρ_θ as well as increasing the number of subclasses. The total number of subclasses l_{total} in this scenario will be 24 subclasses.

Fig. 3.6 shows the performance of the three waveforms in this scenario in terms of P_{cc} vs SNRs. We notice that the performance of the AMD is slightly worse as the number of classes increase. On the other hand, the proposed waveform and the chirp performance improved. In this scenario, we also observe that the chirp waveform performs slightly better than the proposed waveform.

3.2.2.4 Three targets with $\rho_\theta = 8^\circ$ and $\Delta_\theta = 1^\circ$ at an elevation angle $\theta_{el} = 60^\circ$

We change θ_{el} in this scenario to 60° expecting performances to improve as realisations becomes more coherent.

In Fig 3.7, a slight improvement can be noticed in the performance of AMD waveform but not as noticeable as that of the two other waveforms. In this case, we can see the optimised waveform outperforms the chirp.

3.2.2.5 Three targets with $\rho_\theta = 16^\circ$ and $\Delta_\theta = 4^\circ$ at an elevation angle $\theta_{el} = 30^\circ$

In this scenario, we set $\rho_\theta = 16^\circ$ and divide the view into 4 subclasses with $\Delta_\theta = 4^\circ$. In this scenario with results shown in Fig. 3.8, we noticed a huge drop in the performance of the AMD waveform as the modelling each subclass with its mean becomes less accurate. We can see that both the chirp and the proposed waveform perform closely to each other and achieve perfect classification at high SNRs.

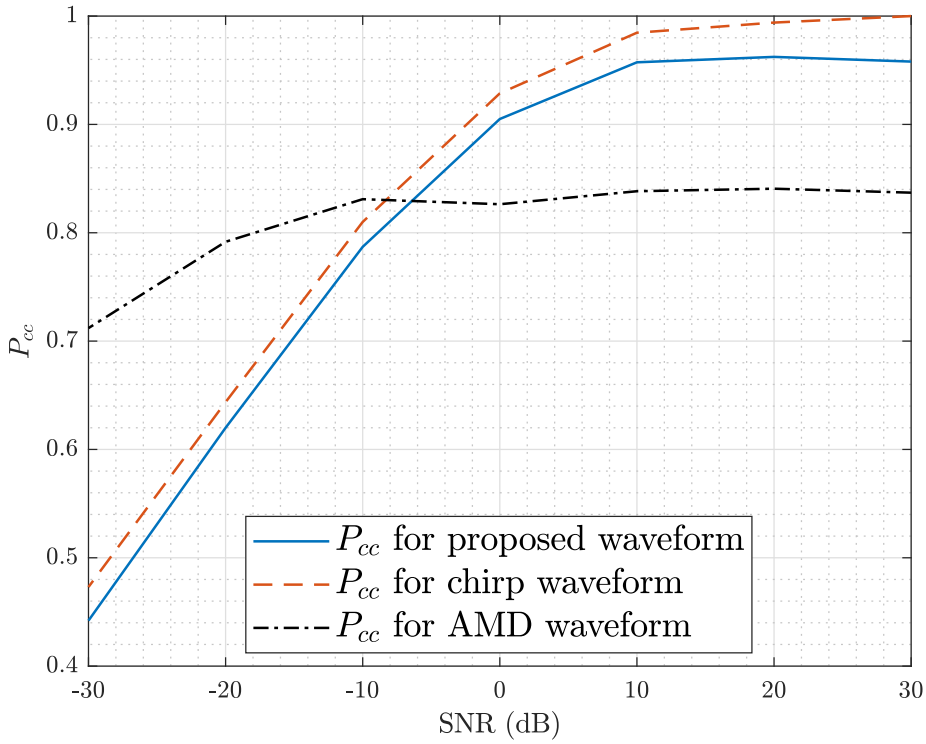

Figure 3.6: *P_{cc} vs SNR for three waveforms: The proposed waveform obtained from the optimisation problem in (3.17) in blue, the LFM/Chirp waveform in red, and the AMD waveform in black; for classifying a Toyota Tacoma, a Mazda MPV and a 1999 Jeep with $\rho_\theta = 8°$ and $\Delta_\theta = 1°$ at an elevation angle $\theta_{el} = 30°$*

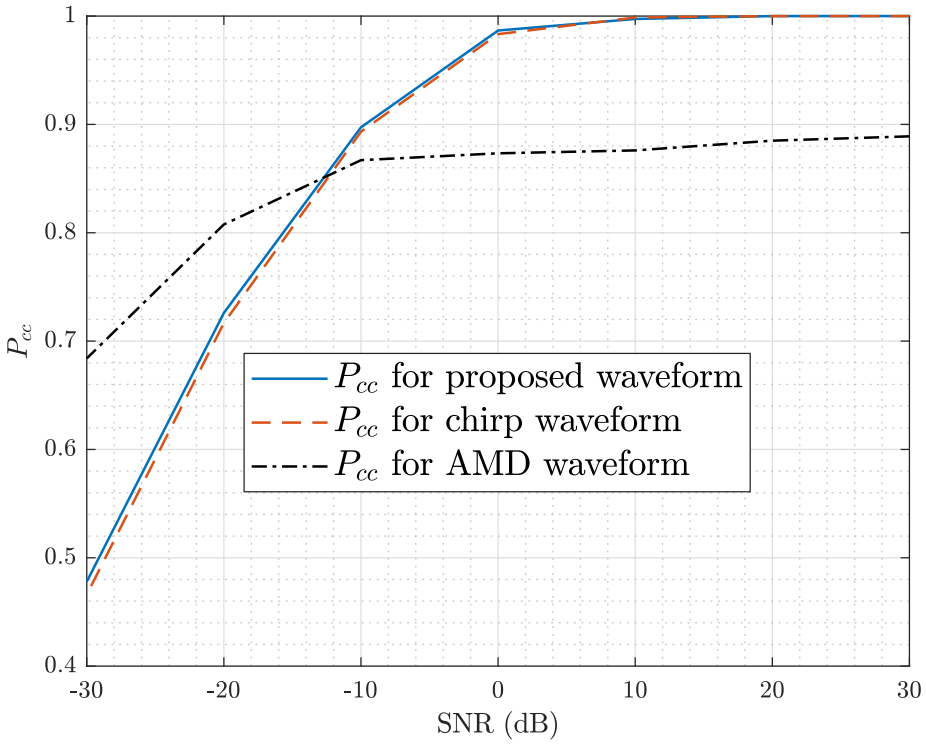

Figure 3.7: *P_{cc} vs SNR for three waveforms: The proposed waveform obtained from the optimisation problem in (3.17) in blue, the LFM/Chirp waveform in red, and the AMD waveform in black; for classifying a Toyota Tacoma, a Mazda MPV and a 1999 Jeep with $\rho_\theta = 8^\circ$ and $\Delta_\theta = 1^\circ$ at an elevation angle $\theta_{el} = 60^\circ$*

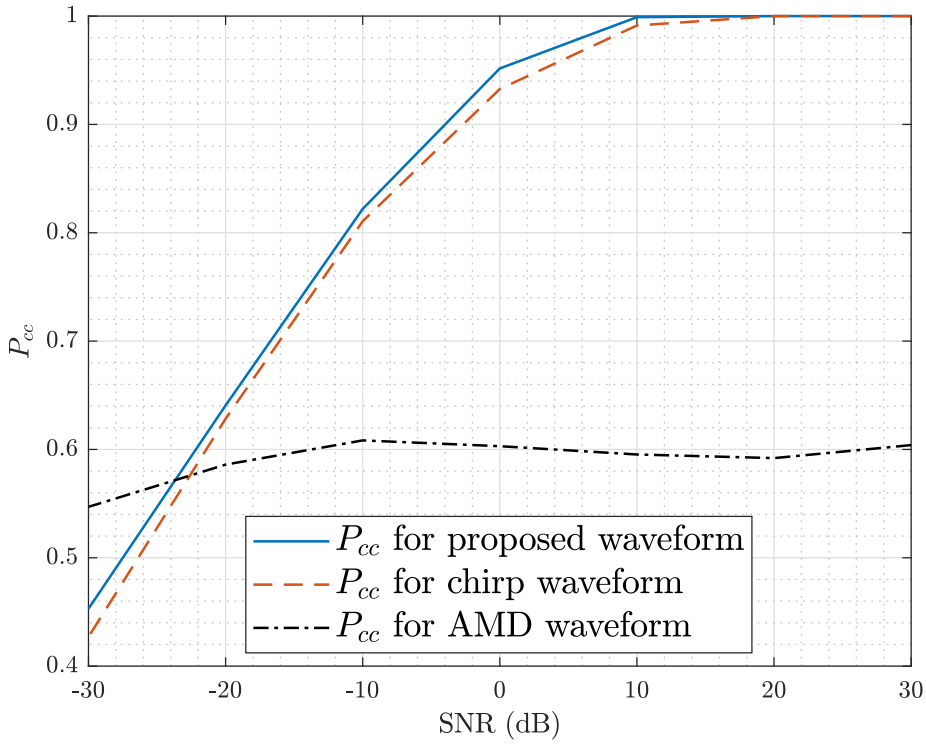

Figure 3.8: *P_{cc} vs SNR for three waveforms: The proposed waveform obtained from the optimisation problem in (3.17) in blue, the LFM/Chirp waveform in red, and the AMD waveform in black; for classifying a Toyota Tacoma, a Mazda MPV and a 1999 Jeep with $\rho_\theta = 16^\circ$ and $\Delta_\theta = 4^\circ$ at an elevation angle $\theta_{el} = 30^\circ$*

3.2.2.6 Three targets with $\rho_\theta = 16^\circ$ and $\Delta_\theta = 4^\circ$ at an elevation angle $\theta_{el} = 60^\circ$

Fig. 3.9 shows the performance in this scenario where θ_{el} is 60°. Again, an insignificant improvement to the AMD performance is observed while it is performing poorly as is the case in the previous scenario. On the other hand, the chirp signal performs closely to the optimised waveform for a majority of SNRs and then fall behind and saturates around $P_{cc} = 0.9$ at high SNR values.

3.2.2.7 Different three targets with $\rho_\theta = 4^\circ$ and $\Delta_\theta = 1^\circ$ at an elevation angle $\theta_{el} = 30^\circ$

In this scenario, we go with similar simulation setup as the first scenario where $\rho_\theta = 4^\circ$, $\Delta_\theta = 1^\circ$ and $\theta_{el} = 30^\circ$ but for different targets. The target classes in this case are: a Toyota Avalon, a Sentra and a Mitsubishi. Fig. 3.10 shows the simulation results for this scenario. The results show how different the results can be than those before, but the trends are almost the same. The AMD waveform and its classifier are underperforming in compare to the previous results. The proposed waveform is shown to perform better achieving $P_{cc} = 1$ but the chirp waveform seems to perform almost the same.

3.2.2.8 Varying Δ_θ while $\rho_\theta = 4^\circ$ at an elevation angle $\theta_{el} = 60^\circ$ with same targets

In this scenario, we repeat the same previous scenario but with $\theta_{el} = 60^\circ$ while varying Δ_θ (sector's angular width) to $1^\circ, 2^\circ$ and 4° to observe how Δ_θ affects the performance of the optimal waveform and AMD waveform.

Fig. 3.11 shows the performance of the proposed and AMD waveform vs SNR at three different values of Δ_θ while $\rho_\theta = 4^\circ$. The line width of each line in the figure corresponds to the values of Δ_θ which are $1^\circ, 2^\circ$ and 4°. We notice that the performance of the optimal waveform improves as Δ_θ is increased. This can be due to the improvement in estimating the distribution of the TFR in each sector as the number of data points increases. On the other hand, while not very large, we notice a degradation in the performance of AMD waveform as Δ_θ is increased. As AMD waveform and classifier rely on averaging responses under angular uncertainty, increasing Δ_θ is expected to make TFRs and TIRs within each sector more

random leading to the assumption that a simple mean is not enough to capture its statistics.

3.3 Conclusions

The chapter have proposed non-adaptive waveform designs and classification schemes to improve radar's target identification performance. The new designs and classifiers are inspired by 2-class and multiclass Fisher discriminant analysis. Fisher's separability function in both analysis is used to formulate the optimisation problem. The optimal waveform is then designed using the optimisation problem. The optimisation problems can be solved using general optimisation software but also, the chapter introduces derived closed-form solutions under LELC conditions. The methods were tested against the non-adaptive waveform AMD design from [13–15] and its classifier. The simulation was conducted using the MSTAR CV dataset in different scenarios and assumptions. We observe that, the new designs and schemes performs better than the AMD waveform especially in high SNR regions. The effect of using real data in simulations appeared as inconsistencies between the relative performance of the waveforms and the values of their objective functions. We conclude that, the proposed designs improve target identification performance under angular uncertainty. The designs are also offline where all the calculations and computations can be done a priori while achieving improved performance. The closed-form solutions in LELC region also shown to achieve comparable performance to optimised designs which lowers the computational requirements.

The chapter have covered the new design procedures in a clutter-free environment. In the next chapter, clutter is introduced in the signal model and closed-form solution for more general scenarios is derived.

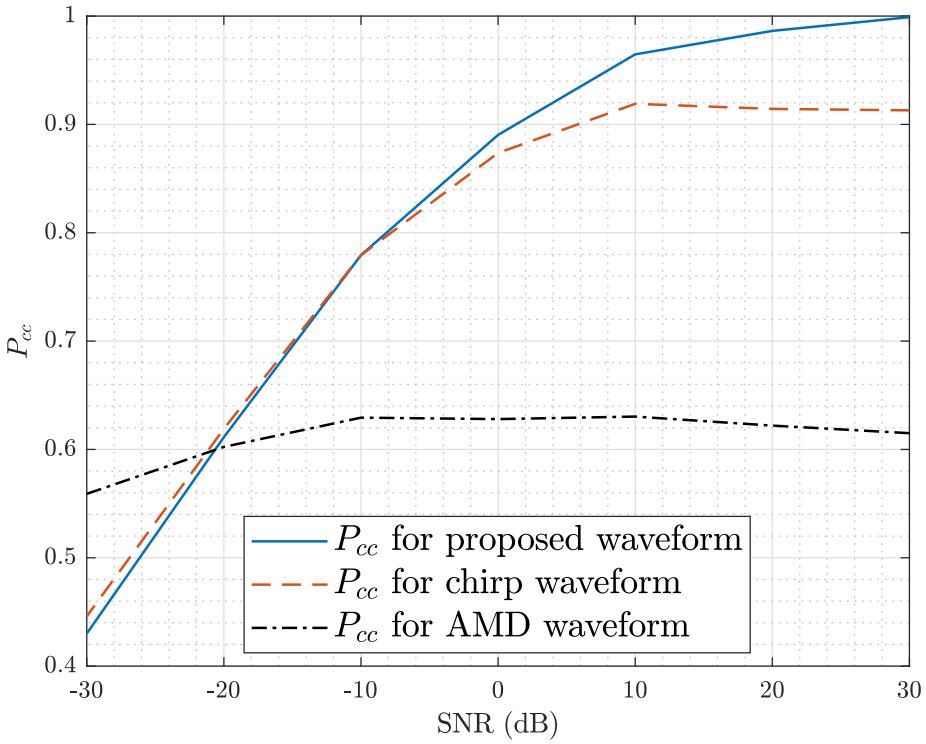

Figure 3.9: *P_{cc} vs SNR for three waveforms: The proposed waveform obtained from the optimisation problem in (3.17) in blue, the LFM/Chirp waveform in red, and the AMD waveform in black; for classifying a Toyota Tacoma, a Mazda MPV and a 1999 Jeep with $\rho_\theta = 4^\circ$ and $\Delta_\theta = 1^\circ$ at an elevation angle $\theta_{el} = 60^\circ$*

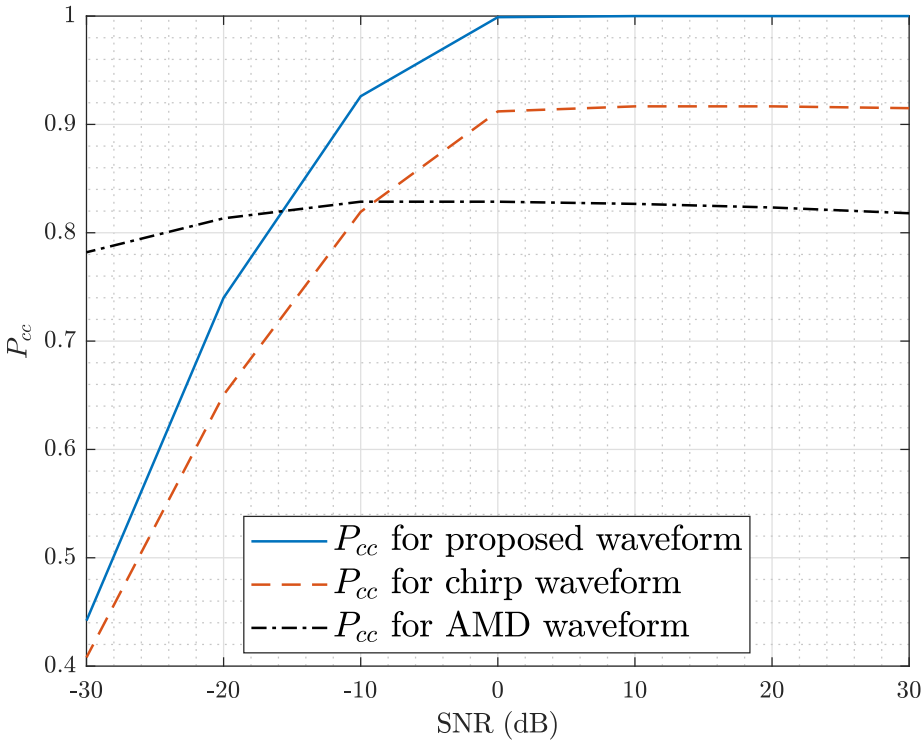

Figure 3.10: *P_{cc} vs SNR for three waveforms: The proposed waveform obtained from the optimisation problem in (3.17) in blue, the LFM/Chirp waveform in red, and the AMD waveform in black; for classifying a Toyota Avalon, a Sentra and a Mitsubishi with $\rho_\theta = 4^\circ$ and $\Delta_\theta = 1^\circ$ at an elevation angle $\theta_{el} = 30^\circ$*

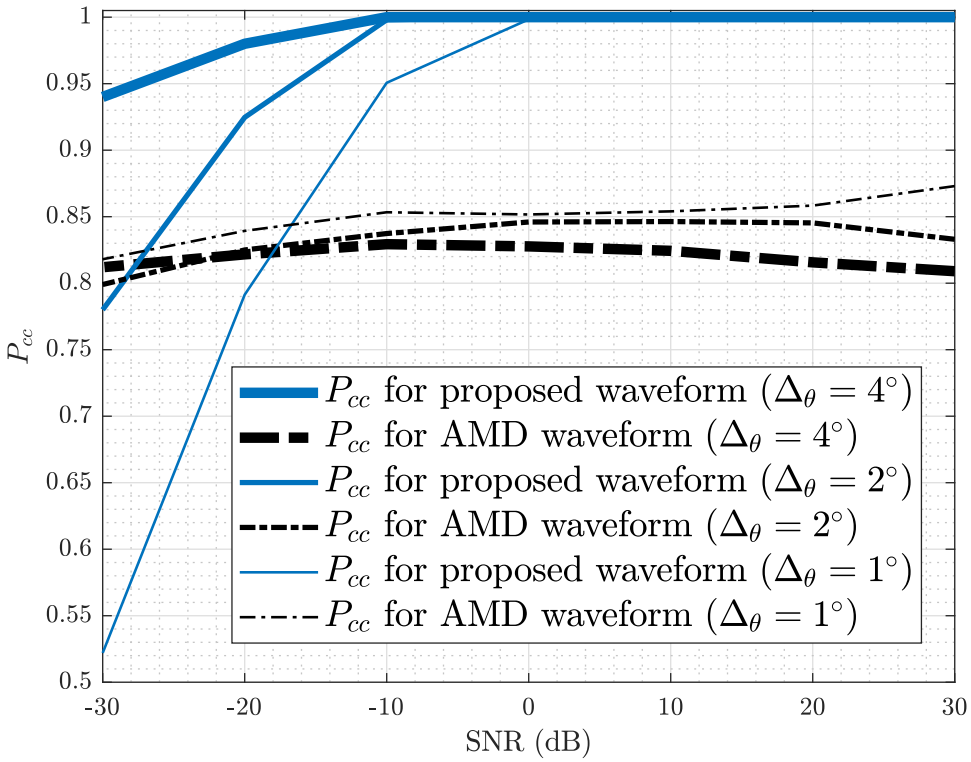

Figure 3.11: *P_{cc} vs SNR for two waveforms: The proposed waveform obtained from the optimisation problem in (3.17) in blue and the AMD waveform in black for $\Delta_\theta = 1°, 2°$ and $4°$; for classifying a Toyota Avalon, a Sentra and a Mitsubishi with $\rho_\theta = 4°$ at an elevation angle $\theta_{el} = 30°$. Note that the line width corresponds to the value of Δ_θ*

Chapter 4
Target Identification Using Closed-form Radar Waveform Design in Presence of Signal-dependent Interference

In this chapter, we consider another scenario where the waveform is designed to optimise target identification in the presence of both signal-dependent and signal-independent interferences. The chapter focuses on waveform design for optimal classification of targets with extended responses in two main scenarios: 1) when classes share the same covariance matrix; 2) when the matrices are different. The design methods presented in the previous chapter result in optimisation problems with no closed-form solutions unless the problem is designed in the LELC regions. These design problems require using numerical optimisation algorithms to solve. In this chapter, we cover the derivation of a closed-form solution for the two main scenario that is valid in all waveform energy levels.

In this chapter, we introduce a closed-form frequency-based solution to the problem of radar waveform design to maximise binary target identification. The proposed solution achieves performance levels comparable to the most optimal waveform in the literature while incurring low computational complexity in comparison to the optimal waveform. The proposed solution is applicable for the two main classification scenarios where the extended target frequency responses (TFRs) are complex, random and normally distributed with unequal mean vectors but their covariance matrices are either 1) identical or 2) different. We expand on these two main scenarios by introducing clutter (signal-dependent interference) in the signal model and studying possible closed-form designs in extreme waveform energy levels. We test the closed-form solution against the available optimal waveforms. The proposed closed-form solution is shown to attain very close performance as that of the optimal waveform without requiring the same computational time and complexity. Simulations are conducted using data synthetically generated in addition to the Civilian Vehicle Data from MSTAR dataset. Initial

results from this chapter were published in [17]. The complete account of the results in this chapter will formed the basis of the second journal submission.

The chapter is divided into four main sections. The first section introduces the new signal model and the updated statistical properties of radar returns. The second section focuses on 1) deriving the objective function and optimisation problems for the two main scenarios 2) expressing the optimal classifier design 3) deriving the waveform design problems based on the optimisation problems in extreme waveform energy levels in addition to deriving the closed-form solution for both main scenarios. The third section is about presenting and discussing the results. The last section is summary.

4.1 Signal Model

4.1.1 Signal Model and Statistical Properties

In this chapter, clutter is not neglected and the signal model defined in chapter 2 is assumed. We assume that the target frequency response, the clutter and the noise are all random with known statistical properties. The vectors R_i, C and N are realisations from complex-valued Gaussian random fields with known means and covariance matrices where R_i is the target frequency response from the class indexed with i for $i = 1, 2$.

Given that the vectors are distributed as follows:

$$R_i \sim \mathcal{CN}(M_{R_i}, \mathbf{\Sigma}_{R_i}) \text{ for } i = 1, 2 \tag{4.1}$$

$$C \sim \mathcal{CN}(M_0, \mathbf{\Sigma}_C) \tag{4.2}$$

$$N \sim \mathcal{CN}(M_0, \mathbf{\Sigma}_N) \tag{4.3}$$

where M_0 is an all-zero vector and assuming that R_i, C and N are all uncorrelated, then, the statistical distribution of Y for the ith class is given by:

$$Y_i \sim \mathcal{CN}(M_{Y_i}, \mathbf{\Sigma}_{Y_i}) \tag{4.4}$$

where:

$$M_{Y_i} = \mathbf{\Omega}_X M_{R_i} \tag{4.5}$$

and

$$\mathbf{\Sigma}_{Y_i} = \mathbf{\Omega}_X(\mathbf{\Sigma}_{R_i} + \mathbf{\Sigma}_C)\mathbf{\Omega}_X^H + \mathbf{\Sigma}_N \tag{4.6}$$

4.2 The Proposed Method

4.2.1 The Objective Function

Given the statistical distributions of Y, the classifier is to be designed to assign the radar return Y_i (aka the data point) to one of two classes with different mean vectors and identical or non-identical covariance matrices. The classifier design depends on the objective function and whether the covariance matrices, $\mathbf{\Sigma}_{R_1}$ and $\mathbf{\Sigma}_{R_2}$, are identical or not.

4.2.1.1 Target Classes with Different Means and Identical Covariance Matrices

In this scenario where two class's distributions share the same covariance matrix with different mean vectors, it is possible to derive a closed-form direct measure of the classification performance, i.e. the probability of misclassification. This allows us to calculate the theoretical performance of the waveform if we are employing the same classifier defined in the derivation. It also allows for comparing the theoretical performance of a waveform against the measured performance obtained using Monte-Carlo simulations. Two targets can have identical covariance matrices if viewed from an angle where they are very similar or share the same source of fluctuation. In this scenario, it is possible to express the probability of misclassification in closed-form.

The classification problem is defined as follows:

- An already detected target with extended impulse/frequency response is to be classified into one of two classes (Binary classification problem)
- i is the class identifier for $i = 1, 2$

- ω_i is the *state of nature* of the target [50]
- All statistical properties of all classes are known a priori
- $M_{Y_1} = \mathbf{\Omega}_X M_{R_1} \neq M_{Y_2}$
- $\mathbf{\Sigma}_{Y_1} = \mathbf{\Omega}_X(\mathbf{\Sigma}_{R_1} + \mathbf{\Sigma}_C)\mathbf{\Omega}_X^H + \mathbf{\Sigma}_N = \mathbf{\Sigma}_{Y_2}$
  $= \mathbf{\Omega}_X(\mathbf{\Sigma}_{R_2} + \mathbf{\Sigma}_C)\mathbf{\Omega}_X^H + \mathbf{\Sigma}_N = \mathbf{\Sigma}_Y$

We can write the minimum-error-rate discriminant function $g_i(Y)$ suited for this scenario as [50]:

$$\begin{aligned} g_i(Y) =& \ln p(Y|\omega_i) + \ln P(\omega_i) \\ =& -(Y - M_{Y_i})^H \mathbf{\Sigma}_Y^{-1}(Y - M_{Y_i}) \\ & - m\ln\pi - \ln|\mathbf{\Sigma}_Y| + \ln P(\omega_i) \end{aligned} \tag{4.7}$$

where $p(Y|\omega_i)$ is the likelihood function of Y given ω_i and $P(\omega_i)$ is the prior probability. If the prior probabilities for all classes are identical (i.e. $P(\omega_1) = P(\omega_2) = 0.5$), it is straightforward to derive the minimum-error-rate classifier and the best hyperplane for classification by rearranging the linear function: $g_1(Y) = g_2(Y)$ which results in the following equation:

$$\begin{aligned} & \Re\{W^H Y + w_0\} = g_1(Y) - g_2(Y) \\ & \Re\{(M_{Y_1} - M_{Y_2})^H \mathbf{\Sigma}_Y^{-1} Y + \frac{M_{Y_2}^H \mathbf{\Sigma}_Y^{-1} M_{Y_2} - M_{Y_1}^H \mathbf{\Sigma}_Y^{-1} M_{Y_1}}{2}\} \\ & = 0 \end{aligned} \tag{4.8}$$

where the weight vector $W = \mathbf{\Sigma}_Y^{-1}(M_{Y_1} - M_{Y_2})$ and the scalar bias w_0 is given by $w_0 = (M_{Y_2}^H \mathbf{\Sigma}_Y^{-1} M_{Y_2} - M_{Y_1}^H \mathbf{\Sigma}_Y^{-1} M_{Y_1})/2$.

The probability of misclassification can be calculated given the distribution of the classifier function in (4.8) which is defined as:

$$f(Y) = (M_{Y_1} - M_{Y_2})^H \mathbf{\Sigma}_Y^{-1} Y + \frac{M_{Y_2}^H \mathbf{\Sigma}_Y^{-1} M_{Y_2} - M_{Y_1}^H \mathbf{\Sigma}_Y^{-1} M_{Y_1}}{2} \tag{4.9}$$

using the equation:

$$P_{mc} = p(\Re f(Y) \leq 0|\omega_1)P(\omega_1) + p(\Re f(Y) > 0|\omega_2)P(\omega_2) \tag{4.10}$$

where: $f(Y) \sim \mathbb{CN}(\mu_{fi}, \sigma_f^2)$ for $i = 1, 2$. The mean μ_{fi} can be derived as follows:

$$\begin{aligned} \mu_{fi} &= \mathbb{E}\{f(Y)|\omega_i\} \\ &= (M_{Y_1} - M_{Y_2})^H \mathbf{\Sigma}_Y^{-1} M_{Y_i} + \frac{M_{Y_2}^H \mathbf{\Sigma}_Y^{-1} M_{Y_2} - M_{Y_1}^H \mathbf{\Sigma}_Y^{-1} M_{Y_1}}{2} \end{aligned} \tag{4.11}$$

and similarly, the variance σ_f^2:

$$\begin{aligned} \sigma_f^2 &= \mathbb{E}\{(f(Y) - \mathbb{E}\{f(Y)\})(f(Y) - \mathbb{E}\{f(Y)\})^H\} \\ &= (M_{Y_1} - M_{Y_2})^H \mathbf{\Sigma}_Y^{-1} (M_{Y_1} - M_{Y_2}) \end{aligned} \tag{4.12}$$

Also, it can be shown that $\Re\mu_{f1} = +\sigma_f^2/2$ and $\Re\mu_{f2} = -\sigma_f^2/2$. Then,

$$\begin{aligned} &p(\Re f(Y) \leq 0|\omega_1) = \\ &\qquad \int_{-\infty}^{0} \int_{-\infty}^{\infty} \xi(\Re f(Y))\xi(\Im f(Y)) \cdot \mathrm{d}\Im f(Y) \cdot \mathrm{d}\Re f(Y) \end{aligned} \tag{4.13}$$

and,

$$\begin{aligned} &p(\Re f(Y) > 0|\omega_2) = \\ &\qquad \int_{0}^{\infty} \int_{-\infty}^{\infty} \xi(\Re f(Y))\xi(\Im f(Y)) \cdot \mathrm{d}\Im f(Y) \cdot \mathrm{d}\Re f(Y) \end{aligned} \tag{4.14}$$

where: $\xi(x) = \dfrac{1}{\sqrt{\pi\sigma_x^2}} \exp\{-\dfrac{(x - m_x)^H (x - m_x)}{\sigma_x^2}\}$.

By solving the integration by substitution in addition to employing the definition of the Q-function,

$$p(\Re f(Y) \leq 0\}|\omega_1) = \mathrm{Q}(+\sqrt{2}\Re\mu_{f1}/\sigma_f) \tag{4.15}$$

$$p(\Re f(Y) > 0\}|\omega_2) = \mathrm{Q}(-\sqrt{2}\Re\mu_{f2}/\sigma_f) \tag{4.16}$$

it can be shown that

$$P_{mc} = \mathrm{Q}\Big(\sqrt{(M_{Y_1} - M_{Y_2})^H \mathbf{\Sigma}_Y^{-1} (M_{Y_1} - M_{Y_2})/2}\Big) \tag{4.17}$$

While P_{mc} can be used as the objective function that should be minimised to maximise the

classification performance, we can also make use of the properties of the Q-function and the square root function to further reduce the optimisation problem objective to only maximise the term inside the square-root in (4.17) which is $(M_{Y_1} - M_{Y_2})^H \mathbf{\Sigma}_Y^{-1} (M_{Y_1} - M_{Y_2})$.

The optimisation problem is then:

$$\begin{aligned} \underset{\mathbf{\Omega}_X}{\arg\max} \quad & \mathrm{g}_1(\mathbf{\Omega}_X) = (M_{Y_1} - M_{Y_2})^H \mathbf{\Sigma}_Y^{-1} (M_{Y_1} - M_{Y_2}) \\ \text{s.t.} \quad & \mathrm{trace}(\mathbf{\Omega}_X \mathbf{\Omega}_X^H) = m\epsilon_x \end{aligned} \tag{4.18}$$

where ϵ_x is the energy of the time-domain waveform in $\mathbf{x}$.

4.2.1.2 Target Classes with Different Means and Different Covariance Matrices

In this scenario, the two distribution have different mean vectors and covariance matrices which makes the derivation of the probability of misclassification a challenging problem.

In this scenario,

- An already detected target with extended impulse/frequency response is to be classified into one of two classes (Binary classification problem)
- i is the class identifier for $i = 1, 2$
- All statistical properties of all classes are known a priori
- $M_{Y_1} = \mathbf{\Omega}_X M_{R_1} \neq M_{Y_2}$
- $\mathbf{\Sigma}_{Y_1} = \mathbf{\Omega}_X (\mathbf{\Sigma}_{R_1} + \mathbf{\Sigma}_C) \mathbf{\Omega}_X^H + \mathbf{\Sigma}_N$
  $\neq \mathbf{\Sigma}_{Y_2} = \mathbf{\Omega}_X (\mathbf{\Sigma}_{R_2} + \mathbf{\Sigma}_C) \mathbf{\Omega}_X^H + \mathbf{\Sigma}_N$

for this kind of classification problems, the performance can be enhanced by employing the concepts of Fisher discriminant analysis [50].

Basically, the analysis aims at finding the projection vector $\mathbf{w}$ that maximises the distance between classes' means while minimising the variance of each class [50]. This is achieved by

maximising the classes' separation which is defined by Fisher separation function as follows:

$$\mathrm{f}(\mathbf{w}) = \frac{\mathbf{w}^H (M_{Y_1} - M_{Y_2})(M_{Y_1} - M_{Y_2})^H \mathbf{w}}{\mathbf{w}^H (\Sigma_{Y_1} + \Sigma_{Y_2})\mathbf{w}} \tag{4.19}$$

The optimal projection vector $\mathbf{w}_{opt}$ that maximises Fisher's separation function $\mathrm{f}(\mathbf{w})$ is well defined and is given by:

$$\mathbf{w}_{opt} = \alpha(\Sigma_{Y_1} + \Sigma_{Y_2})^{-1}(M_{Y_1} - M_{Y_2}) \tag{4.20}$$

where α is a constant [50].

By substituting (4.5), (4.6) and (4.20) in (4.19), the objective function becomes variable only in $\mathbf{\Omega}_X$ which is dependent on X (the Fourier transform of the radar probing signal $\mathbf{x}$).

Let $\mathrm{g}_2(\mathbf{\Omega}_X)$ be the objective function resulting from the substitutions, then (4.19) can be written as:

$$\mathrm{g}_2(\mathbf{\Omega}_X) = \frac{\Delta M_R^H \mathbf{\Omega}_X^H \mathbf{S}^{-1} \mathbf{\Omega}_X \Delta M_R (\Delta M_R^H \mathbf{\Omega}_X^H \mathbf{S}^{-1} \mathbf{\Omega}_X \Delta M_R)}{(\Delta M_R^H \mathbf{\Omega}_X^H \mathbf{S}^{-1} \mathbf{\Omega}_X \Delta M_R)}$$

$$= \Delta M_R^H \mathbf{\Omega}_X^H \left(\mathbf{\Omega}_X(\mathbf{\Psi})\mathbf{\Omega}_X^H + 2\mathbf{\Sigma}_N\right)^{-1} \mathbf{\Omega}_X \Delta M_R \tag{4.21}$$

where $\mathbf{S} = \mathbf{\Omega}_X(\mathbf{\Psi})\mathbf{\Omega}_X^H + 2\mathbf{\Sigma}_N$, $\mathbf{\Psi} = \mathbf{\Sigma}_{R_1} + \mathbf{\Sigma}_{R_2} + 2\mathbf{\Sigma}_C$ and $\Delta M_R = M_{R_1} - M_{R_2}$.

The new objective function $\mathrm{g}_2(\mathbf{\Omega}_X)$ then becomes dependent only on the radar waveform X which can be designed so that the classification is set where the maximum Fisher's separation can be achieved. We use a constant energy constraint to limit the energy of the waveform to the constant value ϵ_x. The energy constraint is used here because it is tractable. The optimisation problem is then can be written as follows:

$$\begin{aligned} \underset{\mathbf{\Omega}_X}{\arg\max} \quad & \mathrm{g}_2(\mathbf{\Omega}_X) \\ \text{s.t.} \quad & \mathrm{trace}(\mathbf{\Omega}_X \mathbf{\Omega}_X^H) = m\epsilon_x \end{aligned} \tag{4.22}$$

4.2.2 Classifier Design

Here, as in [16], the classifier assigns the target to the class closest to the target return Y in terms of the Mahalanobis distance after projecting all the received data and the means by $\mathbf{w}$. The projection vector $\mathbf{w}$, depending on the scenario, is given by:

- $\mathbf{w} = (\mathbf{\Sigma}_Y)^{-1}(M_{Y_1} - M_{Y_2})$ when the covariance matrices are identical
- $\mathbf{w} = (\mathbf{\Sigma}_{Y_1} + \mathbf{\Sigma}_{Y_2})^{-1}(M_{Y_1} - M_{Y_2})$ when they are not identical

the Mahalanobis distance for the ith class is then given by:

$$d_i = \sqrt{\frac{|\mathbf{w}^H(Y - M_{Y_i})|^2}{\mathbf{w}^H \mathbf{\Sigma}_{Y_i} \mathbf{w}}} \tag{4.23}$$

the target is assigned to the classes with the minimum d_i.

4.2.3 Waveform Design

The waveform design section is divided into three subsections. The first two sections present optimal waveform design methods for the two main scenarios where the covariance matrices for classes distributions are 1) identical 2) different. The third section covers the closed-form solution for the waveform design problems which is can be used for the two main scenarios without major changes.

4.2.3.1 Optimal Waveform Design for Two Classes with Identical Covariance Matrices

Maximising the classification performance is directly influenced by reducing classification errors which translates into minimising the probability of misclassification. Minimising P_{mc} can be achieved, as derived in Section 4.2.1.1, by maximising $(M_{Y_1} - M_{Y_2})^H \mathbf{\Sigma}_Y^{-1}(M_{Y_1} - M_{Y_2})$. By expanding this term and substituting the expressions of $\mathbf{\Sigma}_Y$, M_{Y_1} and M_{Y_2}, we can express $\mathrm{g}_1(\mathbf{\Omega}_X)$ that is variable only in $\mathbf{\Omega}_X$ as follows:

$$\mathrm{g}_1(\mathbf{\Omega}_X) = \Delta M_R^H \mathbf{\Omega}_X^H (\mathbf{\Omega}_X(\mathbf{\Sigma}_R + \mathbf{\Sigma}_C)\mathbf{\Omega}_X^H + \mathbf{\Sigma}_N)^{-1} \mathbf{\Omega}_X \Delta M_R \tag{4.24}$$

where $\Delta M_R = M_{R_1} - M_{R_2}$.

The design of the optimal radar waveform is then achieved by solving the optimisation problem in (4.18). Solving (4.18) to find a closed-form solution is a challenging problem. However, a numerical solution for the optimisation problem in (4.18) can be computed using MATLAB optimisation toolbox for example [17].

In some special situations, it is possible to derive a closed-form solution to the optimisation problems. Designing the optimal waveform in these situations will require significantly less computations. The two main special situations explored here are dependent on the relationship of the two terms in (4.24):

i. The signal and clutter term: $\mathbf{\Omega}_X(\mathbf{\Sigma}_R + \mathbf{\Sigma}_C)\mathbf{\Omega}_X^H$

ii. The noise term: $\mathbf{\Sigma}_N$

The first situation is defined when the waveform energy is very high such that the following approximation is accurate:

$$(\mathbf{\Omega}_X(\mathbf{\Sigma}_R + \mathbf{\Sigma}_C)\mathbf{\Omega}_X^H + \mathbf{\Sigma}_N)^{-1} \approx (\mathbf{\Omega}_X^H)^{-1}(\mathbf{\Sigma}_R + \mathbf{\Sigma}_C)^{-1}(\mathbf{\Omega}_X)^{-1}$$

The approximation becomes more accurate as the magnitude of each element in the signal and clutter term becomes much higher than the magnitude of the corresponding element in the noise term such that the noise term becomes negligible in (4.24).

In this situation, we can see that the waveform design no longer matters as (4.24) becomes independent of $\mathbf{\Omega}_X$. This means that, as long as no element in X equals zero (see (4.17)), the probability of misclassification will always be given by:

$$P_{mc} = \mathrm{Q}\Big(\sqrt{\Delta M_R^H(\mathbf{\Sigma}_R + \mathbf{\Sigma}_C)^{-1}\Delta M_R/2}\,\Big) \tag{4.25}$$

The second situation is the opposite situation where the waveform energy is too low such that

the approximation below is valid:

$$(\mathbf{\Omega}_X(\mathbf{\Sigma}_R + \mathbf{\Sigma}_C)\mathbf{\Omega}_X^H + \mathbf{\Sigma}_N)^{-1} \approx (\mathbf{\Sigma}_N)^{-1}$$

This means (4.24), in this situation, can be expressed as

$$\mathrm{g}_1(\mathbf{\Omega}_X) = X^H \mathbf{\Omega}_M^H (\mathbf{\Sigma}_N)^{-1} \mathbf{\Omega}_M X \tag{4.26}$$

where $\mathbf{\Omega}_M = \mathrm{diag}(\Delta M)$.

The values of X that maximises the new objective function is obtained using the eigenvector $\Upsilon_{\lambda_{max}}$ of the matrix $\mathbf{\Omega}_M^H (\mathbf{\Sigma}_N)^{-1} \mathbf{\Omega}_M$ which corresponds to its maximum eigenvalue λ_{max}. Finally, the optimal X equals $\Upsilon_{\lambda_{max}}$ scaled by $\sqrt{m\epsilon_x}/\sqrt{\Upsilon_{\lambda_{max}}^H \Upsilon_{\lambda_{max}}}$ to satisfy the energy constraint.

The probability of misclassification in this situation can be calculated using:

$$P_{mc} = \mathrm{Q}\Big(\sqrt{m\epsilon_x \lambda_{max}/2}\Big) \tag{4.27}$$

The probability of correct classification P_{cc} is then given by :

$$P_{cc} = 1 - P_{mc} \tag{4.28}$$

4.2.3.2 Optimal Waveform Design for Two Classes with Different Covariance Matrices

A similar waveform design strategy can be adopted for the scenario where target classes have different means and difference covariance matrices. In this scenario, minimising P_{mc} is replaced with maximising Fisher separation and the optimisation problem in (4.18) is replaced with (4.22). This is because deriving P_{mc} for classes with different means vectors and different covariance matrices is very challenging problem. Fisher discriminant analysis on the other hand are used regardless of whither the matrices are identical or not.

4.2.3.3 Closed-form Waveform Design

The problem in (4.18) and (4.22) can be solved using optimisation toolbox of MATLAB. The solution to the optimisation problem is used to design the optimal X and ultimately obtain the optimal radar waveform $x(t)$ that maximises the performance of target identification. However, in the following section, we propose a closed-form solution to the problem, which is derived using Lagrange multipliers given that Σ_{R_1}, Σ_{R_2}, Σ_C and Σ_N can be approximated to be diagonal matrices (off-diagonal elements are negligible) as established in [54]. This solution can be used also when the covariance matrices are not identical. The only difference is that the solution will maximise Fisher's separation function and not minimise P_{mc} directly [16].

Let $\mathbf{\Psi} = \mathbf{\Sigma}_{R_1} + \mathbf{\Sigma}_{R_2} + 2\mathbf{\Sigma}_C = \mathrm{diag}(P)$ and $\mathbf{\Sigma}_N = \mathrm{diag}(\Xi)$ where $P = [p_1^2, p_2^2, \cdots, p_m^2]^T$ and $\Xi = [\sigma_1^2, \sigma_2^2, \cdots, \sigma_m^2]^T$ and $\Delta M_R = [\Delta\mu_1, \Delta\mu_2, \cdots, \Delta\mu_m]^T$, then $\mathrm{g}_2(\mathbf{\Omega}_X)$ in (4.2.1.2) can be expressed as:

$$\begin{aligned}\mathrm{g}_2(\mathbf{\Omega}_X) =& \Delta M_R^H \mathbf{\Omega}_X^H \left(\mathbf{\Omega}_X(\mathbf{\Psi})\mathbf{\Omega}_X^H + 2\mathbf{\Sigma}_N\right)^{-1} \mathbf{\Omega}_X \Delta M_R \\ =& \sum_{i=1}^{m} \left(\frac{|\Delta\mu_i|^2 |x_i|^2}{|x_i|^2(p_i^2) + 2\sigma_i^2}\right) \\ =& \sum_{i=1}^{m} \frac{\frac{|\Delta\mu_i|^2}{(p_i^2)}|x_i|^2}{|x_i|^2 + \frac{2\sigma_i^2}{(p_i^2)}} = \sum_{i=1}^{m} \frac{\alpha_i |x_i|^2}{|x_i|^2 + \beta_i}\end{aligned} \tag{4.29}$$

assuming $p_i^2 \neq 0 \; \forall i$

The optimisation problem becomes:

$$\arg\max_{|x_i|} \sum_{i=1}^{m} \frac{\alpha_i |x_i|^2}{|x_i|^2 + \beta_i} \text{ s.t. } \sum_{i=1}^{m} |x_i|^2 = m\epsilon_x \tag{4.30}$$

where $\alpha_i = \dfrac{|\Delta\mu_i|^2}{(p_i^2)}$ and $\beta_i = \dfrac{2\sigma_i^2}{(p_i^2)}$.

To solve this problem, we use a Lagrange multipliers approach. It is important to note that using Lagrange multipliers does not necessary finds the global maxima of the optimisation

problem if the strong duality does not hold and the duality gap is not zero. T'his means there is always the possibility that there is a better waveform than the diagonal waveform which can be found by other methods. We define the Lagrangian of our primal problem $\mathcal{L}(X,\gamma)$ as follows:

$$\mathcal{L}(X,\gamma)=\sum_{i=1}^{m}\frac{\alpha_i|x_i|^2}{|x_i|^2+\beta_i}-\gamma\bigg(\sum_{i=1}^{m}|x_i|^2-m\epsilon_x\bigg) \tag{4.31}$$

we define the dual function $L_D(\gamma)=\max_{|x_i|}\mathcal{L}(X,\gamma)$.

Then, maximising $\mathcal{L}(X,\gamma)$ w.r.t absolute of each element of X amounts to:

$$\begin{aligned}&\frac{\partial\mathcal{L}(X,\gamma)}{\partial|x_i|}=\frac{2\alpha_i\beta_i|x_i|}{(|x_i|^2+\beta_i)^2}-2\gamma|x_i|=0\Rightarrow\\&[-2\gamma(|x_i|^2)^2-4\gamma\beta_i|x_i|^2+(2\alpha_i\beta_i-2\gamma\beta_i^2)]|x_i|=0\end{aligned} \tag{4.32}$$

we neglect the first solution

$$|x_i|=0 \tag{4.33}$$

which corresponds to a saddle point where the objective function is at a global minimum and hence not wanted. This can be concluded by observing the objective function.

The other four possible solutions come from:

$$\begin{aligned}|x_i|^2=&\frac{4\gamma\beta_i\pm\sqrt{(-4\gamma\beta_i)^2-4(-2\gamma)(2\alpha_i\beta_i-2\gamma\beta_i^2)}}{-4\gamma}\\=&\frac{\gamma\beta_i\pm\sqrt{\gamma\alpha_i\beta_i}}{-\gamma}\\=&-\beta_i\mp\frac{\sqrt{\alpha_i\beta_i}}{\sqrt{\gamma}}\end{aligned} \tag{4.34}$$

Please note that γ is not restricted by a sign because the multipliers of equality constraints are not restricted to be positive or negative but can be either.

Now, substituting (4.34) in (4.32), we can write:

$$
\begin{aligned}
&L_D(\gamma) = \\
&\sum_{i=1}^{m} \frac{\alpha_i \dfrac{\gamma\beta_i \pm \sqrt{\gamma\alpha_i\beta_i}}{-\gamma}}{\dfrac{\gamma\beta_i \pm \sqrt{\gamma\alpha_i\beta_i}}{-\gamma} + \beta_i} - \gamma\left(\sum_{i=1}^{m} \frac{\gamma\beta_i \pm \sqrt{\gamma\alpha_i\beta_i}}{-\gamma} - m\epsilon_x\right) \\
&= \sum_{i=1}^{m} \frac{\alpha_i\gamma\beta_i \pm \alpha_i\sqrt{\gamma\alpha_i\beta_i}}{\gamma\beta_i \pm \sqrt{\gamma\alpha_i\beta_i} - \gamma\beta_i} + \sum_{i=1}^{m}\left(\gamma\beta_i \pm \sqrt{\gamma\alpha_i\beta_i}\right) + \gamma m\epsilon_x \\
&= \sum_{i=1}^{m} \frac{\alpha_i\gamma\beta_i \pm \alpha_i\sqrt{\gamma\alpha_i\beta_i}}{\pm\sqrt{\gamma\alpha_i\beta_i}} + \sum_{i=1}^{m}\left(\gamma\beta_i \pm \sqrt{\gamma\alpha_i\beta_i}\right) + \gamma m\epsilon_x \\
&= \sum_{i=1}^{m}\left(\pm\sqrt{\gamma\alpha_i\beta_i} + \alpha_i\right) + \sum_{i=1}^{m}\left(\gamma\beta_i \pm \sqrt{\gamma\alpha_i\beta_i}\right) + \gamma m\epsilon_x \\
&= \pm\sum_{i=1}^{m}\sqrt{\gamma\alpha_i\beta_i} + \sum_{i=1}^{m}\alpha_i + \sum_{i=1}^{m}\gamma\beta_i \pm \sum_{i=1}^{m}\sqrt{\gamma\alpha_i\beta_i} + \gamma m\epsilon_x \\
&= \left(m\epsilon_x + \sum_{i=1}^{m}\beta_i\right)(\sqrt{\gamma})^2 \pm 2\sum_{i=1}^{m}\sqrt{\alpha_i\beta_i}(\sqrt{\gamma}) + \sum_{i=1}^{m}\alpha_i
\end{aligned}
\tag{4.35}
$$

which is quadratic in $(\sqrt{\gamma})$ and convex.

In order to minimise the dual function $L_D(\gamma)$, now that we know it is convex and quadratic, we just need to derive $\sqrt{\gamma}$ which satisfies $\dfrac{\partial L_D(\gamma)}{\partial\sqrt{\gamma}} = 0$.

$$
\begin{aligned}
\frac{\partial L_D(\gamma)}{\partial\sqrt{\gamma}} &= 2\left(m\epsilon_x + \sum_{i=1}^{m}\beta_i\right)\sqrt{\gamma} \pm 2\sum_{i=1}^{m}\sqrt{\alpha_i\beta_i} = 0 \Rightarrow \\
\sqrt{\gamma} &= \mp\frac{\sum_{i=1}^{m}\sqrt{\alpha_i\beta_i}}{m\epsilon_x + \sum_{i=1}^{m}\beta_i}
\end{aligned}
\tag{4.36}
$$

We then substitute the value of γ to obtain the optimal value of $|x_i|$ as follows:

$$\begin{aligned}
|x_i|^2 =& \frac{4\gamma\beta_i \pm \sqrt{(-4\gamma\beta_i)^2 - 4(-2\gamma)(2\alpha_i\beta_i - 2\gamma\beta_i^2)}}{-4\gamma} \\
=& -\beta_i \mp \frac{\sqrt{\alpha_i\beta_i}}{\sqrt{\gamma}} \\
=& -\beta_i \mp \frac{\sqrt{\alpha_i\beta_i}}{\mp\frac{\sum_{l=1}^{m}\sqrt{\alpha_l\beta_l}}{m\epsilon_x + \sum_{l=1}^{m}\beta_l}} \\
=& -\beta_i \mp \left(\mp \frac{\sqrt{\alpha_i\beta_i}}{\frac{\sum_{l=1}^{m}\sqrt{\alpha_l\beta_l}}{m\epsilon_x + \sum_{l=1}^{m}\beta_l}} \right) \\
=& \frac{(m\epsilon_x + \sum_{l=1}^{m}\beta_l)\sqrt{\alpha_i\beta_i}}{\sum_{l=1}^{m}\sqrt{\alpha_l\beta_l}} - \beta_i \\
=& \frac{(m\epsilon_x + \sum_{l=1}^{m}\frac{2\sigma_l^2}{(p_l^2)})\sqrt{\frac{|\Delta\mu_i|^2}{(p_i^2)}\frac{2\sigma_i^2}{(p_i^2)}}}{\sum_{l=1}^{m}\sqrt{\frac{|\Delta\mu_l|^2}{(p_l^2)}\frac{2\sigma_l^2}{(p_l^2)}}} - \frac{2\sigma_i^2}{(p_i^2)}
\end{aligned} \tag{4.37}$$

Because $|x_i|$ in (4.37) has to be positive, we concludes that the amplitude of each element of the solution waveform $X_{solution}$ is given by:

$$|x_i| = \begin{cases} \sqrt{|x_i|^2} & \text{if } |x_i|^2 \geq 0 \\ 0 & \text{otherwise} \end{cases} \tag{4.38}$$

and the phase can be arbitrary. Finally, x_i can be scaled to satisfy the energy constraint.

4.3 Results and Discussion

In this section, we present the simulation results generated using synthetic and real targets data to study the performance of the closed-form solution derived in Section 4.2.3.3 (from here on referred to as "the diagonal solution" and the waveform as "the diagonal waveform")

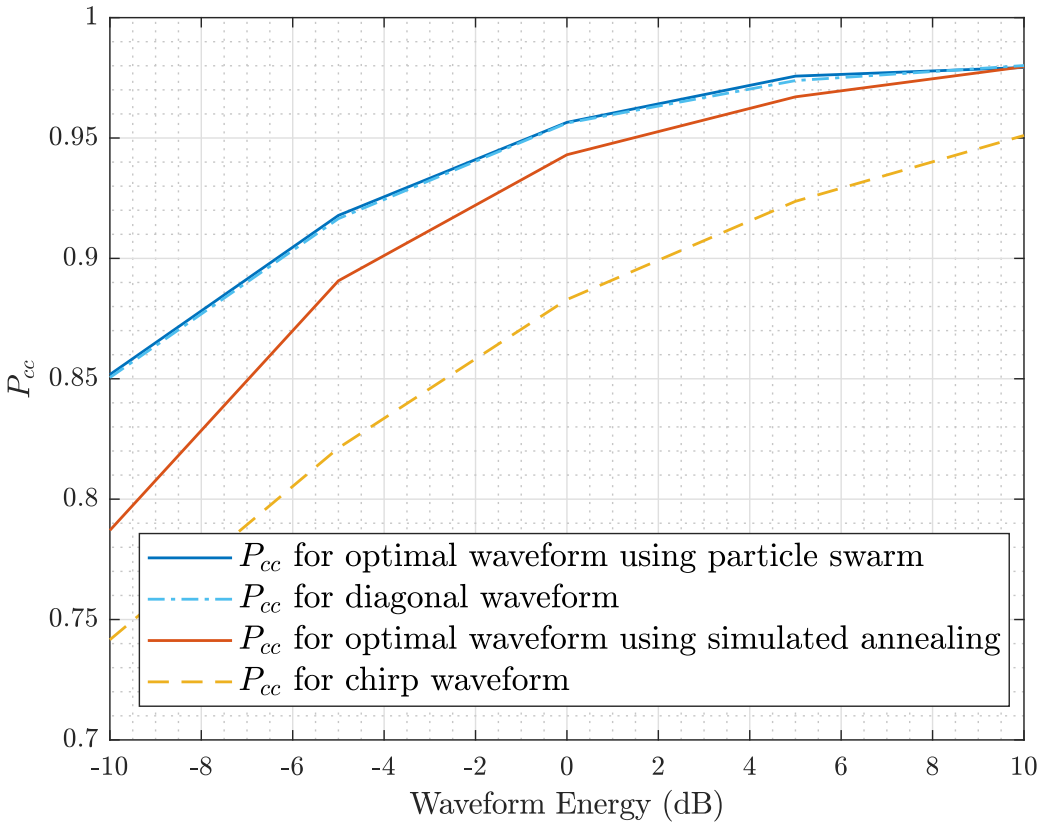

Figure 4.1: *Measured P_{cc} vs waveform energy ϵ_x for different waveform design methods for the scenario where the two classes have identical covariance matrices and no clutter is present*

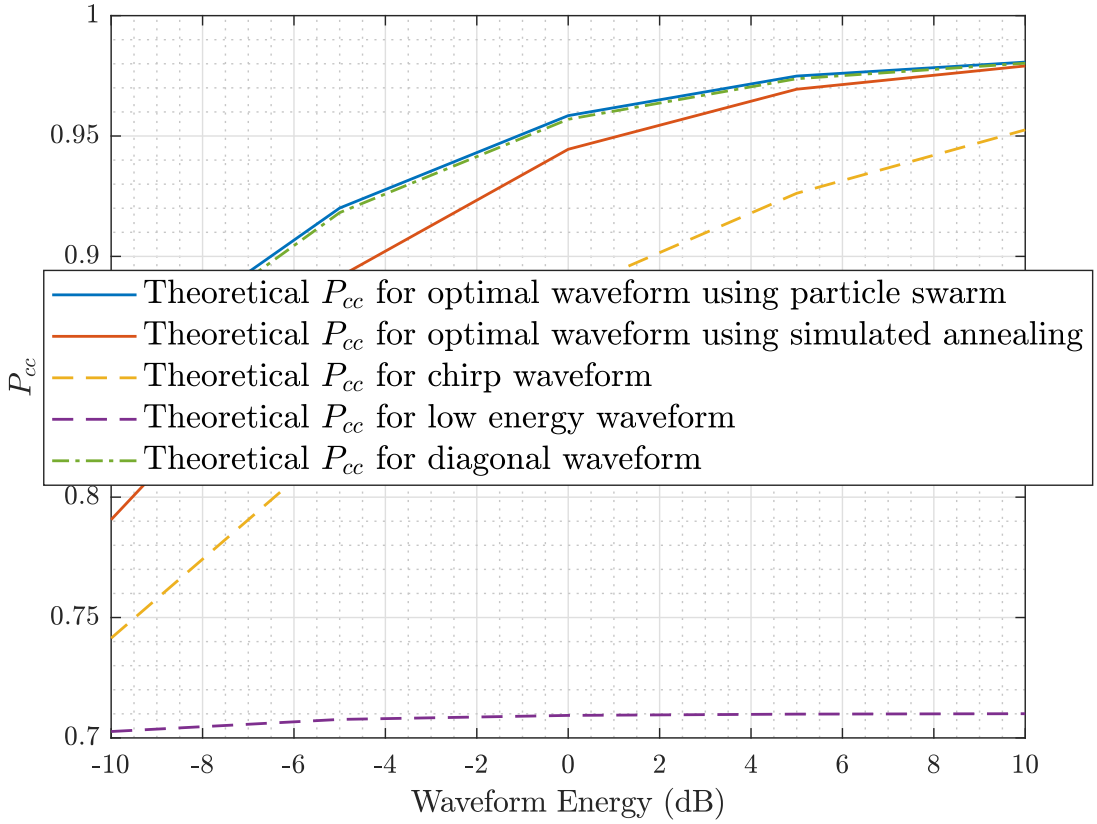

Figure 4.2: *Theoretical P_{cc} vs waveform energy ϵ_x for different waveform design methods for the scenario where the two classes have identical covariance matrices and no clutter is present*

against other radar waveforms found in the literature [16]. Note that in this chapter we are not comparing the results against the AMD waveform as it is not designed for presence of clutter and angular uncertainty simultaneously [12–15, 27–29].

4.3.1 Results Generated Using Synthetic Data

The common simulation setup is shown in table 4.1.

Parameter	Value
Number of frequency bins m	64
Noise	Complex AWGN with with of 1
Clutter	Complex AWGN with of 0.5
Number of Monte Carlo runs n	10,000
Mean vectors and covariance matrices for all target classes	generated arbitrarily at the start of the simulation
Optimisation algorithm	Simulated annealing
Simulated annealing max number of iterations	200
Simulated annealing other parameters	default
The realisations of the Target response R, noise vector N and clutter vector C	different at each run (i.e. generated from pulse-to-pulse)

Table 4.1: *Table of common simulation parameters and setup*

4.3.1.1 The theoretical performance vs the measured performance when the covariance matrices of the classes are identical (i.e. $\mathbf{\Sigma}_{R_1} = \mathbf{\Sigma}_{R_2}$) and clutter is negligible ($\sigma_c^2 = 0$)

We start first by studying the scenario where no significant clutter response is received in the radar system (e.g. radar looking above ground) and the two classes of targets share the same covariance matrix. The standard measure of the classification performance that we will be using from here on is the probability of correct classification Pcc which is the complement probability of P_{mc} (i.e. $P_{cc} = 1 - P_{mc}$.).

In this scenario, we study the performance of the diagonal solution and three other waveforms (defined below) while also showing the difference between the classification performance obtained from running Monte-Carlo simulation and the performance calculated directly from

the theoretical probability of misclassification as derived and expressed in (4.17).

The four main waveform design methods to be studied in this scenario are as follows:

- The diagonal waveform: the waveform generated from computing the optimal waveform using the diagonal solution proposed in this chapter in (4.38)
- The chirp waveform: a wideband flat spectrum linearly frequency-modulated waveform
- The SA optimal waveform: obtained using MATLAB optimisation toolbox to solve (4.18) or (4.22) where the algorithm "Simulated Annealing" is used seeded by the chirp waveform.
- The PS optimal waveform: obtained using MATLAB optimisation toolbox to solve (4.18) or (4.22) where the algorithm "Particle Swarm" is used.

Figures 4.1 and 4.2 show the measured and theoretical performance of the four aforementioned waveforms in terms of the probability of correct classification P_{cc} vs the time-domain waveform energy ϵ_x respectively. As the noise variance is unchanged in the two figures, we expect every point on the x-axis to correspond to different signal-to-noise ratio (SNR) which is also expected to be monotonically increasing with ϵ_x.

The two figures show an almost non-existent difference between the measured performance and the theoretical one which was calculated using (4.17).

Also, we notice that in this case the particle swarm algorithm was able to perform better than simulated annealing and all other waveform design methods. This can be due to the optimisation problem providing favourable conditions for one algorithm over another. This shows the importance of employing multiple global optimisation algorithms and choosing the one that performs better. We notice that the diagonal solution also attained better performance than simulated annealing without requiring the same computations.

On the other hand, the optimal waveform designed using particle swarm algorithm is shown to outperform all other waveforms with slight advantage over the diagonal solution. This,

of course, comes at the expense of more computational complexity required to obtain the optimal waveform in comparison to the diagonal solution [55].

4.3.1.2 The performance when the covariance matrices are identical (i.e. $\mathbf{\Sigma}_{R_1} = \mathbf{\Sigma}_{R_2}$) and clutter is present ($\sigma_c^2 = 0.5$)

In this second scenario, we study the performance of the same four waveform design methods when the two classes also share the same covariance matrix but in the presence of clutter and noise. The clutter and noise vector as mentioned before are both assumed white with spectral variance of 0.5 and 1 respectively.

Fig. 4.3 shows the measured performance of the four waveforms in terms of P_{cc} vs ϵ_x. The figure shows no difference in the relative performances of the four waveforms between this scenario and the previous one. However, the overall performance of all waveforms has clearly degraded due to the presence of the clutter where, for example, the PS optimal and the diagonal waveform can only attain around $P_{cc} = 0.95$ at $\epsilon_x = 10$ dB while it attained higher than that, at the same energy level, in the previous scenario where no clutter is present.

4.3.1.3 The performance when the covariance matrices are identical (i.e. $\mathbf{\Sigma}_{R_1} = \mathbf{\Sigma}_{R_2}$) and clutter is negligible ($\sigma_c^2 = 0$) against very low ϵ_x and very high ϵ_x waveforms

In this scenario, we study the performance of the extreme ϵ_x waveforms derived in Section 4.2.3.1 vs the other waveforms we studied so far. This is to validate the results obtained in (4.25) and (4.26) where the performance of the extreme ϵ_x waveforms was derived. The clutter in this scenario is negligible.

The measured P_{cc} vs ϵ_x for this scenario is shown in Fig. 4.4. The high ϵ_x performance limit is calculated using (4.25). We can see that the performance of no waveform can surpass that of the high ϵ_x limit and the waveforms with best performance start saturating as it get closer to the high ϵ_x limit value. The figure also shows the performance of the low ϵ_x waveform which performs worse in comparison to other waveforms in the current energy levels where ϵ_x is not very low.

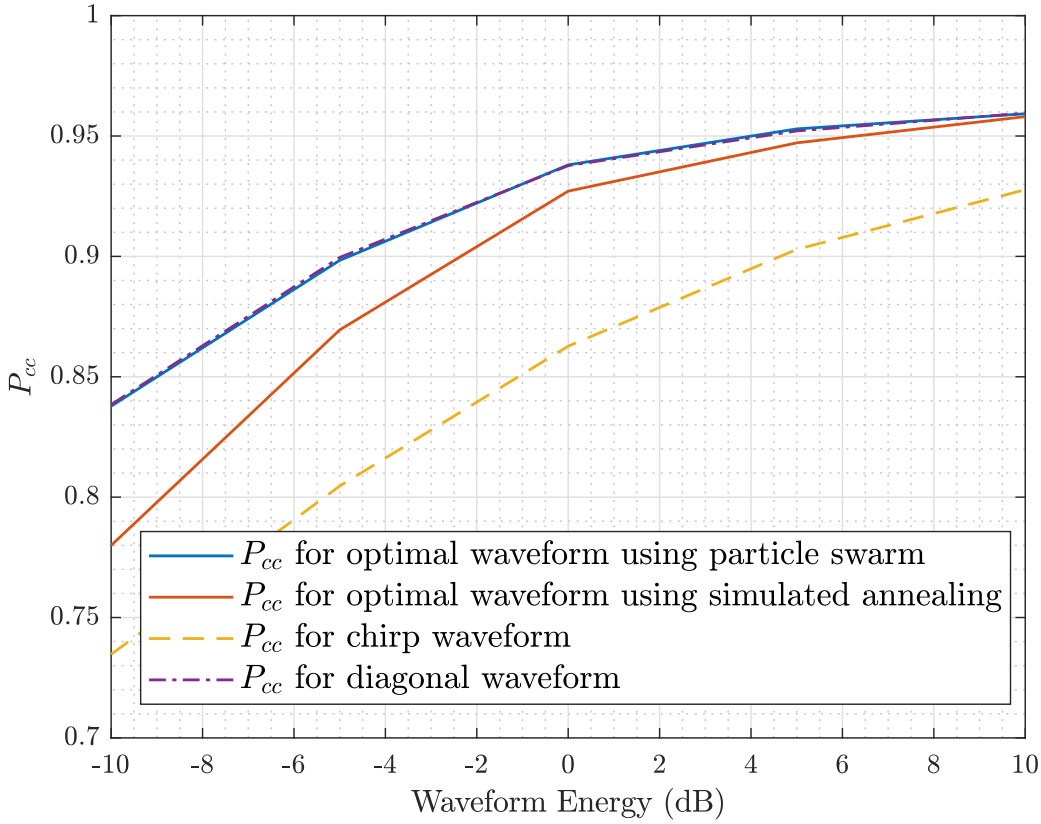

Figure 4.3: *Measured P_{cc} vs waveform energy ϵ_x for different waveform design methods for the scenario where the two classes have identical covariance matrices and clutter is present*

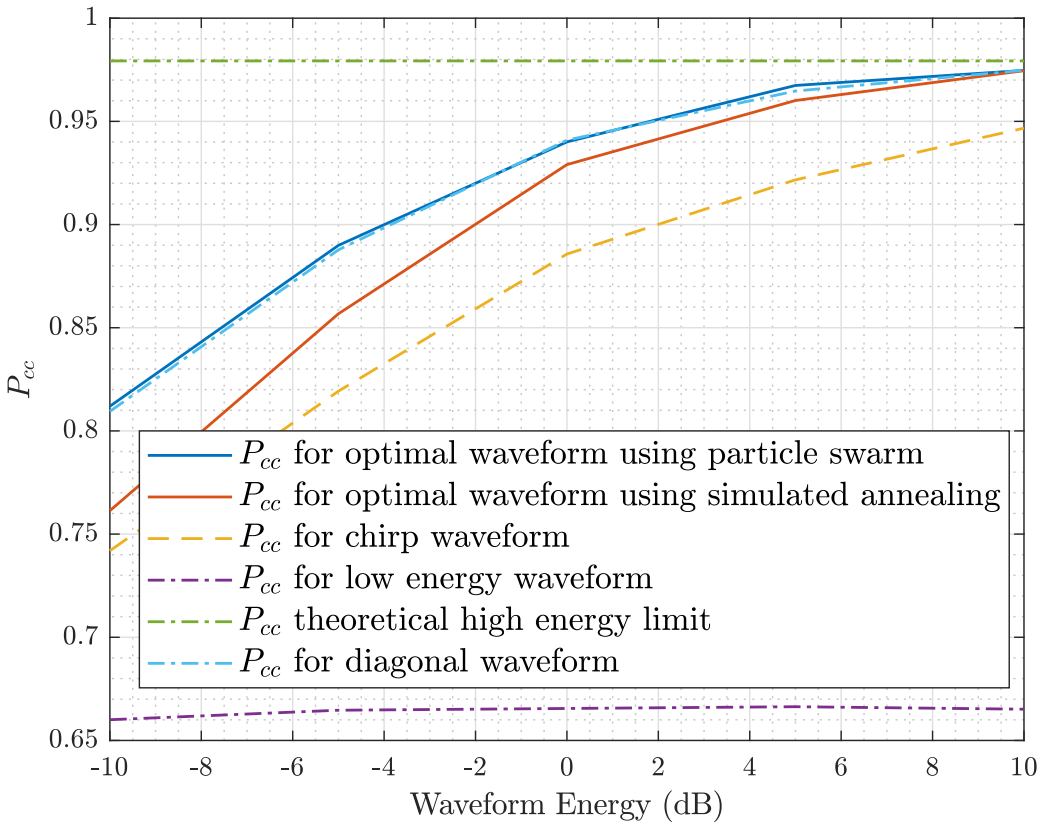

Figure 4.4: *Measured P_{cc} vs waveform energy ϵ_x for different waveform design methods for the scenario where the two classes have identical covariance matrices and no clutter is present along with the P_{cc} limit when the ϵ_x is very high*

When we rerun this scenario at a much lower waveform energy levels, we get the classification performance shown in Fig. 4.5. It is very clear from the figure that the energy level where the low ϵ_x assumption becomes accurate. We can see the low ϵ_x waveform almost outperforming all other waveforms at energy levels below $\epsilon_x = -25$ dB. We call the interval of ϵ_x values below $\epsilon_x = -25$ dB the low ϵ_x region. However, we can also see that it is still possible to find an optimal waveform using particle swarm algorithm that will slightly surpass the low ϵ_x waveform around the start of the low ϵ_x region.

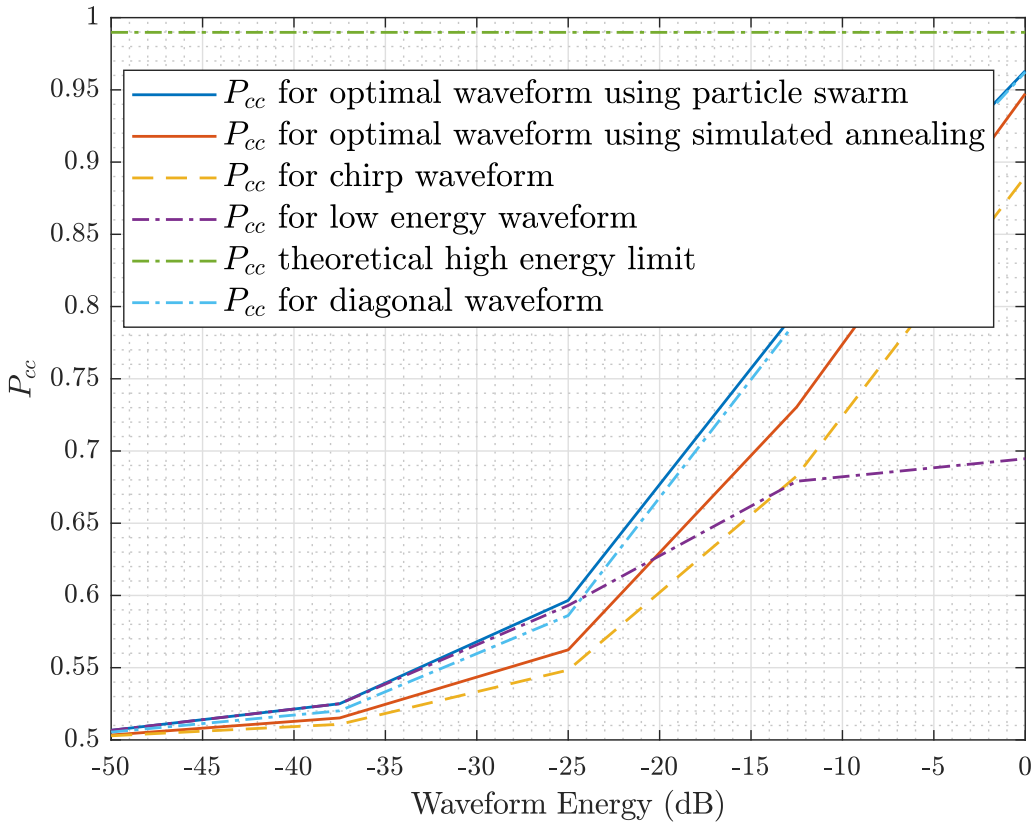

Figure 4.5: *The performance of low waveform energy waveform in Measured P_{cc} vs waveform energy ϵ_x against different waveforms for the scenario where the two classes have identical covariance matrices and no clutter is present*

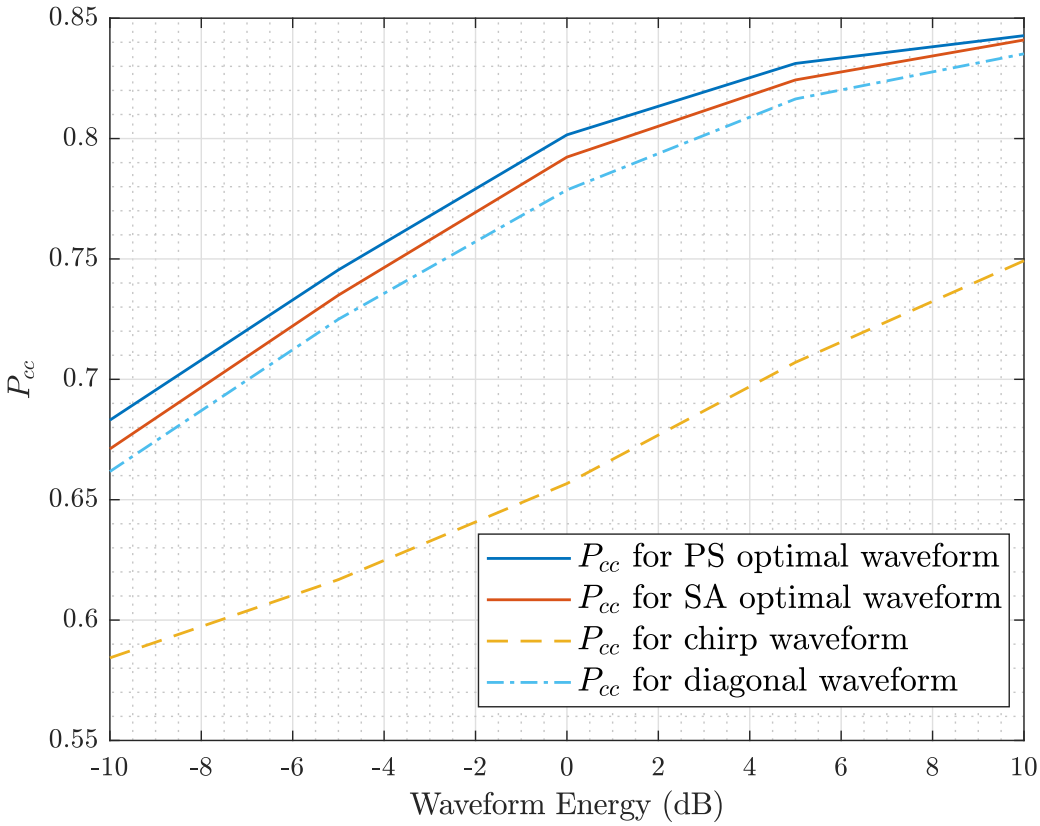

Figure 4.6: *Measured P_{cc} vs waveform energy ϵ_x for different waveform design methods for the scenario where the two classes have different covariance matrices and no clutter is present*

4.3.1.4 The performance when the covariance matrices are different (i.e. $\mathbf{\Sigma}_{R_1} \neq \mathbf{\Sigma}_{R_2}$) and clutter is negligible ($\sigma_c^2 = 0$)

Next we study the more general scenario where the two classes have different mean vectors and covariance matrices. Also, the clutter is assumed negligible in this scenario.

Figure 4.6 shows P_{cc} vs ϵ_x for the four main waveforms. The figure shows a noticeable degradation in the overall performance of all waveforms where the maximum expected P_{cc} at $\epsilon_x = 10$ dB is around $P_{cc} = 0.85$. We can see that in this scenario, the gap between the PS optimal waveform and the diagonal waveform has broadened. We also notice that the SA optimal waveform is now outperforming the diagonal solution while also being outperformed by the PS optimal waveform.

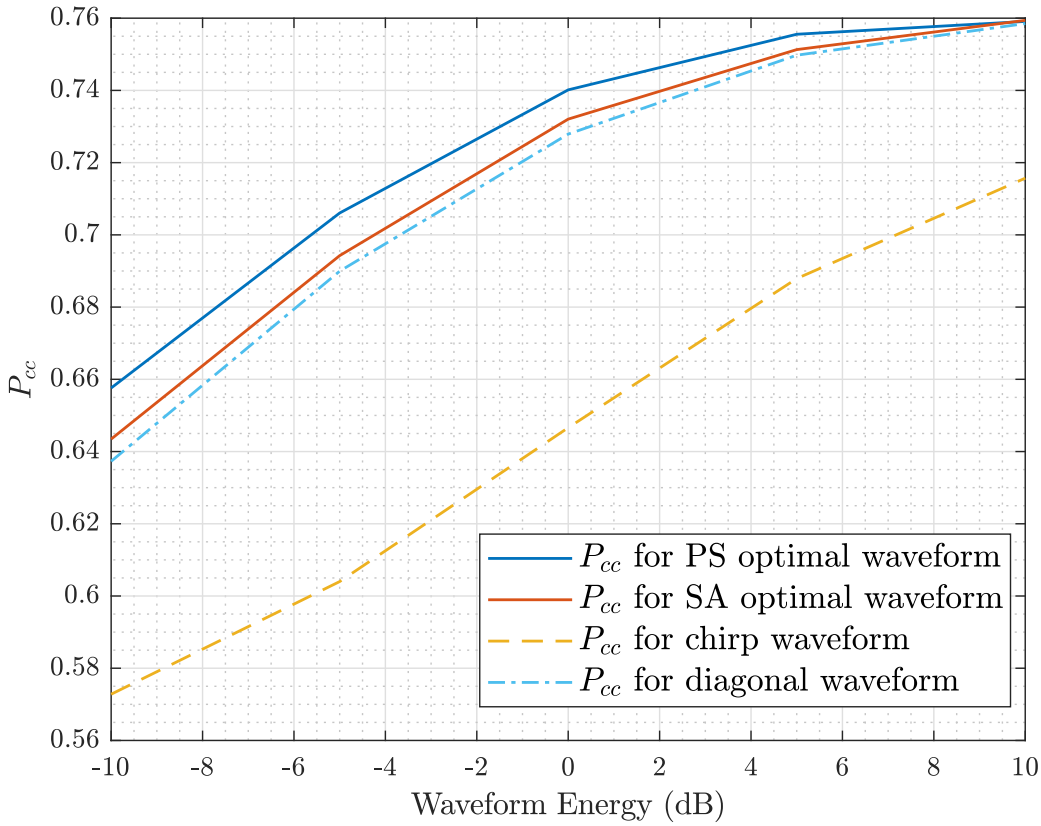

Figure 4.7: *Measured P_{cc} vs waveform energy ϵ_x for different waveform design methods for the scenario where the two classes have different covariance matrices and clutter is present*

4.3.1.5 The performance when the covariance matrices are different (i.e. $\boldsymbol{\Sigma}_{R_1} \neq \boldsymbol{\Sigma}_{R_2}$) and clutter is present ($\sigma_c^2 = 0.5$)

The performance of the four waveforms and their objective function values are shown in Fig. 4.7. As expected, the performance of the waveforms looks like the previous scenario except it is now lower due to clutter. The maximum P_{cc} at $\epsilon_x = 10$ dB is now $P_{cc} = 0.76$ in comparison to around $P_{cc} = 0.85$ attained in the clutter-less scenario.

4.3.2 Results Generated Using Real Dataset

In this section, the synthetic target data is replaced with real data from the MSTAR dataset [22]. The dataset is made up of extended complex target Frequency responses (TFRs) of

ten civilian vehicles. The TFRs are captured at four different elevation angles θ_{el} and 5760 azimuth angles covering the 360° of the target. The statistical properties of the classes of targets are estimated from the data and the rest of the data is used in results generation. Clutter and noise vectors are generated synthetically from white complex Gaussian random fields. We assume that the set of TFRs in a sector from the 360° of the target, consist of realisations from the same given distribution that can be estimated from the responses in the sector. We use ρ_θ to refer to the sector width in degrees.

The three main waveforms to be studied in this scenario are as follows:

- The diagonal waveform: the waveform generated from computing the optimal waveform using the diagonal solution proposed in this chapter
- The chirp waveform: a wideband flat spectrum linearly frequency-modulated waveform
- The optimal waveform: obtained using MATLAB optimisation toolbox to solve (4.22) where the algorithm "Particle Swarm" is used.

Note that, we no longer need to test the SA optimal waveform here as the PS optimal showed superiority in all previous scenarios.

4.3.2.1 The performance of classifying the target into 'Toyota Tacoma' or 'Toyota Avalon' with $\theta_{el} = 60°$, $\rho_\theta = 4°$ and no clutter is present $\sigma_c^2 = 0$

In this scenario, we study the classification performance of the diagonal solution against the PS optimal waveform and the chirp waveform. The radar is to classify an already detected target into either a 'Toyota Tacoma' or 'Toyota Avalon' using its extended TFR [22]. The radar-target orientation is assumed unknown but it is given that it is within the first 4 degrees of the target (in the CVS dataset $\theta_{az} = 0°$ is at the front of the vehicle) in azimuth ($\rho_\theta = 4°$) at $\theta_{el} = 60°$. The only type of interference present, in this scenario, is noise which is generated synthetically to be white with unity spectral variance σ_n^2.

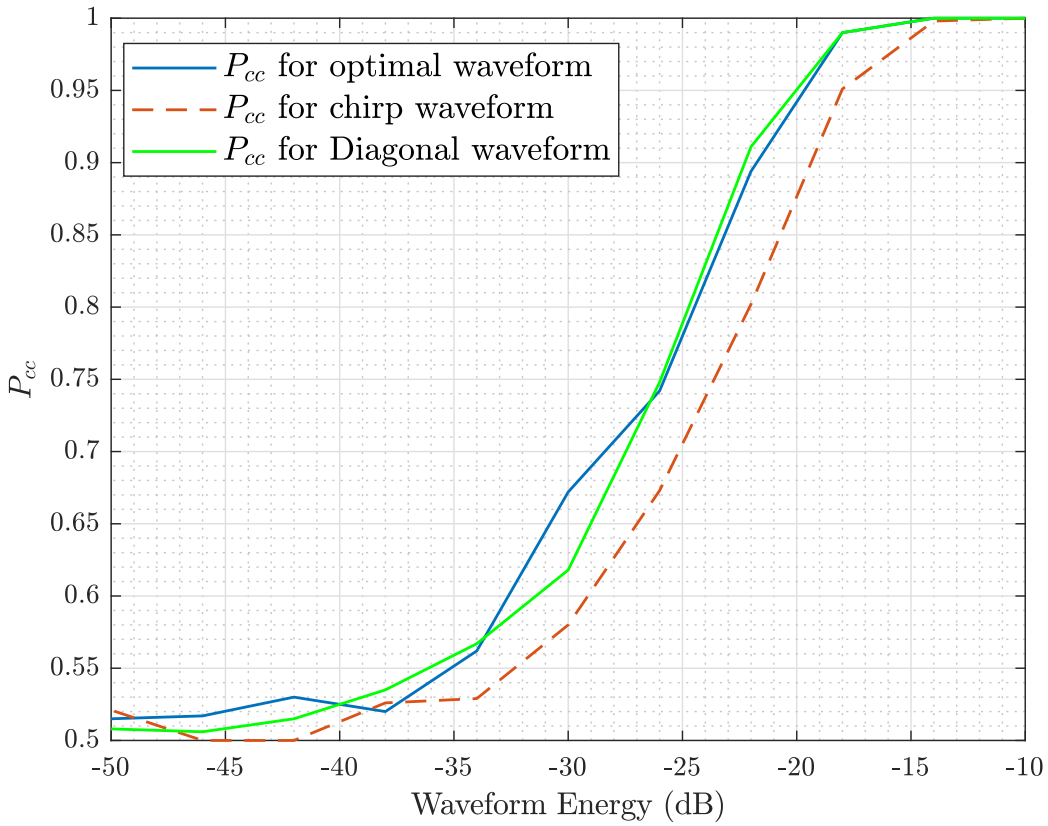

Figure 4.8: *The probability of correct classification P_{cc} vs waveform energy ϵ_x for different waveform design methods for the scenario where the radar to classify the target into 'Toyota Tacoma' or 'Toyota Avalon' where $\theta_{el} = 60°$, $\rho_\theta = 4°$ and no clutter is present $\sigma_c^2 = 0$ where the optimal waveform is designed using Particle Swarm*

The classification performance in terms of P_{cc} vs ϵ_x for the three waveforms considered here is shown in Fig. 4.8. The figure shows that on average, the PS optimal and diagonal waveform perform better than the chirp waveform. It also shows how the diagonal waveform attains a performance close to the PS optimal waveform.

4.3.2.2 The performance of classifying the target into 'Toyota Tacoma' or 'Toyota Avalon' with $\theta_{el} = 60°$, $\rho_\theta = 4°$ and clutter is present $\sigma_c^2 = 0.5$

When the same scenario as Section 4.3.2.1 is considered but clutter is present, the resulting classification performance is as shown in Fig. 4.9. In general, we see an expected degradation due to the presence of clutter but the relative difference between the waveforms is almost the

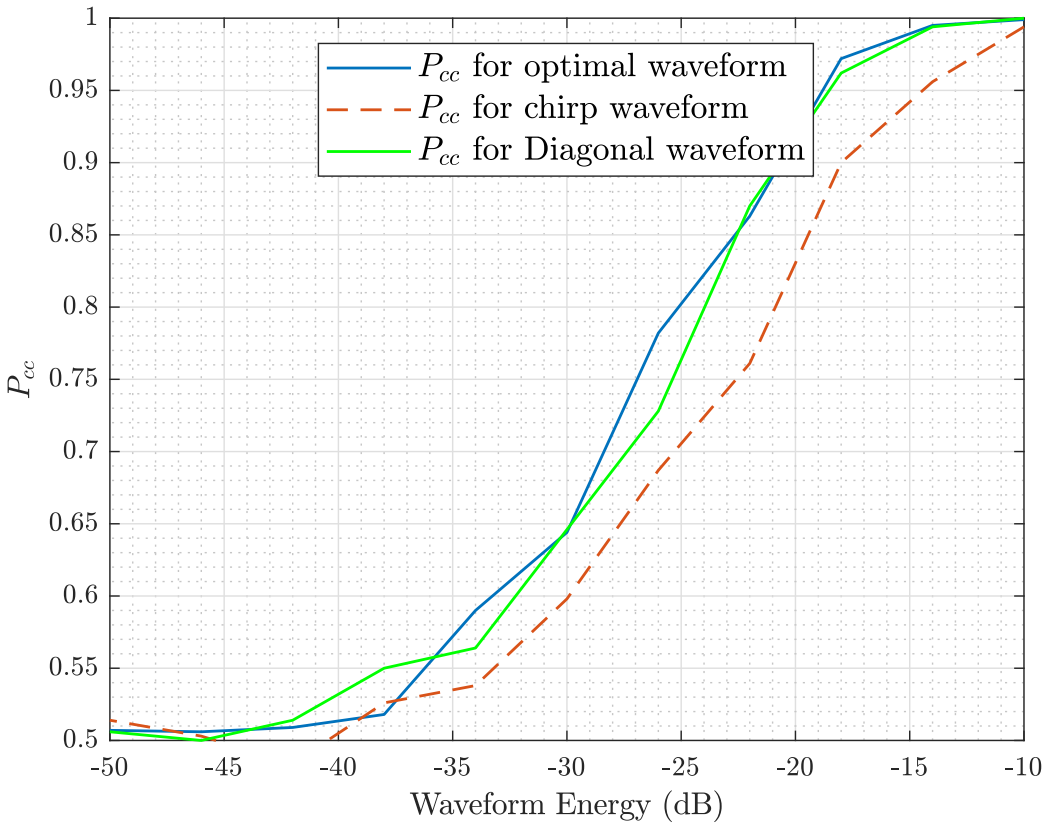

Figure 4.9: *The probability of correct classification P_{cc} vs waveform energy ϵ_x for different waveform design methods for the scenario where the radar to classify the target into 'Toyota Tacoma' or 'Toyota Avalon' where $\theta_{el} = 60°$, $\rho_\theta = 4°$ and clutter is present $\sigma_c^2 = 0.5$ where the optimal waveform is designed using Particle Swarm*

same as the previous scenario of Section 4.3.2.1

4.4 Conclusions

This chapter proposed a closed-form solution for the two main optimisation problems to maximise classification performance in two main scenarios were the TFRs are complex and normally distributed with different mean vectors, but their covariance matrices are either identical or non-identical. The chapter expanded on these two scenarios with introduction of clutter (signal-dependent interference) and studied other possible designs in extreme ϵ_x levels. The derivations of the extreme ϵ_x solutions shows the best performance that the spe-

cial closed-form solutions achieves at these extreme levels. The closed-form solutions were tested against optimal waveforms solved using optimisation software as derived in the literature (with different optimisation algorithms) and showed that the proposed closed-form solution (diagonal solution) attains close if not similar performance as that of the best optimal waveform the optimisation software can design without all the computation time and complexity needed to design the optimal waveform. Some simulations were conducted using data synthetically generated and the other utilised the Civilian Vehicle Data from MSTAR dataset. In both scenarios the gap between the optimal solution and the proposed solution was almost negligible.

Chapter 5
Conclusions

The thesis has studied and presented new waveform and receiver design procedures that optimise the performance of target identification in radar. The importance of signal processing in radar were discussed especially waveform design and its role in shaping the radar performance. Also, the background and the relevant literature to radar waveform design in optimising target identification performance were presented.

The thesis was motivated by the following:

- waveform design plays an important role, that is recognised by the literature, in improving target performance.
- although target identification can be as important as detection, optimising target identification using waveform design is not as much researched as optimal design for target detection.
- a great body of the research in target identification optimisation is focused on adaptive waveform design which requires more computations and more advanced hardware than that required in non-adaptive waveform design.
- many of the relevant literature does not consider angular uncertainty or practical targets responses which can cause significant drop in the performance.

The solutions presented in this thesis for these motivation are as follows:

- The thesis proposed two non-adaptive waveform design procedures inspired by 2-class and multiclass Fisher discriminant analysis in a clutter-free noisy environment. The procedures provided general solutions obtainable using general optimisation solvers.

Also, two closed-form solutions (one for each scenario) to the waveform design optimisation problems were derived under low-energy/low-covariance (LELC) assumption. The results showed that the proposed classification schemes and waveform designs outperform the non-adaptive methods found in the literature especially in high SNR regions.

- The thesis proposed two other non-adaptive design procedures where signal-dependent interference/clutter is present. In presence of signal-dependent interference, the thesis provided the following: 1) Introduction of signal-dependent interference and clutter to the signal model for the two cases: i) when the target classes share the same covariance matrix ii) when they have different matrices 2) formulation of the waveform design problem based on the new signal model for both cases 3) derivation of a frequency-based closed-form solution for radar waveform design problem. The thesis tested the closed-form solution against 1) flat spectrum wideband waveform, 2) optimised waveforms obtained from the optimisation algorithms and 3) extreme energy waveforms when the waveform energy is either extremely low or high.

5.1 Future Work

The thesis presented optimal non-adaptive waveform design methods based on Fisher discriminant analysis to improve target identification. The non-adaptive waveform design allows for pre-design of the waveform and the receiver based on previously obtained knowledge about target classes, noise, clutter and environment. This may limit the design to perform well in conditions matched to the assumptions. Any mismatch may result in significant drop in the performance. For future work, Fisher discriminants analysis can be introduced to more advanced systems where this mismatch will have less impact on the radar performance after deployment. An adaptive waveform design technique based on Fisher analysis, for example, may provide the system with updated prior knowledge preventing performance drops.

In chapter 4, clutter was introduced to the signal model and the waveform design problem where a closed-form solution was derived for designing the waveform and the optimal receiver. Accurate knowledge about clutter is not always available especially for airborne

radars. For future work, the presented methods can be adjusted to update clutter statistical properties on-the-fly and the closed-form solution can be updated for enhanced performance.

Additional constraints can be added like constraining the time-domain waveform to have constant modulus, for example, and low peak-to-average-power ratio (PAPR). This can result in degradation in the classification performance but it can result in designing waveform more practical for old radar systems with non-linear power amplifiers.

Also, variety of more analysis tools can be used for more comprehensive understanding of the performance and the proposed designs properties can be used like confusion matrices where the types of errors and sources of errors can be studied. Also, studying computational complexities and times can provide explicit measure of the computational differences between proposed designs here in this thesis and in the literature.

Appendix A

Derivation for Two Classes ($c = 2$) Problem in Noisy Environment

General Solution for Two Classes ($c = 2$) Problem

With only two classes to classify, the transformation matrix $\mathbf{W}$ reduces to a vector. The within-class scatter matrix is as follows:

$$\begin{aligned}\mathbf{S}_W =& \mathbf{\Omega}_X \mathbf{\Sigma}_1 \mathbf{\Omega}_X^H + \mathbf{\Sigma}_N + \mathbf{\Omega}_X \mathbf{\Sigma}_2 \mathbf{\Omega}_X^H + \mathbf{\Sigma}_N \\ =& \mathbf{\Omega}_X \big(\mathbf{\Sigma}_1 + \mathbf{\Sigma}_2\big) \mathbf{\Omega}_X^H + 2\mathbf{\Sigma}_N\end{aligned} \tag{A.1}$$

while between-class scatter matrix is

$$\mathbf{S}_B = \mathbf{\Omega}_X (M_1 - M_2)(M_1 - M_2)^H \mathbf{\Omega}_X^H \tag{A.2}$$

The objective function is defined as the ratio $\mathrm{f}(\mathbf{w})$:

$$\mathrm{f}(\mathbf{w}) = \frac{\mathbf{w}^H \mathbf{S}_B \mathbf{w}}{\mathbf{w}^H \mathbf{S}_W \mathbf{w}} \tag{A.3}$$

The optimal $\mathbf{w}$ for which $\mathrm{f}(\mathbf{w})$ can be maximised is as follows:

$$\mathbf{w}_{opt} = (\mathbf{S}_W)^{-1} \mathbf{\Omega}_X \Delta M \tag{A.4}$$

where $\Delta M = (M_1 - M_2)$.

Finally, we define the objective function $\mathrm{g}(\mathbf{\Omega}_X)$ which is a function of the radar waveform in

$\mathbf{\Omega}_X$ as follows:

$$\begin{aligned}
&\mathrm{g}(\mathbf{\Omega}_X) = \mathrm{f}(\mathbf{w})_{|\mathbf{w}_{opt}=[\mathbf{\Omega}_X(\mathbf{\Sigma}_1+\mathbf{\Sigma}_2)\mathbf{\Omega}_X^H+2\mathbf{\Sigma}_N]^{-1}\mathbf{\Omega}_X\Delta M} \\
&=\frac{\Delta M^H\mathbf{\Omega}_X^H(\mathbf{S}_W)^{-1}\mathbf{\Omega}_X\Delta M\Delta M^H\mathbf{\Omega}_X^H(\mathbf{S}_W)^{-1}\mathbf{\Omega}_X\Delta M}{\Delta M^H\mathbf{\Omega}_X^H(\mathbf{S}_W)^{-1}\mathbf{S}_W(\mathbf{S}_W)^{-1}\mathbf{\Omega}_X\Delta M} \\
&=\Delta M^H\mathbf{\Omega}_X^H(\mathbf{S}_W)^{-1}\mathbf{\Omega}_X\Delta M \\
&=\Delta M^H\mathbf{\Omega}_X^H\big(\mathbf{\Omega}_X(\mathbf{\Sigma}_1+\mathbf{\Sigma}_2)\mathbf{\Omega}_X^H+2\mathbf{\Sigma}_N\big)^{-1}\mathbf{\Omega}_X\Delta M
\end{aligned}$$

$$\begin{aligned}
&\mathrm{g}(\mathbf{\Omega}_X) = \\
&\Delta M^H\mathbf{\Omega}_X^H\big(\mathbf{\Omega}_X(\mathbf{\Sigma}_1+\mathbf{\Sigma}_2)\mathbf{\Omega}_X^H+2\mathbf{\Sigma}_N\big)^{-1}\mathbf{\Omega}_X\Delta M
\end{aligned} \tag{A.5}$$

The optimisation problem is then the same as (3.17) with different definition for $\mathrm{g}(\mathbf{\Omega}_X)$.

LELC Solution Under AWGN for Two Classes ($c = 2$) Problem

In this scenario, we derive the closed-form solution at LELC's SNR/energy level where the approximation $\mathbf{S}_W \approx 2\mathbf{\Sigma}_N$ is valid.

With $\mathbf{\Omega}_X\big(\mathbf{\Sigma}_1 + \mathbf{\Sigma}_2\big)\mathbf{\Omega}_X^H$ no longer affecting $\mathrm{g}(\mathbf{\Omega}_X)$, the objective function becomes identical to that in [17] under similar assumptions about the SNR and energy level. The optimal solution in this case is the waveform consisting of the largest eigenvector of the maximum eigenvalue of the matrix $\mathbf{C}$ which is defined as:

$$\mathbf{C} = \mathrm{diag}(M_1 - M_2)^H(\mathbf{\Sigma}_N)^{-1}\mathrm{diag}(M_1 - M_2) \tag{A.6}$$

The waveform is then normalised by $\sqrt{\|X\|^2}$ and multiplied with $\sqrt{m\epsilon_x}$ to match the energy constraint of the optimisation problem.

The Derivation of The Classifier

The classifier in this case is not very different than that in multiclass case. The difference now is that the transformation matrix $\mathbf{W}_{opt}$ is just a vector $\mathbf{w}_{opt}$. This means that it will transform

all the vectors into complex scalars.

The scalars will be given by:

$$\tilde{y} = \mathbf{w}_{opt}^{H} Y \tag{A.7}$$

$$\tilde{m}_{Y_{ki}} = \mathbf{w}_{opt}^{H} M_{Y_{ki}} = \mathbf{w}_{opt}^{H} \mathbf{\Omega}_X M_{k_i} \tag{A.8}$$

$$\begin{aligned} \tilde{\sigma}_{Y_{ki}}^{2} &= \mathbf{w}_{opt}^{H} \mathbf{\Sigma}_{Y_{ki}} \mathbf{w}_{opt} \\ &= \mathbf{w}_{opt}^{H} (\mathbf{\Omega}_X \mathbf{\Sigma}_{ki} \mathbf{\Omega}_X^{H} + \mathbf{\Sigma}_N) \mathbf{w}_{opt} \end{aligned} \tag{A.9}$$

and the Mahalanobis distance of the subclass i of class k from the received signal Y is then given by:

$$d_{k_i} = \sqrt{\frac{|\tilde{m}_{Y_{ki}} - \tilde{y}|^2}{\tilde{\sigma}_{Y_{ki}}^2}} \tag{A.10}$$

Algorithm 3 shows in step-by-step how the classifier assign a target to a class from the received signal Y.

Algorithm 3 Identify target class from received signal Y in 2-class scenario

Require: Y, $\mathbf{\Omega}_X$,M_1,M_2, $\mathbf{\Sigma}_1$, $\mathbf{\Sigma}_2$ and $\mathbf{\Sigma}_N$
  $\mathbf{S}_W \Leftarrow \mathbf{\Omega}_X \big(\mathbf{\Sigma}_1 + \mathbf{\Sigma}_2\big) \mathbf{\Omega}_X^{H} + 2\mathbf{\Sigma}_N$
  $\mathbf{w}_{opt} = (\mathbf{S}_W)^{-1}(M_1 - M_2)$
  $\tilde{y} \Leftarrow \mathbf{w}_{opt}^{H} Y$
  for $k = 1$ to 2 **do**
    $\tilde{m}_{Y_k} \Leftarrow \mathbf{w}_{opt}^{H} \mathbf{\Omega}_X M_k$
    $\tilde{\mathbf{\Sigma}}_{Y_k} \Leftarrow \mathbf{w}_{opt}^{H} (\mathbf{\Omega}_X \mathbf{\Sigma}_k \mathbf{\Omega}_X^{H} + \mathbf{\Sigma}_N) \mathbf{w}_{opt}$
    $d_k \Leftarrow \sqrt{\frac{|\tilde{m}_{Y_k} - \tilde{y}|^2}{\tilde{\sigma}_{Y_k}^2}}$
  end for
  if $d_1 < d_2$ **then**
    Assign target to the class 1
  else
    Assign target to the class 2
  end if

References

[1] P. M. Woodward and I. Davies, "Xcii. a theory of radar information," *The London, Edinburgh, and Dublin Philosophical Magazine and Journal of Science*, vol. 41, no. 321, pp. 1001–1017, 1950.

[2] M. R. Bell, "Information theory and radar waveform design," *IEEE Transactions on Information Theory*, vol. 39, no. 5, pp. 1578–1597, Sep 1993.

[3] Zhaofu Chen, J. Li, X. Tan, H. He, Bin Guo, P. Stoica, and M. Datum, "On probing waveforms and adaptive receivers for active sonar," in *OCEANS 2010 MTS/IEEE SEATTLE*, 2010, pp. 1–10.

[4] H. He, P. Stoica, and J. Li, "Waveform design with stopband and correlation constraints for cognitive radar," in *2010 2nd International Workshop on Cognitive Information Processing*, 2010, pp. 344–349.

[5] A. Aubry, A. DeMaio, A. Farina, and M. Wicks, "Knowledge-aided (potentially cognitive) transmit signal and receive filter design in signal-dependent clutter," *IEEE Transactions on Aerospace and Electronic Systems*, vol. 49, pp. 93–117, 2013.

[6] A. Aubry, A. De Maio, M. Piezzo, M. M. Naghsh, M. Soltanalian, and P. Stoica, "Cognitive radar waveform design for spectral coexistence in signal-dependent interference," in *2014 IEEE Radar Conference*, 2014, pp. 0474–0478.

[7] A. Aubry, A. D. Maio, M. Piezzo, and A. Farina, "Radar waveform design in a spectrally crowded environment via nonconvex quadratic optimization," *IEEE Transactions on Aerospace and Electronic Systems*, vol. 50, pp. 1138–1152, 2014.

[8] W. Rowe, P. Stoica, and J. Li, "Spectrally constrained waveform design [sp tips&tricks]," *IEEE Signal Processing Magazine*, vol. 31, pp. 157–162, 2014.

[9] M. M. Naghsh, M. Soltanalian, P. Stoica, M. Modarres-Hashemi, A. D. Maio, and A. Aubry, "A doppler robust design of transmit sequence and receive filter in the presence of signal-dependent interference," *IEEE Transactions on Signal Processing*, vol. 62, pp. 772–785, 2014.

[10] J. R. Guerci and S. U. Pillai, "Adaptive transmission radar: the next "wave"?" in *Proceedings of the IEEE 2000 National Aerospace and Electronics Conference. NAECON 2000. Engineering Tomorrow (Cat. No.00CH37093)*, Oct 2000, pp. 779–786.

[11] L. K. Patton and B. D. Rigling, "Modulus constraints in adaptive radar waveform design," in *IEEE Radar Conference*, May 2008, pp. 1–6.

[12] J. R. Guerci and S. U. Pillai, "Theory and application of optimum transmit-receive radar," in *Proc. Record of the IEEE 2000 Int. Radar Conf. [Cat. No. 00CH37037]*, May 2000, pp. 705–710.

[13] S. U. Pillai, D. C. Youla, H. S. Oh, and J. R. Guerci, "Optimum transmit-receiver design in the presence of signal-dependent interference and channel noise," in *Proc. and Computers (Cat Conf. Record of the Thirty-Third Asilomar Conf. Signals, Systems No.CH37020)*, vol. 2, Oct. 1999, pp. 870–875 vol.2.

[14] D. A. Garren, M. K. Osborn, A. C. Odom, J. S. Goldstein, S. U. Pillai, and J. R. Guerci, "Enhanced target detection and identification via optimised radar transmission pulse shape," *IEE Proceedings - Radar, Sonar and Navigation*, vol. 148, no. 3, pp. 130–138, June 2001.

[15] D. A. Garren, M. K. Osborn, A. C. Odom, J. S. Goldstein, S. U. Pillai, and J. R. Guerci, "Optimal transmission pulse shape for detection and identification with uncertain target aspect," in *Proc. IEEE Radar Conf. (Cat. No.01CH37200)*, May 2001, pp. 123–128.

[16] S. Z. Alshirah, S. Gishkori, and B. Mulgrew, "Frequency-based optimal radar waveform design for classification performance maximization using multiclass Fisher analysis," *IEEE Transactions on Geoscience and Remote Sensing*, 2020.

[17] ——, "Frequency-domain based waveform design for binary extended-target classification," in *Proc. Speech and Signal Processing (ICASSP) ICASSP 2019 - 2019 IEEE Int. Conf. Acoustics*, May 2019, pp. 4450–4453.

[18] P. R. Venkata and N. A. Goodman, "Novel iterative techniques for radar target discrimination," in *2006 International Waveform Diversity Design Conference*, Jan 2006, pp. 1–7.

[19] S. Haykin, "Cognitive radar: a way of the future," *IEEE Signal Processing Magazine*, vol. 23, no. 1, pp. 30–40, Jan 2006.

[20] J. Ender, "The meaning of k-space for classical and advanced SAR-techniques," *Proc. PSIP*, vol. 2001, 2001.

[21] M. A. Richards, *Fundamentals of radar signal processing*. Tata McGraw-Hill Education, 2005.

[22] Civilian vehicle data dome overview. [Online]. Available: https://www.sdms.afrl.af.mil/index.php

[23] S. J. A. Melvin, William L., "5.9 overview of prf regimes," p. 226, 2014. [Online]. Available: https://app.knovel.com/hotlink/khtml/id:kt00U54KK4/principles-modern-radar/overview-prf-regimes

[24] N. J. Willis and H. D. Griffiths, *Advances in bistatic radar*. SciTech Publishing, 2007, vol. 2.

[25] J. Whitaker, *The RF Transmission Systems Handbook*. CRC Press, 2017.

[26] S. D. Blunt and E. L. Mokole, "Overview of radar waveform diversity," *IEEE Aerospace and Electronic Systems Magazine*, vol. 31, no. 11, pp. 2–42, November 2016.

[27] D. A. Garren, A. C. Odom, M. K. Osborn, J. S. Goldstein, S. U. Pillai, and J. R. Guerci, "Full-polarization matched-illumination for target detection and identification," *IEEE Transactions on Aerospace and Electronic Systems*, vol. 38, no. 3, pp. 824–837, July 2002.

[28] S. U. Pillai, H. S. Oh, and J. R. Guerci, "Multichannel matched transmit-receiver design in presence of signal-dependent interference and noise," in *Proc. IEEE Sensor Array and Multichannel Signal Processing Workshop. SAM 2000 (Cat. No.00EX410)*, Mar. 2000, pp. 385–389.

[29] S. U. Pillai and H. S. Oh, "Optimum MIMO transmit-receiver design in presence of interference," in *Proc. Int. Symp. Circuits and Systems ISCAS '03*, vol. 4, May 2003, p. IV.

[30] J. Guerci, *Cognitive Radar: The Knowledge-aided Fully Adaptive Approach*, ser. Artech House radar library. Artech House, 2010. [Online]. Available: https://books.google.co.uk/books?id=8Mn_C-iOzeEC

[31] H. Chernoff, "Sequential analysis and optimal design. society for industrial and applied," 1972.

[32] S. Kay, "Optimal signal design for detection of Gaussian point targets in stationary Gaussian clutter/reverberation," *IEEE Journal of Selected Topics in Signal Processing*, vol. 1, no. 1, pp. 31–41, June 2007.

[33] J. H. Bae and N. A. Goodman, "Adaptive waveforms for target class discrimination," in *2007 International Waveform Diversity and Design Conference*, June 2007, pp. 395–399.

[34] N. A. Goodman, P. R. Venkata, and M. A. Neifeld, "Adaptive waveform design and sequential hypothesis testing for target recognition with active sensors," *IEEE Journal of Selected Topics in Signal Processing*, vol. 1, no. 1, pp. 105–113, June 2007.

[35] N. A. Goodman, "Closed-loop radar with adaptively matched waveforms," in *2007 International Conference on Electromagnetics in Advanced Applications*, Sep. 2007, pp. 468–471.

[36] R. Romero and N. A. Goodman, "Information-theoretic matched waveform in signal dependent interference," in *2008 IEEE Radar Conference*, May 2008, pp. 1–6.

[37] R. A. Romero and N. A. Goodman, "Waveform design in signal-dependent interference and application to target recognition with multiple transmissions," *IET Radar, Sonar Navigation*, vol. 3, no. 4, pp. 328–340, August 2009.

[38] J. Bae and N. A. Goodman, "Evaluation of modulus-constrained matched illumination waveforms for target identification," in *2010 IEEE Radar Conference*, May 2010, pp. 871–876.

[39] D. Bhaskar, S. N. Sur, S. Bera, and R. Bera, "Improvement in target detectability through miso radar," *IJCA Proceedings on International Symposium on Devices MEMS, Intelligent Systems & Communication (ISDMISC)*, no. 6, pp. 10–15, 2011, full text available.

[40] D. J. Rabideau and P. Parker, "Ubiquitous mimo multifunction digital array radar," in *The Thrity-Seventh Asilomar Conference on Signals, Systems Computers, 2003*, vol. 1, 2003, pp. 1057–1064 Vol.1.

[41] T. B. Butler and N. A. Goodman, "Multistatic target classification with adaptive waveforms," in *2008 IEEE Radar Conference*, May 2008, pp. 1–6.

[42] J. Bae and N. A. Goodman, "Widely separated MIMO radar with adaptive waveform for target classification," in *2011 4th IEEE International Workshop on Computational Advances in Multi-Sensor Adaptive Processing (CAMSAP)*, Dec 2011, pp. 21–24.

[43] ——, "Target recognition with high-fidelity target signatures and adaptive waveforms in MIMO radar," in *2015 IEEE 6th International Workshop on Computational Advances in Multi-Sensor Adaptive Processing (CAMSAP)*, Dec 2015, pp. 285–288.

[44] ——, "Automatic target recognition with unknown orientation and adaptive waveforms," in *2011 IEEE RadarCon (RADAR)*, May 2011, pp. 1000–1005.

[45] R. Romero and N. A. Goodman, "Improved waveform design for target recognition with multiple transmissions," in *2009 International Waveform Diversity and Design Conference*, Feb 2009, pp. 26–30.

[46] Q. J. O. Tan, R. A. Romero, and D. C. Jenn, "Target recognition with adaptive waveforms in cognitive radar using practical target RCS responses," in *IEEE Radar Conference*, April 2018, pp. 0606–0611.

[47] Q. J. O. Tan and R. A. Romero, "Jammer nulling adaptive waveforms with cognitive radar for aircraft RCS recognition in presence of frequency sweep and base jammers," in *Proc. and Computers 2018 52nd Asilomar Conf. Signals, Systems*, Oct. 2018, pp. 1339–1343.

[48] ——, "Ground vehicle target signature identification with cognitive automotive radar using 24–25 and 76–77 ghz bands," *Sonar Navigation IET Radar*, vol. 12, no. 12, pp. 1448–1465, 2018.

[49] S. J. A. Melvin, William L., "1.6 u.s. military radar nomenclature," p. 9, 2014. [Online]. Available: https://app.knovel.com/hotlink/khtml/id:kt00U54G75/principles-modern-radar/military-radar-nomenclature

[50] R. O. Duda, *Pattern Classification*, second edition. ed. New York: Wiley, 2000.

[51] S. Z. Alshirah and B. Mulgrew, "Improved 2-class target classification performance using radar waveform design," in *Proc. IEEE Radar Conf. (RadarConf18)*, Apr. 2018, pp. 0458–0461.

[52] K. B. Petersen and M. S. Pedersen, "The matrix cookbook," nov 2012, version 20121115. [Online]. Available: http://localhost/pubdb/p.php?3274

[53] K. E. Dungan, C. Austin, J. Nehrbass, and L. C. Potter, "Civilian vehicle radar data domes," in *Algorithms for Synthetic Aperture Radar Imagery XVII*, E. G. Zelnio and F. D. Garber, Eds., vol. 7699, International Society for Optics and Photonics. SPIE, 2010, pp. 242 – 253. [Online]. Available: https://doi.org/10.1117/12.850151

[54] C. F. Van Loan and G. H. Golub, *Matrix computations*. Johns Hopkins University Press Baltimore, 1983.

[55] L. Ingber, "Adaptive simulated annealing (asa): Lessons learned," *arXiv preprint cs/0001018*, 2000.